



Structure-function relationships of some phosphorus compounds
by Alvin Fitzgerald

A thesis submitted to the Graduate Faculty in partial fulfillment of the requirements for the degree of DOCTOR OF PHILOSOPHY in Chemistry
Montana State University
© Copyright by Alvin Fitzgerald (1973)

Abstract:

The crystal and molecular structures of two cyclic organophosphorus compounds were solved by the X-ray diffraction method. A hypothesis relating the free energy of hydrolysis of p-substituted monoaryl phosphates to the length of the P-O ester bonds has been presented. Huckel molecular orbital calculations were carried out as one test of the hypothesis. The structure of a sodium salt of phenyl phosphate was accurately determined as the initial work in a second test of the hypothesis.

2,2,3,3,4-Pentamethyl-1-phenylphosphetane-1-oxide crystallized in space group P21/c with $a=17.165(16)\text{\AA}$, $b=7.226(2)\text{\AA}$, $c=11.365(10)\text{\AA}$ $\beta=102.24(7)^\circ$, and $Z=4$. This is the first unsymmetrical phosphetane oxide structure to be determined and indicates the reactivity of this group of compounds towards base is directly related to the amount of steric hindrance due to substitution on the α -carbons. The final R is 6.5% for 1244 observed reflections.

1-Iodomethyl-3-methyl-1-phenylphospholanium iodide crystallizes in the space group P21 /c with $a=7.217(3)\text{\AA}$, $b=14.261(6)\text{\AA}$, $c=14.778(6)\text{\AA}$ $\beta=106.54(3)^\circ$, and $Z=4$. The determination of this structure allowed workers in the field to assign structures to ten other compounds that are related to it through stereospecific reactions. The final R is 4.5% for 1434 observed reflections.

Data were presented indicating that the length of a P-O(Ar) bond, L, can be related to the equilibrium constant for the hydrolysis reaction by the equation.

$L=(k/\rho)\text{Log}(K\text{ArR}/K_0)$ Huckel molecular orbital calculations were carried out for para-substituted phenols, benzoic acids and phenyl phosphates. The results of these calculations are consistent with the proposed hypothesis.

Disodium phenylphosphate-2-methoxyethanol trihydrate molecular complex crystallizes in the space group P21/c with $a=14.69(2)\text{\AA}$, $b=7.960(6)\text{\AA}$, $c=13.68(1)\text{\AA}$, $\beta=107.3(2)^\circ$, and $Z=4$. Comparison of the intramolecular distances in the phenylphosphate dianion with those of a previously determined structure showed significant differences in some of the non-bonded intramolecular distances. These differences were found to be due to a difference in the orientation of the phenyl ring with respect to the phosphate group. The final R is 5.6% for 969 observed reflections.

STRUCTURE-FUNCTION RELATIONSHIPS OF SOME
PHOSPHORUS COMPOUNDS

by

ALVIN FITZGERALD

A thesis submitted to the Graduate Faculty in partial
fulfillment of the requirements for the degree

of

DOCTOR OF PHILOSOPHY

in

Chemistry

Approved:

E. W. Guicker

Head, Major Department

Charles N. Caughlan

Chairman, Examining Committee

Henry L. Parsons

Graduate Dean

MONTANA STATE UNIVERSITY
Bozeman, Montana

December, 1973

ACKNOWLEDGMENTS

I would like to thank the faculty of the Chemistry Department of Montana State University for their help and guidance and in particular the following: Dr. Charles N. Caughlan for his assistance as my thesis advisor, Dr. G. David Smith for providing invaluable assistance in keeping the Crystallography Computing Library up to date and discussion on many topics, Dr. Patrik R. Callis for much needed help on the molecular orbital calculations, and Mr. Terry Maffit for determining the NMR spectra.

I wish to acknowledge the National Aeronautic and Space Administration and the National Science Foundation for support while working on part of the research. Also I wish to thank the Computing Center of Montana State University for grants of computing time.

Finally, I wish to thank my wife, Linda, for being an understanding wife, breadwinner, and mother while this research was being completed. Allison and Patrik provided inspiration and were very understanding during the writing of the thesis.

TABLE OF CONTENTS

CHAPTER	PAGE
INTRODUCTION	1
I. THE CRYSTAL AND MOLECULAR STRUCTURE OF	
2,2,3,3,4-PENTAMETHYL-1-PHENYLPHOSPHETANE	
1-OXIDE	3
Introduction	3
Preparation of Crystals	5
Density Determination	6
Determination of Space Group and Cell	
Parameters	6
Collection of the Data	7
Treatment of the Data	9
Structure Determination	11
Discussion of the Structure	13
II. THE CRYSTAL AND MOLECULAR STRUCTURE OF	
1-IODOMETHYL-3-METHYL-1-PHENYLPHOSPHOLANIUM	
IODIDE	30
Introduction	30
Choice of a Crystal	31
Density	31
Determination of Space Group and Unit Cell	
Dimensions	31

CHAPTER	PAGE
Determination of Accurate Unit Cell	
Dimensions	32
Data Collection	32
Treatment of Data	34
Structure Determination	34
Discussion of the Structure	44
III. HYPOTHESIS RELATING FREE ENERGY OF HYDROLYSIS TO THE LENGTH OF THE P-O BOND BEING HYDROLYZED IN ARYL PHOSPHATES.	53
Introduction.	53
Development of the Hypothesis	55
Proposed Hypothesis	61
Proposed Tests of the Hypothesis.	61
IV. HÜCKEL MOLECULAR ORBITAL CALCULATIONS	63
Introduction.	63
Procedure for Carrying Out the HMO Calculations.	66
Results of HMO Calculations	68
Substituted phenols	68
Substituted benzoic acids	68
Para-substituted monophenyl phosphates.	73
Conclusions Based on HMO Calculations	73

CHAPTER	PAGE
V. THE CRYSTAL AND MOLECULAR STRUCTURE OF DISODIUM PHENYL PHOSPHATE·2-METHOXYETHANOL· TRIHYDRATE $\text{Na}_2\text{PO}_4\text{C}_6\text{H}_5\cdot\text{C}_3\text{O}_3\text{H}_9\cdot 3\text{H}_2\text{O}$	83
Introduction.	83
Preparation	83
Choice and Mounting of a Crystal.	83
Determination of Tentative Cell Dimensions.	84
Determination of Space Group and Accurate Cell Dimensions	85
Determination of the Density.	85
Data Collection	87
Treatment of Data	87
Structure Determination	88
Refinement.	89
Discussion of the Molecular Structure	99
The phenyl phosphate dianion.	99
The 2-methoxyethanol molecule	110
Sodium ion coordination	111
Hydrogen bonding scheme	114
Water of hydration.	114
Discussion of the Crystal Structure	116
VI. SUMMARY AND CONCLUSIONS	119
BIBLIOGRAPHY	122

LIST OF TABLES

TABLE	PAGE
I. Crystal Data: 2,2,3,3,4-Pentamethyl-1-phenylphosphetane 1-oxide.	8
II. Positional Parameters for the Non-hydrogen Atoms in 2,2,3,3,4-Pentamethyl-1-phenylphosphetane 1-oxide.	14
III. Anisotropic Thermal Parameters for the Non-hydrogen Atoms in 2,2,3,3,4-Pentamethyl-1-phosphetane 1-oxide.	15
IV. Hydrogen Atoms Positions and Thermal Parameters for 2,2,3,3,4-Pentamethyl-1-phosphetane 1-oxide.	17
V. Observed and Calculated Structure Factors.	19
VI. Equations of Planes Referred to Orthogonal Axes in 2,2,3,3,4-Pentamethyl-1-phenylphosphetane 1-oxide.	27
VII. Crystal Data: 1-Iodomethyl-3-methyl-1-phenylphospholanium Iodide	33
VIII. Observed and Calculated Structure Factors.	38
IX. Positional Parameters for the Non-hydrogen Atoms in 1-Iodomethyl-3-methyl-1-phenylphospholanium Iodide	39

TABLE	PAGE
X. Anisotropic Thermal Parameters for the Non-hydrogen Atoms in 1-Iodomethyl-3-methyl-1-phenylphospholanium Iodide	40
XI. Hydrogen Atom Positions and Thermal Parameters for 1-Iodomethyl-3-methyl-1-phenylphospholanium Iodide	42
XII. Equations of Planes Referred to Orthogonal Axes in 1-Iodomethyl-3-methyl-1-phenylphospholanium Iodide	47
XIII. Values for h_x and k_{yx} Used in HMO Calculations .	67
XIV. Crystal Data: Sodium phenyl phosphate·2-methoxyethanol·trihydrate.	86
XV. Observed and Calculated Structure Factors. . . .	92
XVI. Positional Parameters for the Non-hydrogen Atoms in $\text{Na}_2\text{PO}_4\text{C}_6\text{H}_5 \cdot \text{C}_3\text{O}_3\text{H}_9 \cdot 3\text{H}_2\text{O}$	93
XVII. Anisotropic Thermal Parameters for the Non-hydrogen Atoms in $\text{Na}_2\text{PO}_4\text{C}_6\text{H}_5 \cdot \text{C}_3\text{O}_3\text{H}_9 \cdot 3\text{H}_2\text{O}$	95
XVIII. Hydrogen Atom Positions and Thermal Parameters for $\text{Na}_2\text{PO}_4\text{C}_6\text{H}_5 \cdot \text{C}_3\text{O}_3\text{H}_9 \cdot 3\text{H}_2\text{O}$	97
XIX. Least Squares Planes Referred to Orthogonal Axes in Sodium phenyl phosphate·2-methoxyethanol·trihydrate	107

LIST OF FIGURES

FIGURE	PAGE
I. Isomers for Which Three-dimensional Structures Have Been Determined.	4
II. Molecular Structure of 2,2,3,3,4-Pentamethyl-1-phenylphosphetane 1-oxide at the 50% Probability Level.	20
III. Bond Distances and Angles for 2,2,3,3,4-Pentamethyl-1-phenylphosphetane 1-Oxide.	21
IV. Proposed Reaction Mechanism for Alkaline Hydrolysis of 2,2,3,3,4-Pentamethyl-1-phenylphosphetane 1-Oxide.	23
V. Comparison of Ring Puckering in the Three Isomeric Phosphetane Oxides.	25
VI. Tilt of Phenyl Group Relative to the C(2)-P-C(4) Plane.	26
VII. Stereographic Packing Diagram for 2,2,3,3,4-Pentamethyl-1-phenylphosphetane 1-Oxide.	28
VIII. Normal Probability Plot of $1244 \bar{\sigma}_{R_1}$ Based on F_0	29
IX. Bond Distances and Angles for 1-Iodomethyl-3-methyl-1-phenylphospholanium Iodide.	43

FIGURE	PAGE
X. Molecular Structure of 1-Iodomethyl-3-methyl-1-phenylphospholanium Iodide Illustrating the Thermal Ellipsoids at the 50% Probability Level of Thermal Displacement.	45
XI. Envelope Form of the Five-membered Phospholanium Ring System.	48
XII. Comparison of the Envelope and Half-chair Forms of Cyclopentane and the Phospholanium Ring System	49
XIII. Stereographic Packing Diagram for 1-Iodomethyl-3-methyl-1-phenylphospholanium Iodide	51
XIV. Normal Probability Plot of $1395 \delta_{R_1}$ Based on (F_0)	52
XV. $\ln(k)$ Versus σ Plot for the Hydrolysis of Monoaryl Phosphates.	57
XVI. C(Ph)-C(OOH) Bond Distance Versus σ For Substituted Benzoic Acids.	58
XVII. P-O Bond Distance Versus σ For Some Mono- and Diaryl Phosphate Esters.	59
XVIII. P-O Bond Distance Versus σ For Some Triaryl Phosphate Esters	60

FIGURE.	PAGE
XIX. HMO Bond Orders and Electron Density on the Phenolic Oxygen for p-Substituted Phenols.	69
XX. Electron Density on the Phenolic Hydroxyl Oxygen Atom Versus σ	70
XXI. HMO Bond Orders and Electron Density on Acid Oxygen Benzoic Acids	71
XXII. Electron Density on the Carboxyl OH Oxygen Atom of Substituted Benzoic Acids Versus σ	72
XXIII. HMO Bond Orders and Electron Density on Ester Oxygen - First HMO Approximation for Para-substituted Phenyl Phosphates.	74
XXIV. HMO First Set of Assumptions. Electron Density on Ester Oxygen Atom of Substituted Phenyl Phosphates Versus σ	75
XXV. Bond Order, p , For P-O(ester) Bond in Phenyl Phosphates Versus σ	76
XXVI. HMO Bond Orders and Electron Density on Ester Oxygen - Second HMO Approximation for Para-substituted Phenyl Phosphates	77
XXVII. HMO Bond Orders and Electron Density on Ester Oxygen - Third HMO Approximation for Para-substituted Phenyl Phosphates.	78

FIGURE	PAGE
XXVIII. Calculated P-O(ester) Bond Lengths Versus σ For Phenyl Phosphates: Approximation A	81
XXIX. a-b Projection of the Molecular Structure of $\text{Na}_2\text{PO}_4\text{C}_6\text{H}_5 \cdot \text{C}_3\text{O}_3\text{H}_9 \cdot 3\text{H}_2\text{O}$ Illustrating the Thermal Ellipsoids at the 50% Probability Level	100
XXX. Bond Distances and Angles for the Phenyl Phosphate Dianion	101
XXXI. Bond Distances and Angles for the Solvation Molecule and the Water of Hydration	102
XXXII. Half-normal Probability Plot for All Intra- molecular Distances in the Phenyl Phosphate Dianion from Two Structure Determinations	103
XXXIII. Half-normal Probability Plot for the Intra- molecular Distances Expected to be Identical in the Two Phenyl Phosphate Dianion Structures.	105
XXXIV. Half-normal Probability Plot for the Intra- molecular Distances Expected to be Different in the Two Phenyl Phosphate Dianion Structures.	106

FIGURE	PAGE
XXXV. Normal Probability Plot of 969 δ_{R_1} Based on Observed Structure Factors F_o	109
XXXVI. Sodium Ion Coordination Angles and Distances.	112
XXXVII. Packing Diagram Emphasizing Sodium Ion Coordination.	113
XXXVIII. Packing Diagram Emphasizing Hydrogen Bonding	115
XXXIX. Stereographic Packing Diagram for $\text{Na}_2\text{PO}_4\text{C}_6\text{H}_5 \cdot \text{C}_3\text{O}_3\text{H}_9 \cdot 3\text{H}_2\text{O}$	117

ABSTRACT

The crystal and molecular structures of two cyclic organophosphorus compounds were solved by the X-ray diffraction method. A hypothesis relating the free energy of hydrolysis of p-substituted monoaryl phosphates to the length of the P-O ester bonds has been presented. Hückel molecular orbital calculations were carried out as one test of the hypothesis. The structure of a sodium salt of phenyl phosphate was accurately determined as the initial work in a second test of the hypothesis.

2,2,3,3,4-Pentamethyl-1-phenylphosphetane-1-oxide crystallized in space group $P2_1/c$ with $a=17.165(16)\text{Å}$, $b=7.226(2)\text{Å}$, $c=11.365(10)\text{Å}$, $\beta=102.24(7)^\circ$, and $Z=4$. This is the first unsymmetrical phosphetane oxide structure to be determined and indicates the reactivity of this group of compounds towards base is directly related to the amount of steric hindrance due to substitution on the α -carbons. The final R is 6.5% for 1244 observed reflections.

1-Iodomethyl-3-methyl-1-phenylphospholanium iodide crystallizes in the space group $P2_1/c$ with $a=7.217(3)\text{Å}$, $b=14.261(6)\text{Å}$, $c=14.778(6)\text{Å}$, $\beta=106.54(3)^\circ$, and $Z=4$. The determination of this structure allowed workers in the field to assign structures to ten other compounds that are related to it through stereospecific reactions. The final R is 4.5% for 1434 observed reflections.

Data were presented indicating that the length of a P-O(Ar) bond, L, can be related to the equilibrium constant for the hydrolysis reaction by the equation.

$$L = \frac{k}{\rho} \text{Log} \left(\frac{K_{ArR}}{K_O} \right)$$

Hückel molecular orbital calculations were carried out for para-substituted phenols, benzoic acids and phenyl phosphates. The results of these calculations are consistent with the proposed hypothesis.

Disodium phenylphosphate-2-methoxyethanol trihydrate molecular complex crystallizes in the space group $P2_1/c$ with $a=14.69(2)\text{Å}$, $b=7.960(6)\text{Å}$, $c=13.68(1)\text{Å}$, $\beta=107.3(2)^\circ$, and $Z=4$. Comparison of the intramolecular distances in the phenylphosphate dianion with those of a previously determined structure showed significant differences in some of the non-bonded intramolecular distances. These differences were found to be due to a difference in the orientation of the phenyl ring with respect to the phosphate group. The final R is 5.6% for 969 observed reflections.

INTRODUCTION

This dissertation is divided into five chapters which may be generally considered as two sections. The first section consists of the first two chapters which contain the structures of two compounds. The structures of 2,2,3,3,4-pentamethyl-1-phenylphosphetane 1-oxide and 1-iodomethyl-3-methyl-1-phenylphospholanium iodide were determined as a service to workers in the field of organophosphorus chemistry and as part of a long term study of the structures of phosphorus compounds carried on in this laboratory. Preliminary reports on these structures have appeared (22,23).

The second section of the thesis consists of the last three chapters. Chapter III consists of the evidence for and the derivation of a hypothesis relating the free energy of hydrolysis for monoaryl phosphates to the length of the P-O bond being hydrolyzed. A preliminary report of this hypothesis has been given (12). Huckel molecular orbital (HMO) calculations have been carried out as a preliminary test of the hypothesis and are presented in the fourth chapter. The structure of a sodium salt of phenyl phosphate has been determined as the initial structure analysis in a series of structures that must be accurately determined to test the validity of the hypothesis and is contained in the

fifth chapter.

CHAPTER I

THE CRYSTAL AND MOLECULAR STRUCTURE OF 2,2,3,3,4-PENTAMETHYL-1-PHENYLPHOSPHETANE 1-OXIDE

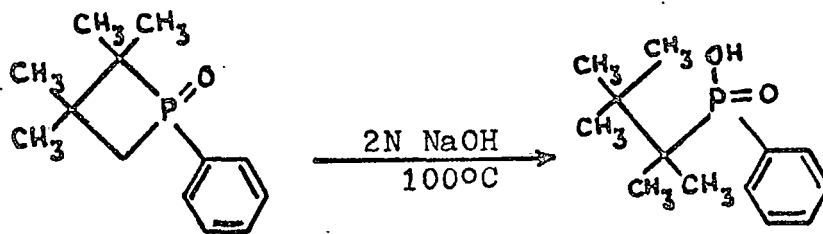
I. INTRODUCTION

The determination of the three-dimensional structure of 2,2,3,3,4-pentamethyl-1-phenylphosphetane 1-oxide is of interest for a number of reasons. Structures of compounds of this type have been studied in this laboratory for several years. Examples of other compounds in this series whose structures have been determined are shown in Figure I.

This is the first unsymmetrical phosphetane oxide whose structure has been determined. Dr. Sheldon Cremer of Marquette University synthesized the compound and supplied the sample. It is of particular interest in regard to organophosphorus chemistry to know if the methyl group on the mono-substituted α -carbon is cis or trans to the phenyl group.

This class of compounds shows surprising stability when subjected to hydrolysis under basic conditions.

Corfield has reported the following two reactions (13):



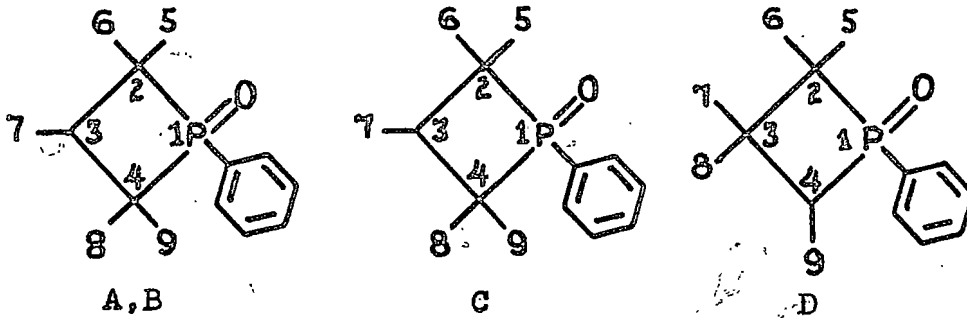
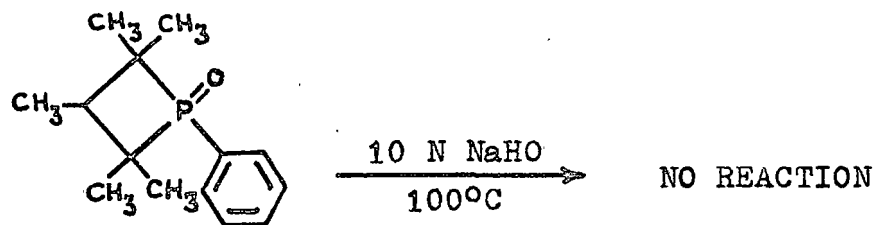
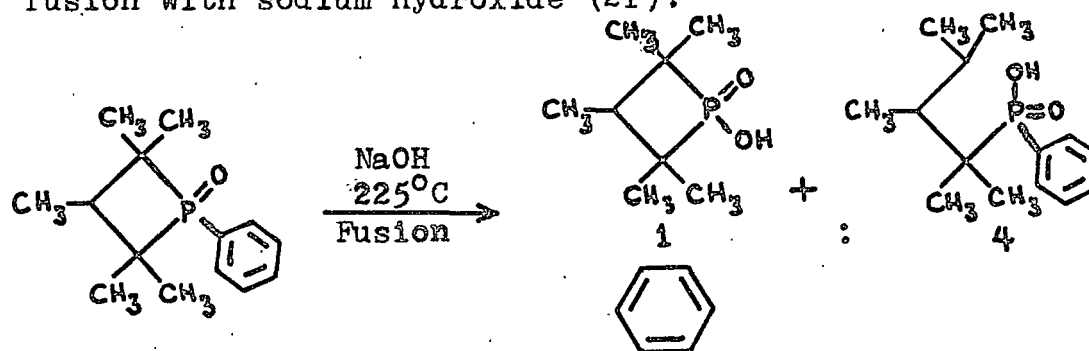


FIGURE I

ISOMERS FOR WHICH THREE-DIMENSIONAL STRUCTURES HAVE BEEN DETERMINED. A, B: METHYL-7 TRANS TO PHENYL (28); C: METHYL-7 CIS TO PHENYL (29); D: THIS WORK



Ezzel has observed that the P-C bond can be cleaved by fusion with sodium hydroxide (21):



These reactions clearly show the effect of α -substitution on the reactivity of the compounds.

It has been suggested that the 1-4 bond may be longer in the unsymmetrical case than the 1-2 bond (37). Solution of this structure should adequately answer that question though ideally one would use a phosphetane-oxide that was disubstituted on a α -carbon and unsubstituted on the other α -carbon.

II. PREPARATION OF CRYSTALS

The compound crystallized readily from solutions of

either benzene or cyclohexane when these were allowed to evaporate slowly. This was achieved by placing a Petri dish of the solution in a dessicator and opening the lid very briefly once a day until crystals formed. Two to three weeks were generally required for crystal growth to occur. The largest crystals were obtained from the cyclohexane solution and one of these was used for the data collection. The crystal was mounted on a glass fiber and sealed in a capillary in as much as the crystals turned opaque in air when exposed to X-rays.

III. DENSITY DETERMINATION

The density of the compound was determined by flotation in a mixture of methanol and carbon tetrachloride. The observed density was 1.12 gram/cm^3 , and the calculated density, assuming four molecules per unit cell, was 1.14 gram/cm^3 .

IV. DETERMINATION OF SPACE GROUP AND CELL PARAMETERS

The crystal was mounted coincident with the b-axis. An oscillation photograph contained a mirror plane perpendicular to the axis of rotation indicating a space group of monoclinic or higher symmetry. The space group extinct reflections, as determined on the General Electric XRD-5 diffractometer, were:

hkl: no conditions

Ok0: $k = 2n + 1$

h0l: $l = 2n + 1$

These extinctions uniquely determine the space group as $P2_1/c$. The unit cell dimensions were determined by least-squares refinement of the 2θ values of 12 general reflections using a General Electric XRD-5 diffractometer equipped with with a G.E. single crystal orienter.

Pertinent crystal data are listed in Table I. It was later discovered that a different cell still in space group $P2_1/c$ could be chosen which would give a β angle nearer to 90° . The data were converted to this cell although the solution of the structure was obtained using the original cell parameters.

V. COLLECTION OF THE DATA

The unique intensity data were collected by the θ - 2θ scan method out to $2\theta = 25.0^\circ$, using zirconium-filtered $\text{MoK}\alpha$ ($\lambda = 0.71069\text{\AA}$) radiation. The General Electric XRD-5 diffractometer used was equipped with a scintillation counter, pulse-height discriminator, and a General Electric single crystal orientator. Each reflection was scanned over an angular width of 2.0° in 2θ at a rate of 2° per minute and background radiation was counted for ten

TABLE I
CRYSTAL DATA

2,2,3,3,4-Pentamethyl-1-phenylphosphetane 1-oxide
 $C_{14}POH_{21}$ F.W. 236.295 F(000) = 512
 Monoclinic, space group $P2_1/c$

ORIGINAL CELL

$$a = 18.50(4)\text{\AA}$$

$$b = 7.222(4)\text{\AA}$$

$$c = 11.36(2)\text{\AA}$$

$$\beta = 114.6(1)^\circ$$

$$\text{Volume of the unit cell} = 1379\text{\AA}^3$$

$$\text{Molecules/unit cell} = 4$$

$$\text{Linear absorption coefficient, } \mu(\text{MoK}\alpha) = 1.78\text{cm}^{-1}$$

Crystal dimensions: 0.18mm x 0.64mm x 0.65mm

Crystal was bound by faces {100}, {010}, and {001} respectively.

NEW CELL

$$a = 17.165(16)\text{\AA}$$

$$b = 7.226(2)\text{\AA}$$

$$c = 11.365(10)\text{\AA}$$

$$\beta = 102.24(7)^\circ$$

$$D_{\text{calc}} = 1.14 \text{ grams/cc.}$$

$$D_{\text{exp}} = 1.12 \text{ grams/cc.}$$

*Unit cell dimensions and standard deviations are those determined for a second data set on a second crystal.

seconds at each end of the 2θ scan. The take-off angle was set at 4.00° . The intensities of the 020, 220, and 002 reflections were monitored during the data collection so that corrections could be made for such things as variations in room temperature, voltage supply, instrumental stability and also to check for decomposition of the crystal during the course of the data collection. A scale factor was calculated for each block of data using these standard reflections. The average value of the scale factor over the complete data collection was 1.08 with a standard deviation of 0.045.

VI. TREATMENT OF THE DATA

Structure factors (F_0) were calculated from the intensities by applying the usual Lorentz-polarization correction for diffractometer data. The weights were calculated for each reflection assuming Poisson counting statistics and a correction factor, k_2 , related to the instrument instability (45). The weight assigned to the individual F_0 is related to the standard deviation, σ_F , as shown below.

$$w = \frac{1}{(\sigma_F)^2}$$

and

$$\sigma_F = \frac{k_1}{2\sqrt{L_p}} \sqrt{\frac{N_T + N_{Bg1} + N_{Bg2} + (k_2 N_{pk})^2}{N_{pk}}}$$

where

w = the weight

σ_F = the standard deviation of F_o

k_1 = the scale constant for the data set

k_2 = the instrument instability constant

p = the polarization factor

L = the Lorentz factor

N_T = the total peak count

N_{Bg1} and N_{Bg2} = the background counts at each end of the scan
(corrected for time)

$N_{pk} = N_T - N_{Bg1} - N_{Bg2}$ = the net peak count

The data set consisted of 1712 reflections of which 1244 were considered observed at the three sigma level. The constant, k_2 , was set at 0.07 based on the average standard deviation of the individual standard reflections (45). The data were corrected for absorption (35). The maximum and minimum transition factors were 0.96 and 0.98, respectively. Scattering factor curves for the non-hydrogen atoms were taken from the International Tables (31) as were the anomalous scattering corrections ($\Delta f'$ and $\Delta f''$) for phosphorus. The scattering factor curve for hydrogen was taken from Stewart,

et al. (44).

VII. STRUCTURE DETERMINATION

Five possible phosphorus positions were located from a Patterson map and refinement was tried on each of them. The fifth peak proved to be the correct phosphorus position.

Refinement is taken to mean least squares refinement where the minimized function is

$$\sum w(|F_o| - \frac{1}{k_1} |F_c|)^2$$

There are several indicators which describe the fit of the model to the data. These will be defined here for use in this chapter and the remaining two structural chapters. The residual index, summed over the observed data only is

$$R = \frac{\sum ||F_o| - |F_c||}{\sum |F_o|}$$

The residual index summed over all data collected is

$$R_{\text{obs} + \text{unobs}} = \frac{\sum ||F_o| - |F_c||}{\sum |F_o|}$$

The weighted residual index summed over the observed data only is defined as

$$R'' = \left[\frac{\sum w (|F_o| - |F_c|)^2}{\sum w |F_o|^2} \right]^{\frac{1}{2}}$$

A fourth indicator, S, the standard deviation of an observation of unit weight summed over the observed data only is

$$S = \left[\frac{\sum w (|F_o| - |F_c|)^2}{N_{\text{obs}} - N_{\text{var}}} \right]^{\frac{1}{2}}$$

where

N_{obs} = the number of observed data

and

N_{var} = the number of variables that are refined in the model

Full matrix least squares refinement of the positional and anisotropic thermal parameters for the 16 heavy atoms produced an R of 0.084 (8). A series of difference Fourier maps were needed to determine the positions of all the hydrogen atoms. The methyl groups appear to be somewhat disordered.

Positional and anisotropic thermal parameters of the 16 non-hydrogen atoms were refined. The positional and

isotropic temperature factors for the 21 hydrogen atoms were included in the refinement. At the completion of the refinement $R = 0.065$, $R'' = 0.080$, $R_{\text{obs} + \text{unobs}} = 0.123$ and $S = 1.70$. The largest shift divided by the standard deviation was less than 0.2 at the end of the refinement.

A final difference map was calculated. The largest peaks on this map were less than $\pm 0.26 \text{e}\text{\AA}^{-3}$ and were found near the phosphorus atom.

VIII. DISCUSSION OF THE STRUCTURE

The positional parameters of the non-hydrogen atoms are listed in Table II. The thermal parameters of the non-hydrogen atoms are listed in Table III. The hydrogen atom parameters are listed in Table IV. Table V contains the observed and calculated structure factors.

Figure II shows an ORTEP drawing of the structure with the thermal ellipsoids calculated at the 50% probability level (32). The bond lengths and angles are presented in Figure III.

The ORTEP drawing clearly shows that the single α -methyl group is trans to the phenyl group. Figure III shows that the two P-C bonds in the ring differ by about eight standard deviations. Moret and Trefonas have suggested that the P-C bond to the least substituted

TABLE II

POSITIONAL PARAMETERS FOR THE NON-HYDROGEN ATOMS IN
2,2,3,3,4-PENTAMETHYL-1-PHENYLPHOSPHETANE 1-OXIDE

<u>ATOM</u>	<u>x/a</u>	<u>y/b</u>	<u>z/c</u>
P	.74713(7) ^a	.23726(16)	.76522(10)
C(2)	.7405(3)	.0113(6)	.7293(5)
C(3)	.6518(3)	.0276(7)	.6599(5)
C(4)	.6633(2)	.2419(7)	.6398(4)
C(5)	.5958(4)	.3776(10)	.6375(7)
C(6)	.6253(4)	.0767(9)	.5422(5)
C(7)	.5923(4)	.0058(9)	.7400(6)
C(8)	.7512(4)	.1382(8)	.8377(6)
C(9)	.7942(3)	.0669(7)	.6439(5)
C(10)	.8344(2)	.3594(6)	.7384(4)
C(11)	.8516(3)	.3804(7)	.6287(5)
C(12)	.9187(4)	.4772(8)	.6143(7)
C(13)	.9679(3)	.5536(8)	.7160(7)
C(14)	.9509(3)	.5353(9)	.8243(7)
C(15)	.8849(3)	.4378(8)	.8386(5)
O	.7327(2)	.2904(5)	.8843(3)

^aThe number in parentheses is the standard deviation and refers to the least significant digits.

TABLE III

ANISOTROPIC THERMAL PARAMETERS FOR THE NON-HYDROGEN ATOMS IN

2,2,3,3,4-PENTAMETHYL-1-PHOSPHETANE 1-OXIDE

ATOM	β_{11}	β_{22}	β_{33}	β_{12}	β_{13}	β_{23}
P	.00258(4)	.01508(24)	.00692(11)	.00017(9)	.00095(4)	-.00007(14)
C(2)	.0033(2)	.0139(9)	.0093(5)	.0005(3)	.0005(2)	-.0012(5)
C(3)	.0030(2)	.0178(10)	.0078(5)	.0006(3)	.0011(2)	-.0009(5)
C(4)	.0023(1)	.0177(10)	.0088(4)	.0003(3)	.0013(2)	-.0005(6)
C(5)	.0030(2)	.0289(17)	.0199(10)	-.0030(5)	.0002(3)	.0001(10)
C(6)	.0048(3)	.0254(14)	.0107(6)	.0033(5)	-.0002(3)	.0025(7)
C(7)	.0038(2)	.0305(17)	.0141(8)	.0027(5)	.0026(3)	-.0033(8)
C(8)	.0063(3)	.0174(13)	.0156(8)	.0017(5)	-.0002(4)	-.0080(8)
C(9)	.0037(2)	.0154(11)	.0127(6)	-.0011(4)	.0012(3)	.0040(6)
C(10)	.0018(2)	.0155(10)	.0093(5)	-.0001(3)	.0004(2)	-.0004(5)
C(11)	.0027(2)	.0228(12)	.0095(5)	.0004(4)	.0012(2)	-.0021(6)
C(12)	.0038(2)	.0260(15)	.0152(8)	-.0003(5)	.0023(3)	-.0051(8)

TABLE III (CONTINUED)

ANISOTROPIC THERMAL PARAMETERS FOR THE NON-HYDROGEN ATOMS IN

2,2,3,3,4-PENTAMETHYL-1-PHOSPHETANE 1-OXIDE

ATOM	β_{11}	β_{22}	β_{33}	β_{12}	β_{13}	β_{23}
C(13)	•0027(2)	•0190(12)	•0184(8)	•0014(4)	•0001(3)	•0032(8)
C(14)	•0036(2)	•0260(15)	•0138(8)	•0015(5)	•0001(3)	•0007(8)
C(15)	•0030(2)	•0193(12)	•0112(6)	•0006(4)	•0003(3)	•0025(6)
O	•0041(2)	•0244(9)	•0096(4)	•0019(3)	•0019(2)	•0016(4)

(e.s.d.'s in parentheses)

The expression for the anisotropic thermal parameters is of the form:

$$\exp(-\beta_{11}h^2 - \beta_{22}k^2 - \beta_{33}l^2 - 2\beta_{12}hk - 2\beta_{13}hl - 2\beta_{23}kl)$$

TABLE IV

HYDROGEN ATOM POSITIONS AND THERMAL PARAMETERS FOR
2,2,3,3,4-PENTAMETHYL-1-PHOSPHETANE 1-OXIDE

ATOM	x/a	y/b	z/c	B_{iso}
H(1)	•690(3) ^a	•258(7)	•585(4)	4•(1)
H(2)	•556(5)	•343(12)	•604(8)	9•(2)
H(3)	•574(5)	•386(11)	•716(7)	9•(2)
H(4)	•614(9)	•538(18)	•651(13)	15•(4)
H(5)	•571(5)	•044(11)	•492(7)	8•(2)
H(6)	•651(4)	•069(8)	•481(6)	6•(1)
H(7)	•616(4)	•178(10)	•565(6)	7•(2)
H(8)	•545(4)	•042(9)	•701(6)	7•(2)
H(9)	•598(4)	•126(11)	•772(7)	8•(2)
H(10)	•604(5)	•056(12)	•824(8)	9•(2)
H(11)	•733(4)	•246(9)	•809(6)	6•(1)
H(12)	•799(4)	•154(9)	•872(6)	6•(1)
H(13)	•721(6)	•091(15)	•890(9)	12•(3)
H(14)	•788(3)	•193(8)	•615(5)	5•(1)
H(15)	•783(6)	•006(12)	•574(9)	11•(3)
H(16)	•857(4)	•078(9)	•711(6)	7•(2)
H(17)	•827(4)	•334(8)	•564(5)	6•(1)

^aThe number in parenthesis is the standard deviation and refers to the least significant digits.

TABLE IV (CONTINUED)
HYDROGEN ATOM POSITIONS AND THERMAL PARAMETERS FOR
2,2,3,3,4-PENTAMETHYL-1-PHOSPHETANE 1-OXIDE

<u>ATOM</u>	<u>x/a</u>	<u>y/b</u>	<u>z/c</u>	<u>B_{iso}</u>
H(18)	.928(4)	=.515(8)	.544(6)	5.(1)
H(19)	1.011(7)	=.612(15)	.702(11)	14.(3)
H(20)	.987(4)	=.563(9)	.919(7)	7.(2)
H(21)	.875(4)	=.427(9)	.912(6)	7.(1)

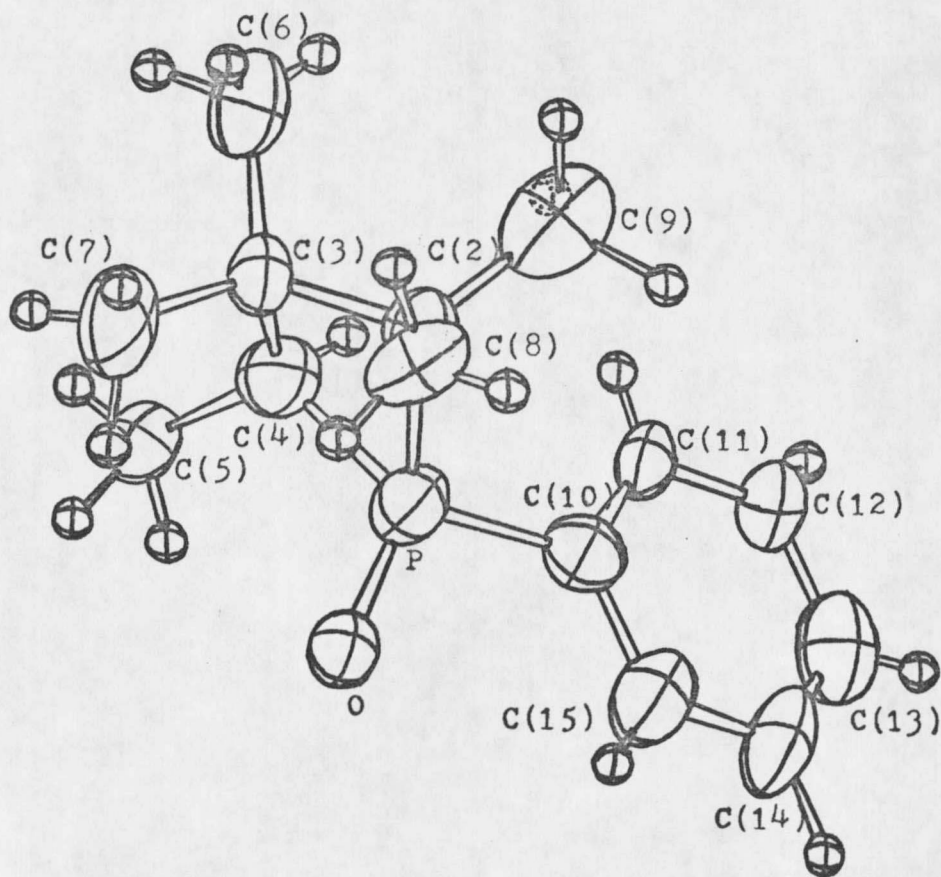


FIGURE II

MOLECULAR STRUCTURE OF
2,2,3,3,4-PENTAMETHYL-1-PHENYLPHOSPHETANE 1-OXIDE
AT THE 50% PROBABILITY LEVEL

The hydrogen atoms were arbitrarily assigned isotropic temperature factors of 1.0 in this illustration.

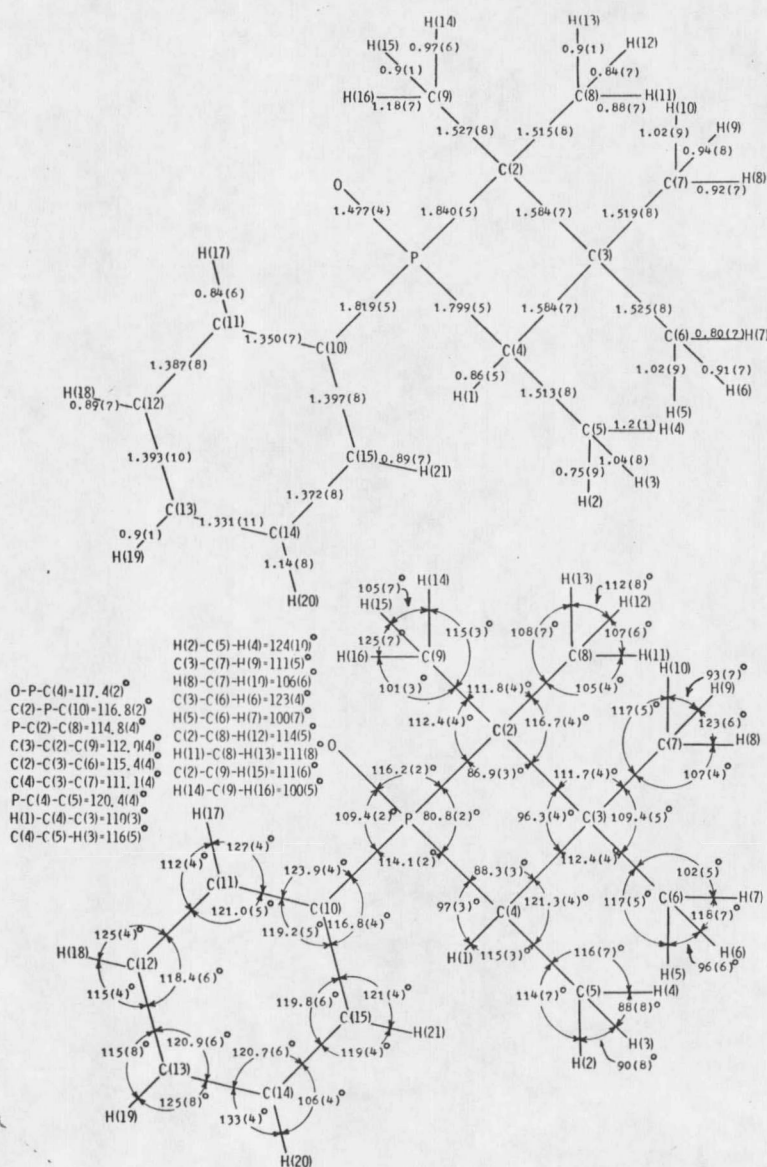


FIGURE III

BOND DISTANCES AND ANGLES FOR
 2,2,3,3,4-PENTAMETHYL-1-PHENYLPHOSPHETANE 1-OXIDE

α -carbon will be longer than the other P-C bond (37). They based this suggestion on the ring opening reactions of this class of compounds. In fact, the P-C bond to the least substituted α -carbon is shorter than the other P-C bond. The observed result is reasonable since increased α -carbon substitution causes an increased number of steric interactions (30). As steric repulsion between groups attached to bonded atoms increases, the distance between the bonded atoms increases. Other than the P-C(4) bond distance, the bond angles and distances are not significantly different from previously reported values for phosphetane oxides (28, 29).

Corfield has proposed a trigonal-bipyramid transition state for basic hydrolysis in which the ring carbons are axial-equatorial (13). Steric hindrance apparently is responsible for the differences in reactivity of this class of compounds. The symmetrical α -disubstituted compounds would provide a great deal of hindrance to the approach of the hydroxide ion. The mono-substituted α -carbon would offer a less hindered approach for the hydroxide ion. A transition state involving a pseudo-rotation (36) must be invoked to explain the cleavage of the P-C bond to the least substituted α -carbon. This is illustrated in Figure IV.

Four-membered rings of this type are expected to be puckered. A comparison of the ring pucker in these three

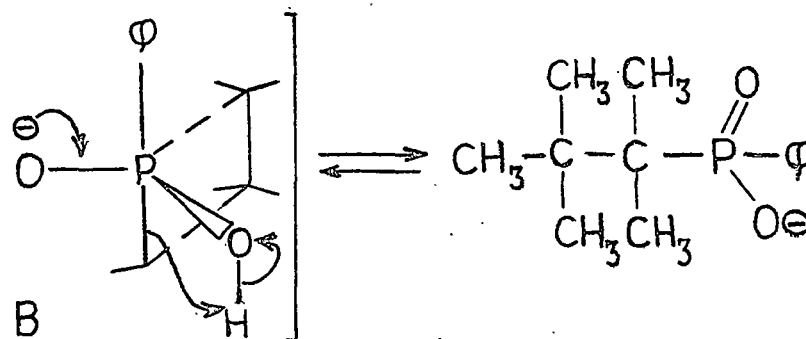
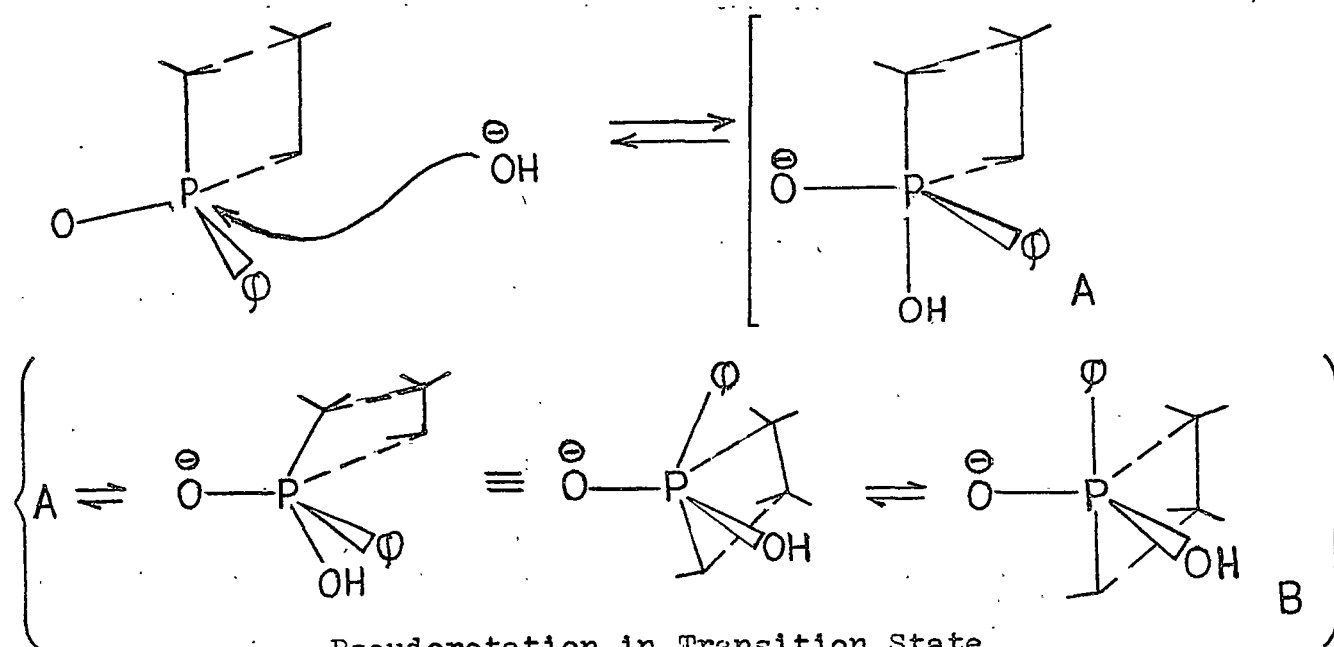


FIGURE IV

PROPOSED REACTION MECHANISM FOR ALKALINE HYDROLYSIS OF
2,2,3,3,4-PENTAMETHYL-1-PHENYLPHOSPHETANE 1-OXIDE

isomers is shown in Figure V. The angle between the planes C(2)-P-C(4) and C(2)-C(3)-C(4) is larger in this compound than in the other compounds. The phenyl group is tilted 12° away from being perpendicular to the C(2)-P-C(4) plane as is illustrated in Figure VI.

The phenyl group is planar with an average displacement from the least squares plane of 0.0034\AA . The maximum displacement from the plane is 0.0062\AA at the C(14) position. The equations for the various planes of interest are given in Table VI.

A stereographic packing diagram is shown in Figure VII. The closest intermolecular contact is $3.1(1)\text{\AA}$ and occurs between H(4) and C(6). There are no intermolecular distances that are significantly less than the sum of the van der Waal radii (38).

A σ_R plot was constructed for this structure and is shown in Figure VIII (1). The slope of the least squares line through the data points was 1.60 with an intercept of 0.01. This indicates underestimation of the standard deviations by a factor of about 1.60. Further discussion of the σ_R plot is contained in Chapter V.

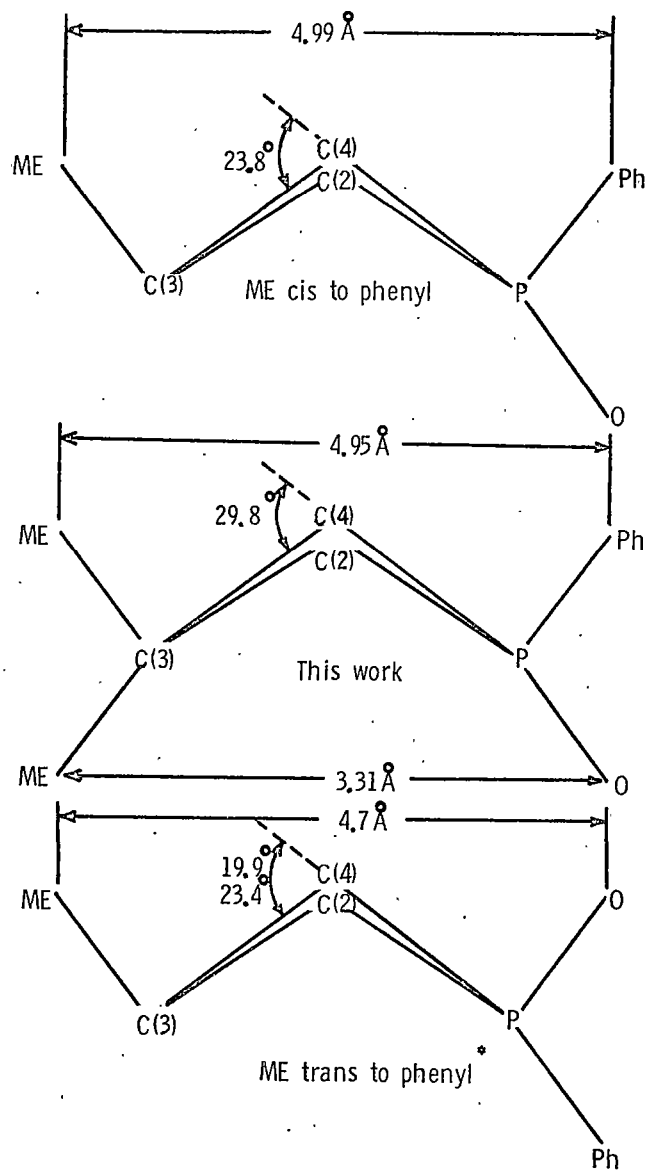


FIGURE V

COMPARISON OF RING PUCKERING IN THE THREE ISOMERIC PHOSPHETANE OXIDES

*Two molecules in the asymmetric unit.

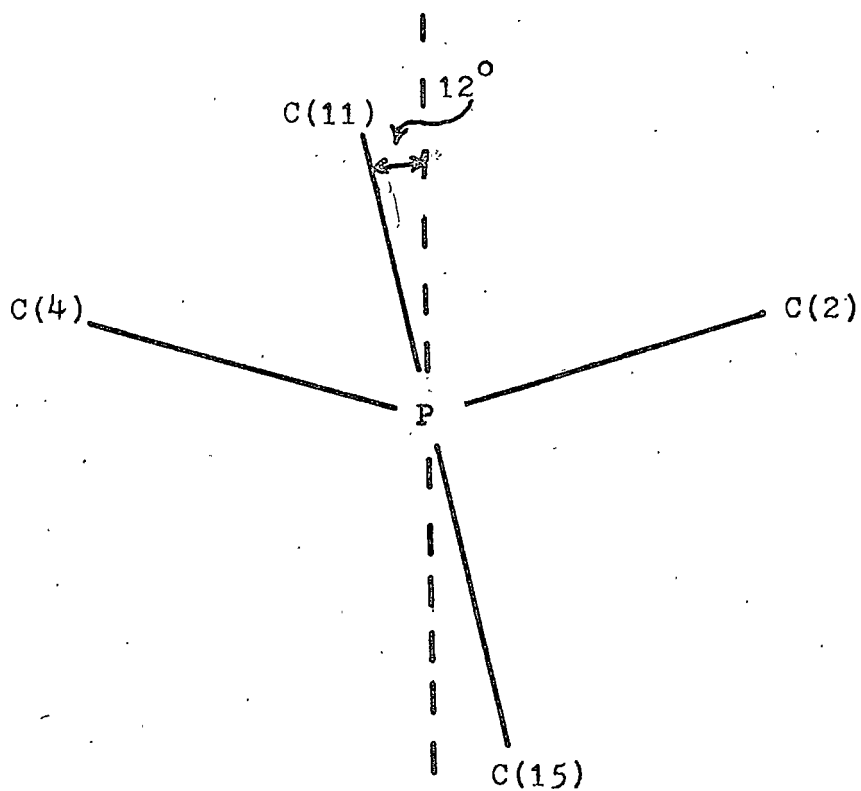


FIGURE VI

TILT OF PHENYL GROUP RELATIVE TO THE C(2)-P-C(4) PLANE

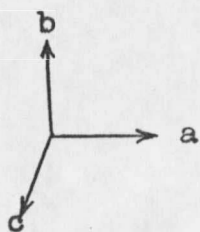
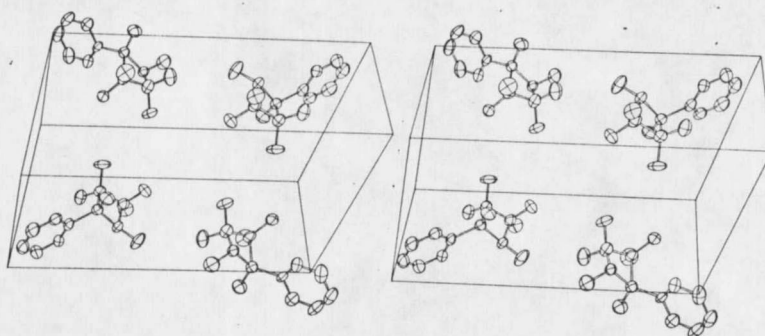
TABLE VI
 EQUATIONS OF PLANES^{a.)} REFERRED TO ORTHOGONAL AXES IN
 2,2,3,3,4-PENTAMETHYL-1-PHENYLPHOSPHETANE 1-OXIDE^{b.)}

<u>ATOMS IN PLANE</u>	<u>l</u>	<u>m</u>	<u>n</u>	<u>p</u>	<u>S(Δ^2)^{c.)}</u>
C(10), C(11), C(12), C(13), C(14), C(15)	0.520	0.843	0.138	5.461	0.00009
C(2), P, C(4)	0.770	-0.127	-0.626	3.353	————
C(2), C(3), C(4)	-0.454	-0.197	0.869	2.052	————

a.) Least squares plane: $lX + mY + nZ - p = 0.0$

b.) Coordinate system for plane is: X along a, Y in a-b plane,
z along c.

c.) $S(\Delta^2)$ is the sum of the squares of the deviations of atoms
from the planes.



Orientation of unit cell

FIGURE VII
STEREOGRAPHIC PACKING DIAGRAM FOR
2,2,3,3,4-PENTAMETHYL-1-PHENYLPHOSPHETANE 1-OXIDE

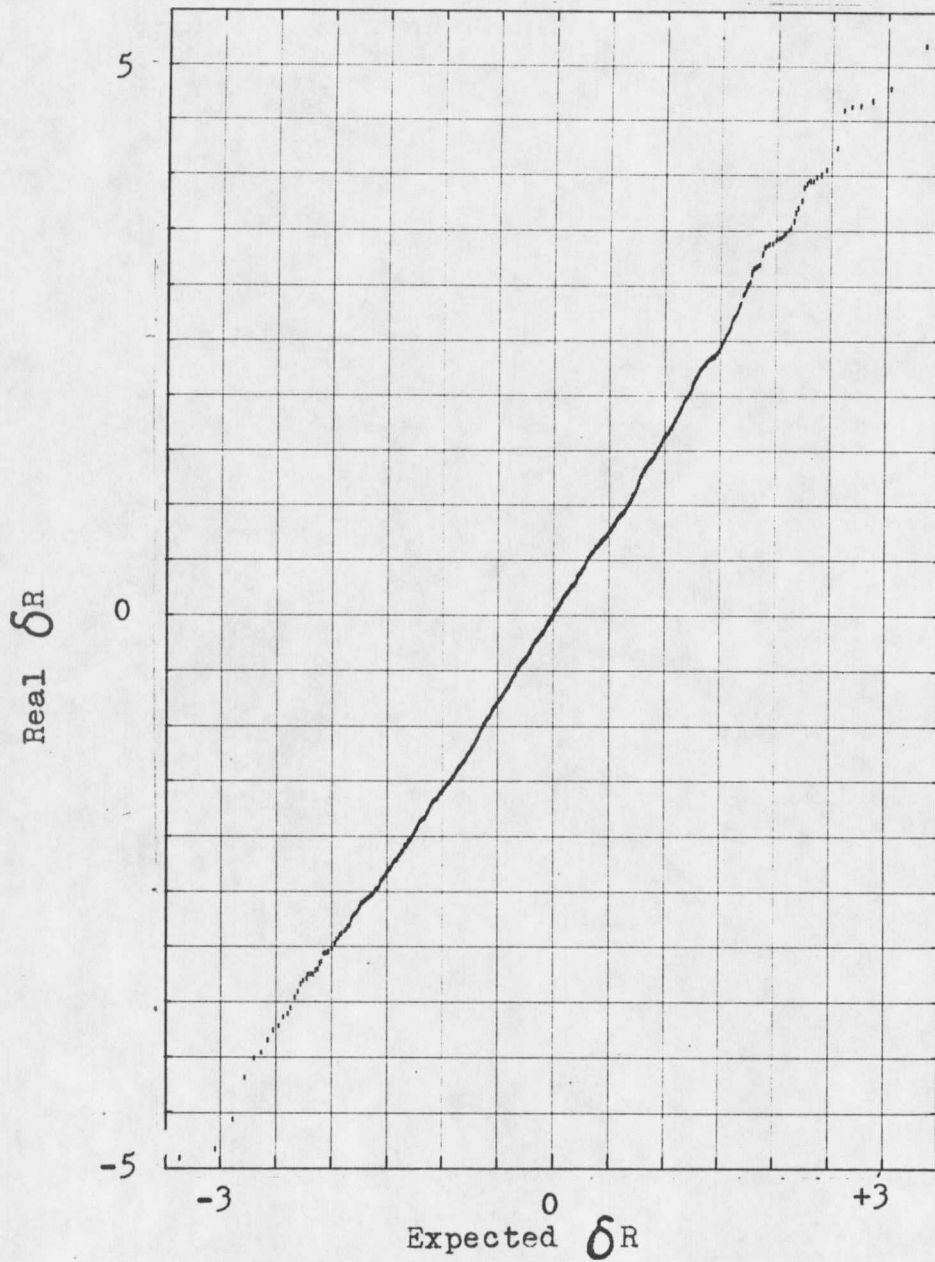


FIGURE VIII

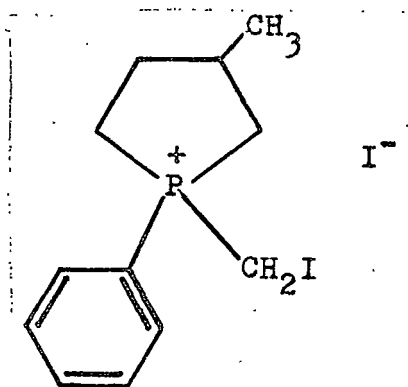
NORMAL PROBABILITY PLOT OF 1244 δ_R BASED ON F_0

CHAPTER II

THE CRYSTAL AND MOLECULAR STRUCTURE OF 1-IODOMETHYL-3-METHYL-1-PHENYLPHOSPHOLANIUM IODIDE

I. INTRODUCTION

The primary purpose for determining the three-dimensional structure of this compound was to correlate structural results with those of others in a series of phosphorus organic compounds. Dr. Kenneth L. Marsi of California State College, Long Beach, prepared the compound and supplied the crystals. It was known that the crystals were a racemic mixture of either the cis or the trans isomer of this structure:



Attempts to determine the configuration of this compound by the use of NMR spectroscopy had proved fruitless. A crystal structure analysis seemed the logical method for obtaining

the desired answers.

II. CHOICE OF A CRYSTAL

The crystal used for the X-ray analysis was chosen because of its small size and well-defined faces. It was a colorless, transparent parallelepiped of dimensions $0.486 \times 0.076 \times 0.064 \text{ mm}^3$. Since the compound could be somewhat hygroscopic, the crystal was mounted on a glass fiber and sealed in a Lindemann glass capillary tube.

III. DENSITY

The density was determined experimentally by the flotation method, using a mixture of carbon tetrachloride and bromoform that would just suspend a crystal. The experimental density, D_{exp} , is 2.12 g/cm^3 and the calculated density, D_{calc} , based on four molecules per unit cell, is 2.03 g/cm^3 .

IV. DETERMINATION OF SPACE GROUP AND UNIT CELL DIMENSIONS

A combination of Weissenberg and oscillation photographs indicated that the compound crystallized in a monoclinic space group and that the crystal was mounted along the a-axis. The precession camera was used to determine the β -angle. Initial unit cell dimensions were

chosen as $a \approx 7.7\text{\AA}$, $b \approx 15.3\text{\AA}$, $c \approx 15.7\text{\AA}$, and $\beta \approx 106.5^\circ$. Using this unit cell the following extinctions were observed.

hkl: no conditions

Ok0: $k = 2n + 1$

h0l: $l = 2n + 1$

These extinctions uniquely determine the space group as $P2_1/c$. In addition, the Weissenberg photographs exhibited a pseudo-A-centering condition which was of some value in the interpretation of the Patterson map.

V. DETERMINATION OF ACCURATE UNIT CELL DIMENSIONS

Accurate unit cell dimensions were determined from a least squares analysis of the 2θ values for eighteen independent reflections. Both $+2\theta$ and -2θ were carefully determined for each reflection and the average 2θ value for the reflection was used in the refinement. The crystal data are listed in Table VII.

VI. DATA COLLECTION

The intensities of the 1946 reflections were measured out to $\theta \approx 22.5^\circ$. The method of data collection was the same as in Chapter I. Three standard reflections (060, 121, $\bar{2}12$

TABLE VII
CRYSTAL DATA

1-Iodomethyl-3-methyl-1-phenylphosphonium Iodide

C PI H F. W. 446.051 F(000)=840

Monoclinic, space group $P2_1/c$

$$a' = 7.217(3)\text{\AA}$$

$$b = 14.261(6)\text{\AA}$$

$$c = 14.778(6)\text{\AA}$$

$$\beta = 106.54^\circ(3)$$

Volume of the unit cell = 1458\AA^3 $D_{\text{calc}} = 2.03$ grams/cc.

Molecules/unit cell = 4 $D_{\text{exp}} = 2.12$ grams/cc.

Linear absorption coefficient, $\mu(\text{MoK}\alpha) = 44.473\text{cm}^{-1}$

Crystal dimensions: 0.486mm x 0.076mm x 0.064mm

Crystal was bound by faces $\{100\}$, $\{0\bar{1}1\}$, and $\{011\}$, respectively.

reflections) were measured at about two hour intervals during the course of the data collection. A scale factor calculated from these was used to scale each block of data to the same scale as the initial data block. The average value of the scale factor over the complete data collection was 1.006 with a standard deviation of 0.026. This indicates little deterioration of the crystal or deviation of conditions over the course of the data collection. The crystal did change to a yellowish-brown color in the course of the data collection.

VII. TREATMENT OF DATA

The intensities were converted to structure factors (F_o) in the usual manner. The weights for each reflection were determined as in Chapter I with an instrument instability constant (k_2) of 0.05 (45).

VIII. STRUCTURE DETERMINATION

The structure was solved from the Patterson map and subsequent Fourier maps. The pseudo-A-centering condition indicated that if one iodine atom was located at x, y, z in the unit cell the other iodine atom was at $x, y + \frac{1}{2}, z + \frac{1}{2}$. The positions determined from the Patterson map were x, y, z and $x - 0.2, y + 0.5, z + 0.5$. Refinement of the iodine positional parameters and isotropic temperature

factors produced an R of 0.23. A Fourier map(2) revealed the positions of all the remaining heavy atoms. All atomic positions except those of the ring-methyl group were included in the full matrix refinement with isotropic temperature factors. Another Fourier map was calculated and the ring-methyl group was clearly shown to be trans to the phenyl group. The heavy atom positional parameters and isotropic temperature factors refined to an R of 0.07 using a unit weighting scheme. Further refinement of the positions and anisotropic thermal parameters using the weighting scheme of Stout and Jensen (45) produced an R of 0.047. A difference map(2) revealed the tentative positions of all the hydrogen atoms except those on the ring-methyl group. Refinement of the positional parameters of all atoms, anisotropic thermal parameters for the heavy atoms and isotropic temperature factors for the hydrogen atoms produced an R of 0.042. It was discovered at this point that the data had been used as decacounts which is roughly the same as considering the data to be observed at the 6-sigma cut-off level.

The data were converted to counts, reduced in the usual manner with 1434 of the 1904 reflections considered observed at the 3-sigma level. Hydrogen atom positions were calculated (42) but not refined at this point as they were not readily observable on a difference map. Refinement of the

heavy atom positions and anisotropic thermal parameters produced an R of 0.066.

The data were very carefully inspected at this point since certain aspects of the model that best fit the data were not reasonable. One of the carbon-carbon single bond distances calculated to be 1.403Å in this model. Some 39 reflections (2.8% of the observed data) were found to be in poor agreement with the rest of the data. The reflections removed all had $|\Delta F|/\sigma_F \geq 6.0$; all data with $|\Delta F|/\sigma_F < 6.0$ at this point were assumed to be in reasonable agreement. The data removed were classified roughly into four groups: obvious error in instrument setting, 5; irregularly shaped backgrounds, 4; high peak count due to short-term variation, 23 (all very low intensity reflections); no obvious error, 7. At the completion of the refinement 5 pieces of data were found to have $|\Delta F|/\sigma_F \geq 6.0$. These were considered to be statistically in agreement with the rest of the data set as will be discussed later in the chapter.

All hydrogen atoms were located from a difference map. Four additional cycles of full matrix refinement of positional parameters of all atoms, anisotropic thermal parameters of the heavy atoms and isotropic temperature factors of the hydrogen atoms completed the refinement. At completion, $R = 0.045$, $R'' = 0.059$, $R_{\text{obs} + \text{unobs}} = 0.085$,

and $S = 1.87$. Final shifts in heavy atom parameters were less than 10% of their standard deviations. Corresponding shifts in the hydrogen atom parameters were less than 25% of their standard deviations.

Maximum and minimum transmission coefficients were 0.77 and 0.72 respectively. When the data were corrected for absorption (35) and refined as above, no significant differences between the two refinements were found. The various indicators were: $R = 0.046$, $R'' = 0.060$, $R_{\text{obs}} + u_{\text{obs}} = 0.086$, and $S = 1.89$.

The observed and calculated structure factors are listed in Table VIII. The positional and thermal parameters for the non-hydrogen atoms are listed in Tables IX and X respectively. The positional and thermal parameters for the hydrogen atoms are listed in Table XI. The bond angles and bond distances are indicated in Figure IX.

The scattering factor curve for the iodide ion was taken from Cromer and Mann (15), the curve for hydrogen from Stewart, et al. (44), and all other curves were from the International Tables (31). The normal phosphorus curve was used since there is no reported curve for a phosphorus with a formal positive charge. Anomalous scattering corrections ($\Delta f'$ and $\Delta f''$) were assumed to be the same for both iodine and iodide ion and were taken from the International Tables (31).

TABLE IX

POSITIONAL PARAMETERS FOR THE NON-HYDROGEN ATOMS IN
1-IODOMETHYL-3-METHYL-1-PHENYLPHOSPHOLANIUM IODIDE

<u>ATOM</u>	<u>x/a</u>	<u>y/b</u>	<u>z/c</u>
I(1)	.90818(10) ^a	.88611(5)	.22996(5)
I(2)	.30387(9)	.61494(5)	.24359(4)
PA *	.3656(3)	.7580(2)	.0815(2)
C(2)	.1005(12)	.7451(7)	.0187(6)
C(3)	.0556(13)	.8258(8)	-.0483(7)
C(4)	.1750(15)	.9089(7)	-.0017(7)
C(5)	.3791(13)	.8767(6)	.0427(7)
C(6)	-.1623(16)	.8452(9)	-.0486(8)
C(7)	.3939(14)	.7515(7)	.2060(7)
C(8)	.5047(12)	.6768(6)	.0426(5)
C(9)	.4522(16)	.6515(7)	-.0516(7)
C(10)	.5658(17)	.5905(7)	-.0825(6)
C(11)	.7267(14)	.5531(7)	-.0230(8)
C(12)	.7787(14)	.5771(7)	.0691(8)
C(13)	.6677(13)	.6387(6)	.1052(7)

^aThe number in parentheses is the standard deviation and refers to the least significant digits.

TABLE X

ANISOTROPIC THERMAL PARAMETERS FOR THE NON-HYDROGEN ATOMS IN

1-IODOMETHYL-3-METHYL-1-PHENYLPHOSPHOLANIUM IODIDE

<u>ATOM</u>	<u>β_{11}</u>	<u>β_{22}</u>	<u>β_{33}</u>	<u>β_{12}</u>	<u>β_{13}</u>	<u>β_{23}</u>
I(1)	.02025(20)	.00576(5)	.00565(5)	.00011(7)	.00348(7)	-.00087(3)
I(2)	.01933(18)	.00569(5)	.00376(4)	.00044(7)	.00286(6)	.00012(3)
P	.0127(5)	.0034(1)	.0042(1)	.0004(2)	.0022(2)	.0000(1)
C(2)	.0165(23)	.0045(6)	.0047(6)	.0011(9)	.0036(9)	.0006(4)
C(3)	.0137(22)	.0057(7)	.0065(6)	.0020(10)	.0033(10)	.0011(5)
C(4)	.0193(24)	.0042(6)	.0064(7)	.0018(10)	.0049(11)	.0009(5)
C(5)	.0155(23)	.0034(5)	.0057(6)	.0000(8)	.0029(9)	-.0004(4)
C(6)	.0195(28)	.0072(7)	.0075(8)	-.0005(12)	-.0019(12)	-.0003(7)
C(7)	.0193(25)	.0046(6)	.0048(6)	-.0005(9)	.0027(9)	-.0016(5)
C(8)	.0126(20)	.0041(5)	.0030(5)	-.0014(8)	.0025(8)	.0003(4)
C(9)	.0275(29)	.0038(6)	.0048(6)	.0010(11)	.0040(11)	.0004(5)
C(10)	.0348(35)	.0056(7)	.0027(5)	.0022(12)	.0063(11)	-.0005(5)

TABLE X (CONTINUED)

ANISOTROPIC THERMAL PARAMETERS FOR THE NON-HYDROGEN ATOMS IN

1-IODOMETHYL-3-METHYL-1-PHENYLPHOSPHOLANIUM IODIDE

ATOM	β_{11}	β_{22}	β_{33}	β_{12}	β_{13}	β_{23}
C(11)	.0187(26)	.0033(6)	.0072(8)	-.0025(9)	.0042(12)	-.0017(5)
C(12)	.0148(23)	.0048(6)	.0068(7)	-.0001(10)	-.0004(10)	-.0002(6)
C(13)	.0147(23)	.0047(6)	.0050(6)	-.0006(9)	.0023(9)	-.0001(5)

(e.s.d.'s in parentheses)

The expression for the anisotropic thermal parameters is of the form:

$$\exp(-\beta_{11}h^2 - \beta_{22}k^2 - \beta_{33}l^2 - 2\beta_{12}hk - 2\beta_{13}hl - 2\beta_{23}kl)$$

TABLE XI

HYDROGEN ATOM POSITIONS AND THERMAL PARAMETERS FOR
1-IODOMETHYL-3-METHYL-1-PHENYLPHOSPHOLANIUM IODIDE

<u>ATOM</u>	<u>x/a</u>	<u>y/b</u>	<u>z/c</u>	<u>B_{iso}</u>
H(1)	.057(16) ^a	.670(9)	-.013(7)	8.(3)
H(2)	.017(13)	.736(6)	.055(6)	5.(2)
H(3)	.097(11)	.843(6)	-.091(5)	3.(2)
H(4)	.119(11)	.929(6)	.037(6)	4.(2)
H(5)	.171(14)	.970(7)	-.051(7)	6.(3)
H(6)	.440(13)	.875(6)	-.002(6)	4.(2)
H(7)	.449(8)	.907(4)	.094(4)	0.(1)
H(8)	-.234(14)	.791(7)	-.112(7)	6.(3)
H(9)	-.233(18)	.868(7)	-.032(8)	7.(3)
H(10)	-.213(15)	.893(7)	-.129(7)	8.(3)
H(11)	.510(15)	.758(6)	.234(6)	5.(2)
H(12)	.310(8)	.805(4)	.222(4)	0.(1)
H(13)	.351(11)	.678(6)	-.093(5)	4.(2)
H(14)	.536(8)	.576(4)	-.144(4)	0.(1)
H(15)	.774(12)	.502(6)	-.045(6)	5.(2)
H(16)	.874(10)	.550(5)	.114(5)	3.(2)
H(17)	.714(9)	.662(4)	.178(4)	1.(1)

^aThe number in parentheses is the standard deviation and refers to the least significant digits.

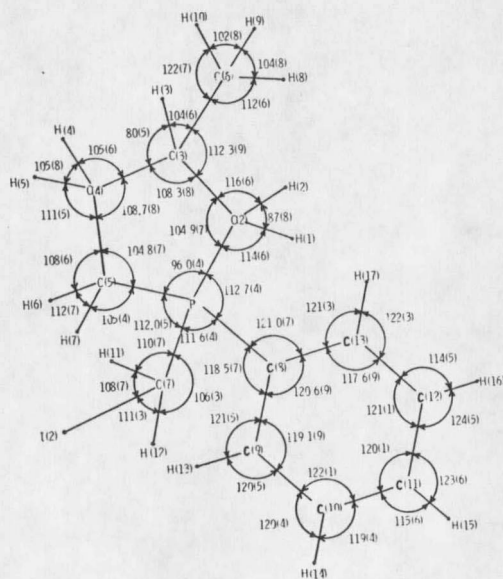
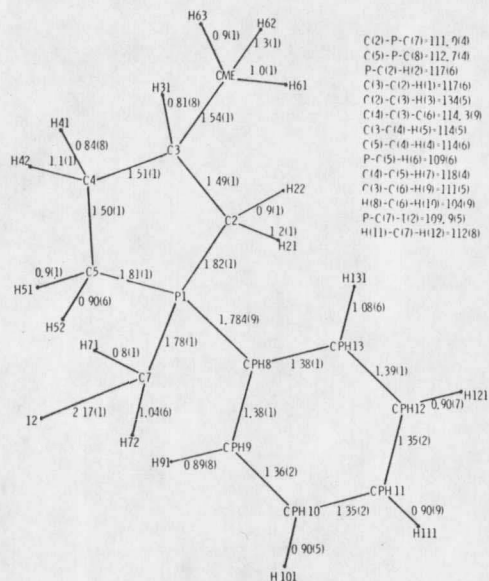


FIGURE IX

BOND DISTANCES AND ANGLES FOR
1-iodomethyl-3-methyl-1-phenylphosphonium iodide

A final difference map was calculated and was essentially flat except for areas about the iodine atom and iodide ion. Peak heights varied from $+1.30$ to $-0.51e\text{\AA}^{-3}$ about these atoms. A number of possible reasons for this behavior can be proposed: extinction problems, absorption, inaccurate model for the anisotropic thermal behavior of the atoms, and problems caused by the close approach of the iodide and iodine atoms. Determining the contribution of each of these factors plus those of any additional unknown factors is essentially impossible.

IX. DISCUSSION OF THE STRUCTURE

The molecule of 1-iodomethyl-3-methyl-1-phenylphospholanium iodide with its thermal ellipsoids (32) is shown in Figure X. Comparison of this structure to the structure of methyl phenyl phospholanium iodide (4) showed all angles and distances to be within three standard deviations of one another (based on the values found in the earlier structure determination). A planar pentagon is expected to have a total of 540° in internal angles. The sum of the angles in the phospholanium ring of methyl phenyl phospholanium iodide is 516° while the sum of the internal angles in the phospholanium ring system of the current structure is 523° . The equations for the various planes of interest are given

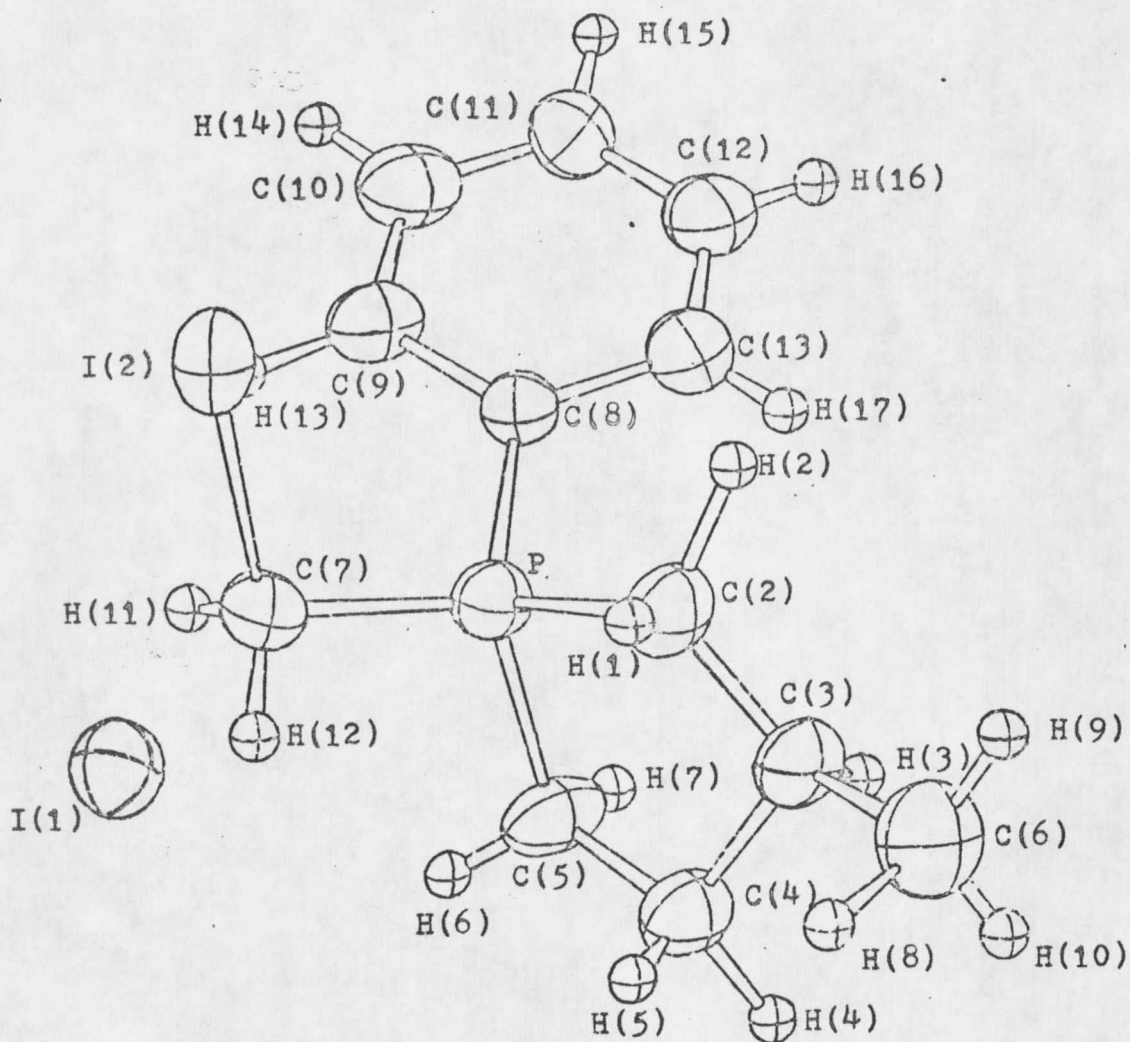


FIGURE X

MOLECULAR STRUCTURE OF 1-IODOMETHYL-3-METHYL-1-PHENYLPHOSPHONIUM IODIDE ILLUSTRATING THE THERMAL ELLIPSOIDS AT THE 50% PROBABILITY LEVEL OF THERMAL DISPLACEMENT

The hydrogen atoms were arbitrarily assigned isotropic temperature factors of 1.0 in this illustration.

in Table XII. The angle formed between the plane of the phenyl group and the C(8)-P-C(2) plane is 34° . The plane of the phenyl group forms an angle of 77° with the C(5)-C(4)-P-C(2) plane. The C(2)-C(3)-C(4) plane forms an angle of 38° with the C(5)-C(4)-P-C(2) plane in the phospholanium ring. The methyl group is trans to the phenyl group and is in an equatorial position as is predicted by calculations on methylcyclopentane (39). The phospholanium ring system would appear to be a good analogue to the methylcyclopentane system in spite of the substituents on the phosphorus atom. Due to the long P-C bonds (relative to a normal C-C bond) the interactions between the substituents on the phosphorus atom and the hydrogens on the α -carbons are negligible. As can be seen from Figure XI, the ring system appears to be in the envelope form with the methyl group equatorial at the point of the flap [C(3)]. Figure XII shows a comparison of the envelope and half-chair forms of cyclopentane (20) and the phospholanium ring system. It appears that the phospholanium ring system approximates the half-chair form. The phospholanium ring system may not be a good analogue to the methylcyclopentane system. Variations in bond angles and lengths due to the presence of the phosphorus atom may cause substantial differences between the two systems.

TABLE XII
 EQUATIONS OF PLANES^{a.)} REFERRED TO ORTHOGONAL AXES IN
 1-iodomethyl-3-methyl-1-phenylphosphonium iodide^{b.)}

<u>ATOMS IN PLANE</u>	<u>l</u>	<u>m</u>	<u>n</u>	<u>p</u>	<u>S(Δ^2)^{c.)}</u>
C(8), C(9), C(10) C(11), C(12), C(13)	0.618	0.763	-0.189	9.38	0.0002
P, C(2), C(4), C(5)	-.438	0.272	0.857	2.89	0.019
C(2), C(3), C(4)	-0.880	0.282	0.382	2.53	————
C(8), P, C(2)	0.310	0.659	-0.686	7.02	————
P, C(2), C(3), C(4), C(5)	-0.559	0.290	0.776	2.80	0.151

a.) Least squares plane: $lX + mY + nZ - p = 0.0$

b.) Coordinate system for plane is: X along a, Y in a-b plane, z along c.

c.) $S(\Delta^2)$ is the sum of the squares of the deviations of atoms from the planes.

47

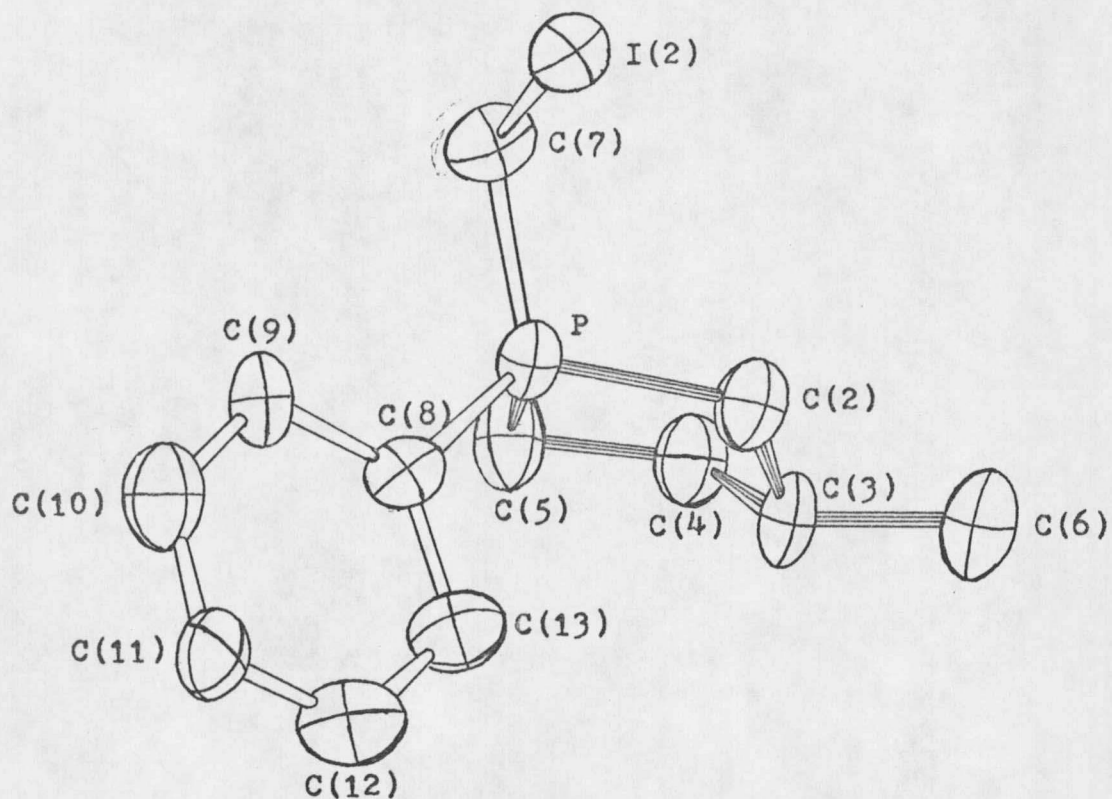
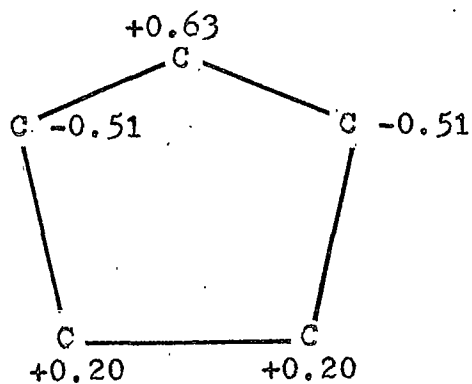
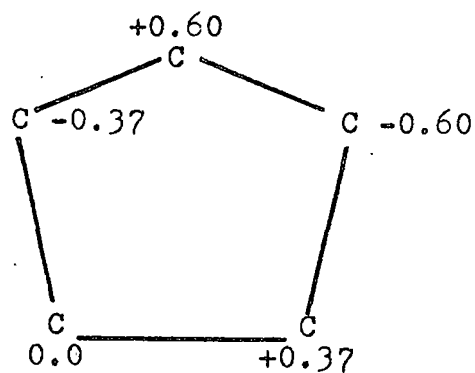


FIGURE XI

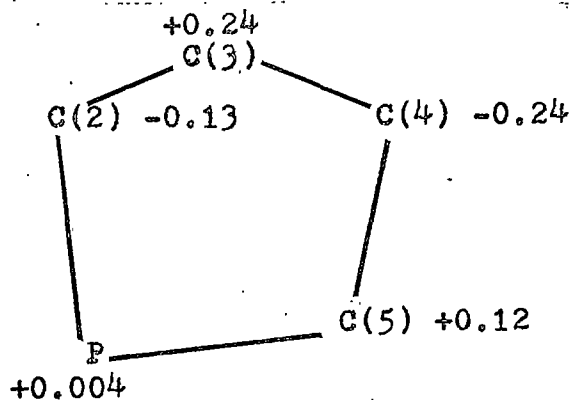
ENVELOPE FORM OF THE FIVE-MEMBERED
PHOSPHOLANIUM RING SYSTEM



CYCLOPENTANE
(Envelope Form)



CYCLOPENTANE
(Half-chair)



PHOSPHOLANIUM RING
SYSTEM

FIGURE XII

COMPARISON OF THE ENVELOPE AND HALF-CHAIR FORMS OF CYCLOPENTANE (20) AND THE PHOSPHOLANIUM RING SYSTEM. [FIGURES INDICATE DISPLACEMENT OF ATOMS, IN ANGSTROMS, ABOVE (POSITIVE) OR BELOW (NEGATIVE) THE PLANE OF THE PAPER.]

The phenyl group is planar with an average displacement from the least squares plane of $0.005\overset{\circ}{\text{Å}}$ and a maximum displacement from the plane of $0.009\overset{\circ}{\text{Å}}$ by atoms C(8) and C(13).

The packing diagram is shown in a stereographic view in Figure XIII. An iodide-iodine distance of $3.672(1)\overset{\circ}{\text{Å}}$ is observed in this structure, which is significantly less than the sum of the Van der Waal's radii of $4.3\overset{\circ}{\text{Å}}$ (38). An intermolecular distance of $3.76\overset{\circ}{\text{Å}}$ between two iodines has been observed in hexaiodobenzene (43). The polarizable nature of the iodine atom probably accounts for the unusually close approaches observed in these two structures. The conformation of the organic portion of the molecule is apparently not affected by packing considerations as there are no other intermolecular interactions that are significantly less than the sum of the van der Waal's radii.

A δR plot was constructed for this structure and is shown in Figure XIV. The slope of the least squares line through the data points was 1.7 with an intercept of -0.04, indicating underestimation of the standard deviations by a factor of about 1.7. Since data are essentially linear it is felt that the data with $|\Delta F|/\sigma_F \geq 6.0$ are in agreement with the rest of the data. Further discussion of the δR plot is contained in Chapter V.

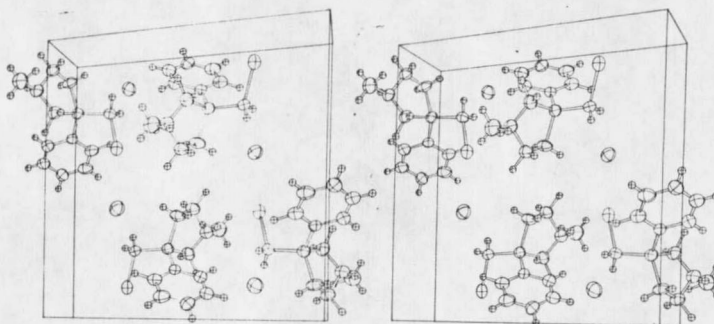
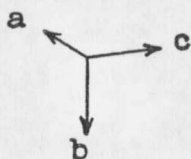


FIGURE XIII

STEREOGRAPHIC PACKING DIAGRAM FOR
1-IODOMETHYL-3-METHYL-1-PHENYLPHOSPHOLANIUM IODIDE



ORIENTATION OF UNIT CELL

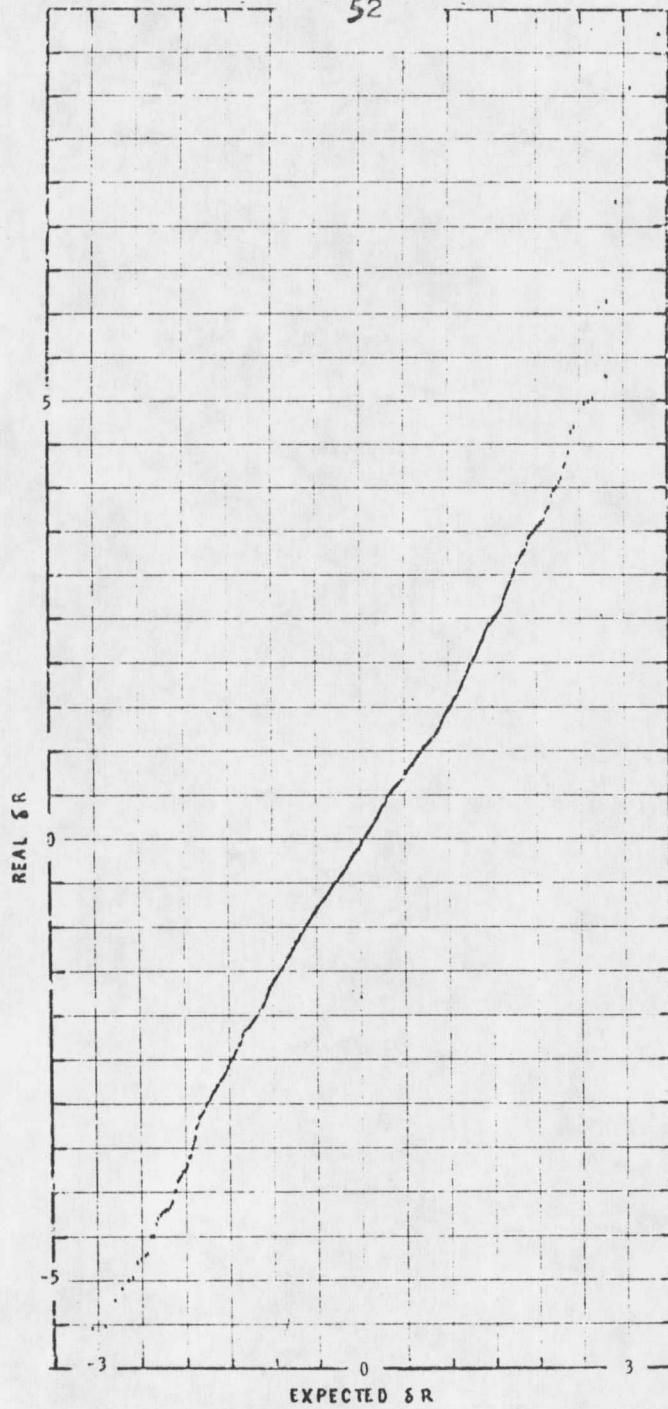


FIGURE XIV

NORMAL PROBABILITY PLOT OF 1395 δR_1 BASED ON (F_0) .

CHAPTER III

HYPOTHESIS RELATING FREE ENERGY OF HYDROLYSIS TO THE LENGTH OF THE P-O BOND BEING HYDROLYZED IN ARYL PHOSPHATES

I. INTRODUCTION

Hammett observed that:

The idea that there is some sort of relationship between the rate of a reaction and the equilibrium constant is one of the most persistently held and at the same time denied concepts in chemical theory. (25)

In this same paper, Hammett reviewed known examples of reactions that exhibited such a relationship and pointed out the quantitative form of the relationship:

$$\log k = x \log K + \log G$$

where k is the rate constant, K is the equilibrium constant, G and x are empirically determined constants. Hammett also showed (26) that the effect of a substituent in the meta or para position of the benzene ring upon the rate or the equilibrium constant may be represented by a simple formula:

$$\log X = \log X^{\circ} + \sigma\rho$$

where X° is either the rate or the equilibrium constant for the reference compound and X is either the rate or the equilibrium constant for the analogous compound with a substituent in the meta or para position. The parameter

σ defined in terms of the acid dissociation equilibrium of substituted benzoic acids in water at 25°C (30) is

$$\sigma_R \equiv \log \frac{K_A^R}{K_A^0}$$

The substituent constant, σ , is a measure of the electron-donating or electron-withdrawing power of the substituent, R. The reaction constant, ρ , is a function of the reaction and indicates how sensitive the rate or equilibrium constant is to changes in σ .

Some typical σ constants and their uncertainties are: p-amino, -0.66(0.1); p-hydroxy, -0.37(0.04); p-methoxy, -0.27(0.02); p-methyl, -0.17(0.02); p-hydrogen, 0.00, p-chloro, 0.23(0.02); p-nitro, +0.78(0.02); [+1.27(0.05) for derivatives of phenols and anilines] (26, 30).

Many reactions of meta and para substituted aromatic compounds have been found to follow the Hammett equation (26, 30). If there is a relationship between the length of the bond being hydrolyzed and the free energy of hydrolysis of phosphate esters the Hammett equation may be used to show this. The choice of the para substituted phenyl phosphates for study has two advantages:

- a. If one assumes that the phenyl phosphates follow the Hammett equation, one needs only to show a

relationship between σ and the length of the bond being hydrolyzed. σ is related to the equilibrium constant and thus to the free energy of hydrolysis. Such a relationship would prove that the free energy of hydrolysis and the length of the bond being broken in hydrolysis are related.

- b. If such a relationship exists it will be much easier to detect with aryl phosphates than with alkyl phosphates. The electronic structure of the molecule is subject to much greater perturbation with the substituted aryl phosphates than would be possible in the sugar phosphates.

II. DEVELOPMENT OF THE HYPOTHESIS

Before one can develop any sort of a hypothesis utilizing the Hammett equation, one must determine whether the hydrolysis of phosphate esters may be expected to follow the Hammett equation. Kinetic data for the reaction of substituted phenyl diethylphosphines with ethyl iodide (17), rate studies of the hydrolysis of substituted benzene-sulfonic ethyl esters (19) and acid catalyzed hydrolysis of substituted aryl sulfuric acids (7) were found by Hammett (26) to obey the Hammett equation. Relative rates of hydrolysis of three aryl monophosphate monoanion esters

have been reported by Barnard, et al. (5). A $\ln(k)$ versus σ plot of their data is shown in Figure XV. Based on these data it seems reasonable to assume that the rate and equilibrium constants for the para-substituted phenyl phosphates follow the Hammett equation.

If there is a relationship between the length of the bond being hydrolyzed and σ both the existence and the form of such a relationship must be determined empirically. A review of the literature shows what type of relationship may be expected. The structures of five benzoic acids have been reported (6, 34, 40, 41, 48). A plot of C(Ph)-C(OOH) bond distance versus σ is shown in Figure XVI. A similar plot of P-OAr) bond lengths versus σ for various di- and tri-aryl phosphate esters is shown in Figures XVII and XVIII (10, 11, 18, 27, 47, 50, 51). It is obvious from Figures XVII and XVIII that there are difficulties in drawing conclusions from these data. The standard deviations of the bond lengths are large enough that one cannot say the bond lengths are significantly different from each other. Also, there are insufficient data to show whether the mono-, di-, and tri-esters are correlated by the same relationship. Further, variations due to the ionic charge of the compound, coordination, packing, hydrogen bonding, etc., may make comparisons between other than analogous compounds of questionable value.

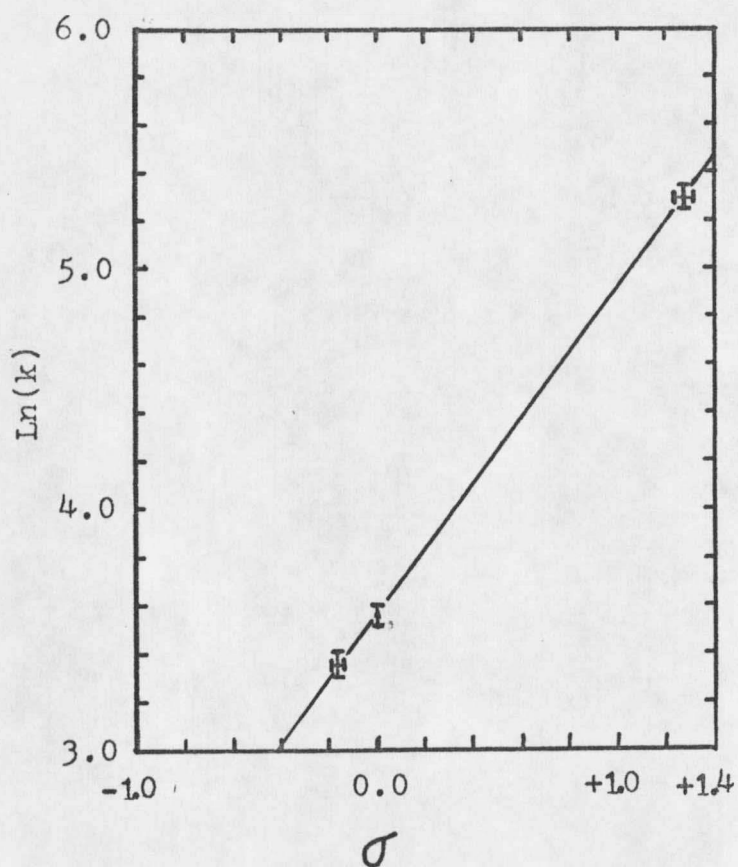


FIGURE XV

$\ln(k)$ VERSUS σ PLOT FOR THE HYDROLYSIS OF MONOARYL PHOSPHATES

Bars Indicate \pm One Standard Deviation.
 $\sigma_{\text{p-NO}_2}$ is that for Derivatives of Phenols (26).

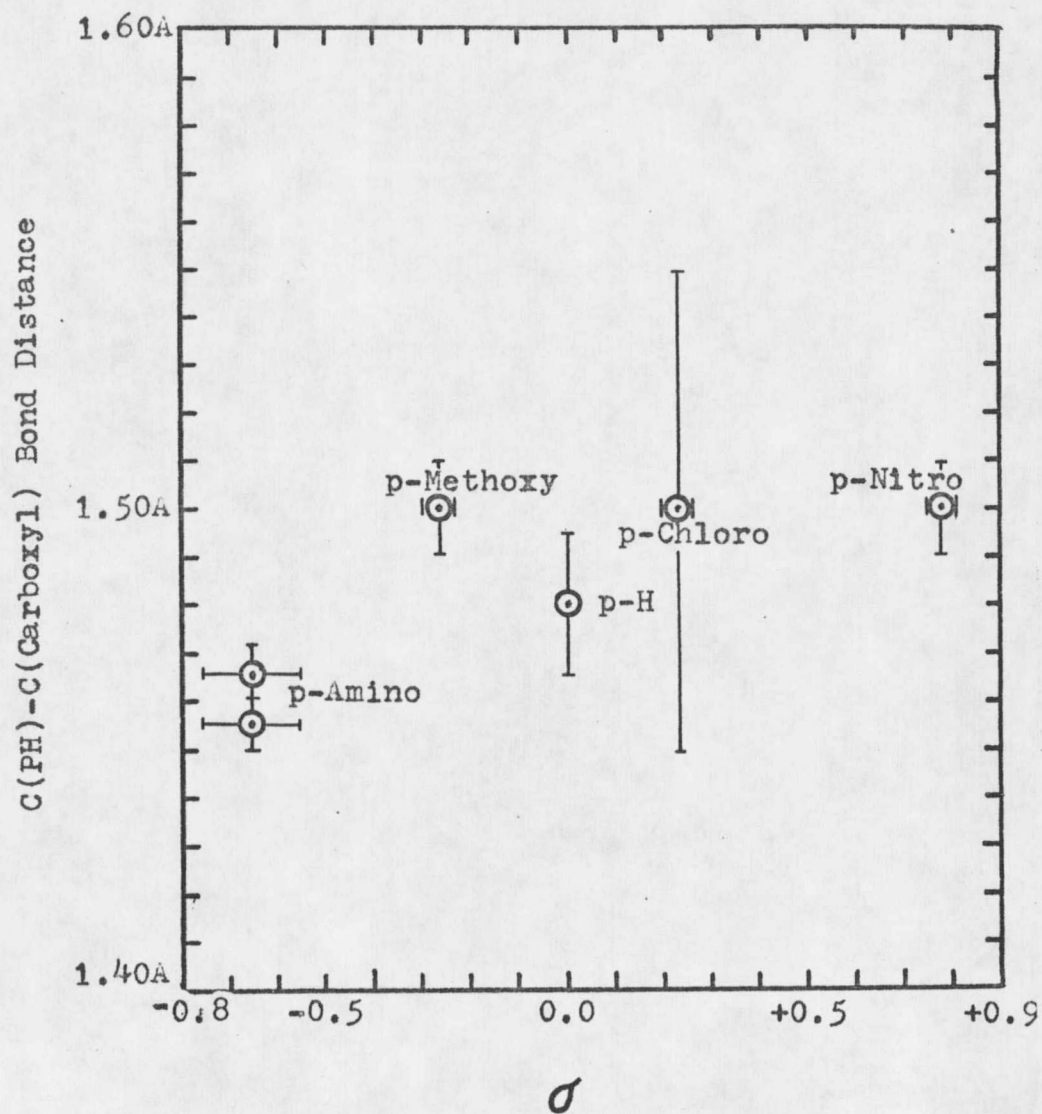


FIGURE XVI

C(Ph)-C(OOH) BOND DISTANCE VERSUS σ FOR
SUBSTITUTED BENZOIC ACIDS

Bars Indicate \pm One Standard Deviation

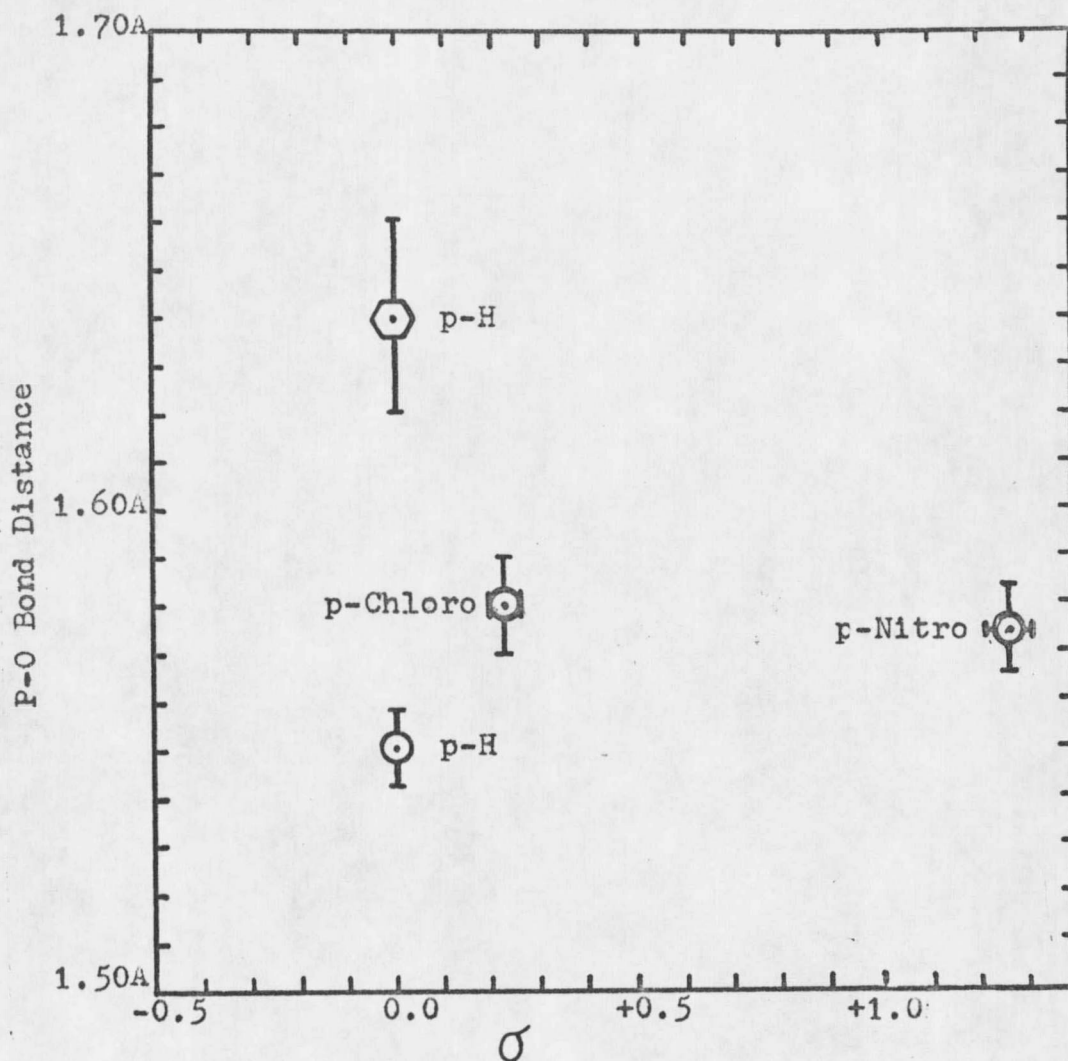


FIGURE XVII

P-O BOND DISTANCE VERSUS σ FOR SOME
MONO- AND DIARYL PHOSPHATE ESTERS

⬡ = Monoester dianion form.

○ = Diester protonated form (average value).

(Bars indicate \pm one standard deviation.)

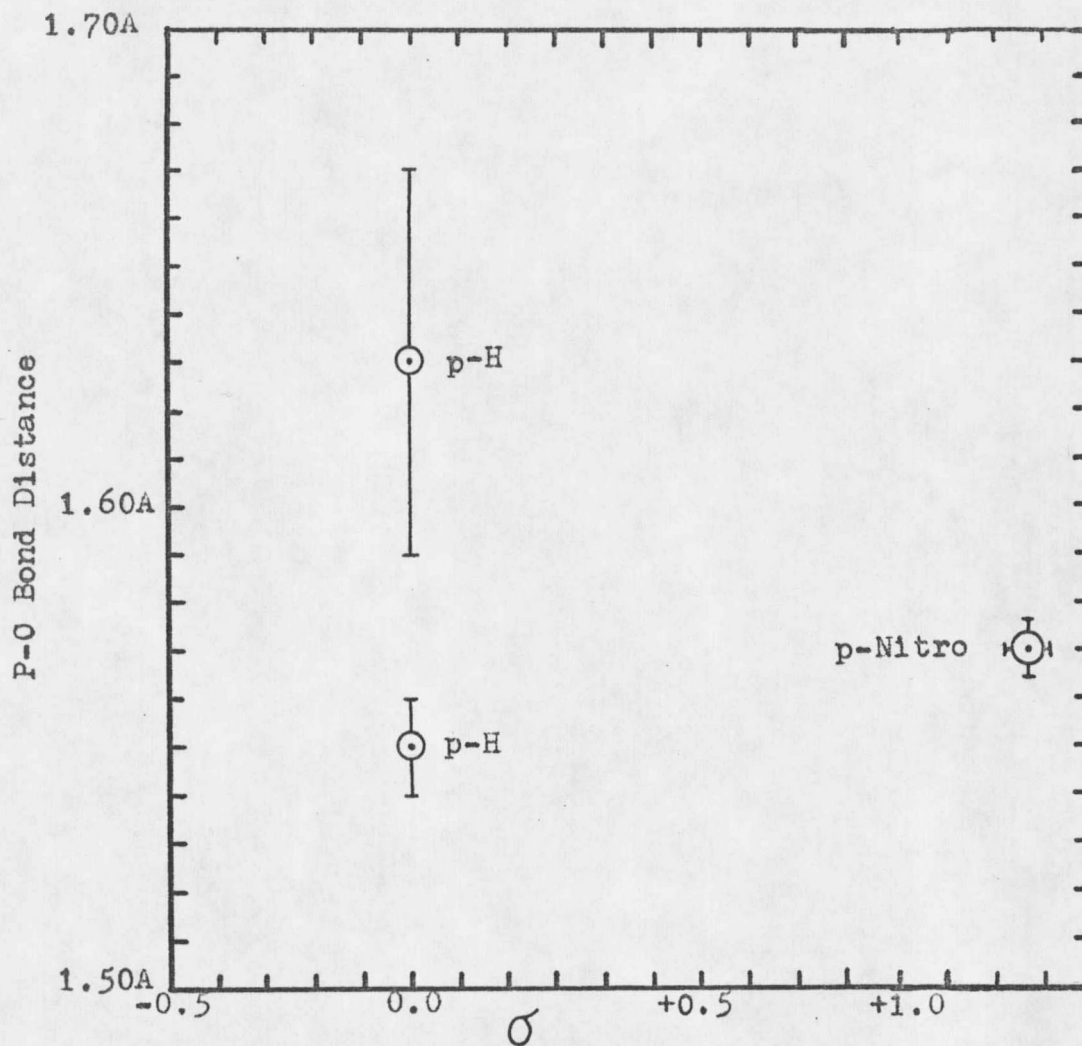


FIGURE XVIII

P-O BOND DISTANCE VERSUS σ FOR SOME
TRIARYL PHOSPHATE ESTERS

Triesters (Average Values)

(Bars indicate \pm one standard deviation.)

III. PROPOSED HYPOTHESIS

The hypothesis to be tested (at least initially) is:

$$\text{Length [P-O(ArR)]} = k\sigma_R$$

where

$$\log\left(\frac{K_R}{K_O}\right) = \rho\sigma_R$$

thus

$$\text{Length [P-O(ArR)]} = \frac{k}{\rho} \log \frac{K_R}{K_O}$$

where k is an empirically determined constant.

IV. PROPOSED TESTS OF THE HYPOTHESIS

It is proposed that the molecular structures of the sodium salts of several para-substituted phenyl phosphate mono-esters be determined. These compounds will probably pack in a similar manner in the crystalline state and, since they are sodium salts, not have undue differences caused by hydrogen bonding.

To justify the hypothesis simple Hückel molecular orbital (HMO) calculations have been carried out for several benzoic acids, phenols, and mono-aryl phosphate esters (see Chapter IV). Calculations such as these are admittedly only qualitative, but they have been very useful to the organic

chemist in suggesting trends.

CHAPTER IV

HÜCKEL MOLECULAR ORBITAL CALCULATIONS

I. INTRODUCTION

The Hückel molecular orbital (HMO) method utilizes several assumptions. First it is assumed that wave functions, Ψ , may be factored sets of non-interacting Φ . For unsaturated molecules $\Psi = \Phi_{\sigma} \Phi_{\pi}$. HMO calculations are concerned primarily with Φ_{π} which is approximated as a product of molecular orbitals, Ψ_j . Each of the Ψ_j are then assumed to be a linear combination of π -type atomic orbitals ($2p_z$ -orbitals in unsaturated hydrocarbons)

$$\Psi_j = c_{j1} \phi_1 + c_{j2} \phi_2 + \dots + c_{jn} \phi_n$$

or

$$\Psi_j = \sum_{r=1}^n c_{jr} \phi_r$$

where

- Ψ_j = the j th molecular orbital
- ϕ_r = the atomic orbital for the r th atom
- c_{jr} = the coefficient of the r th atomic orbital in the j th molecular orbital

The variation principle states

$$\epsilon = \frac{\int \psi H \psi d\tau}{\int \psi^2 d\tau} \approx E_0$$

The ψ is an approximate wave function and E_0 is the actual ground state energy.

Introduction of the symbols

$$H_{rs} = \int \phi_r H \phi_s d\tau$$

$$S_{rs} = \int \phi_r \phi_s d\tau$$

and minimizing ϵ with respect to each of the coefficients, c_t , yields

$$\sum_r c_r (H_{rt} - \epsilon S_{rt}) = 0$$

Since the minimization was carried out with respect to each coefficient there will be n equations of this type.

To solve the equations some further approximations are made. For planar hydrocarbons the Coulomb integrals, H_{rr} , are all assumed to be equal and are replaced by the symbol α . H_{rs} , the bond integrals, are all assumed to be equal to β for atoms r and s which are bonded or zero if r and s are not bonded. The overlap integrals, S_{rs} ,

are taken as zero for $r \neq s$ and one for $r=s$. The set of simultaneous equations can have a nontrivial solution only if the corresponding secular determinant vanishes:

$$\begin{vmatrix} \alpha - \epsilon & \beta_{12} & \beta_{13} & \cdots & \beta_{1n} \\ \beta_{21} & \alpha - \epsilon & \beta_{23} & \cdots & \beta_{2n} \\ \dots & \dots & \dots & \dots & \dots \\ \beta_{n1} & \beta_{n2} & \beta_{n3} & \cdots & \alpha - \epsilon \end{vmatrix} = 0$$

The determinant may be expanded to a polynomial equation which has n real roots of the form

$$\epsilon = \alpha + m_j \beta$$

A more complete analysis of the HMO method is contained in Streitwieser (46).

The values for α_x and β_x , where x denotes a heteroatom are given in terms of the carbon parameters α_0 and β_0 by

$$\alpha_x = \alpha_0 + h_x \beta_0$$

$$\beta_{cx} = k_{cx} \beta_0$$

and the various h_x and k_{cx} were obtained from Streitwieser (46) or as described later in this chapter.

II. PROCEDURE FOR CARRYING OUT THE HMO CALCULATIONS

The program used for the calculations was one developed by Professors P. R. Callis, A. C. Craig, and R. A. Howald of the Montana State University Chemistry Department (9). No overlap was assumed in these calculations. The values of h_x and k_{yx} where $x =$ phosphorus were assumed the same as those given for sulfur (46). Table XIII contains the various values for h_x and k_{yx} that were used in these calculations. The calculations on the phenyl phosphates were carried out using three separate sets of assumptions:

1. The phosphorus atom was assumed to have five 3d orbitals available for π -bonding with the 2p orbitals of the oxygen. The 3d orbitals were assumed to have equal probability of π -bonding with the 2p orbitals. No angular dependence of the p-orbitals with respect to the d-orbitals was considered. The non-ester oxygens were assumed to have one 2p orbital available for overlap. The ester oxygen was assumed to have one 2p orbital with two electrons in it involved in the π -system. The phosphate group was considered to be the dianion in all cases.

TABLE XIII

VALUES FOR h_x AND k_{yx} USED IN HMO CALCULATIONS

Atom Type	h_x	k_{yx}
CARBON		$k_{CC} = 1.0^{\text{a.)}}$
NITROGEN	$h_N = 1.5$	$k_{C-N} = 0.8$ $k_{N-O} = 0.7$
OXYGEN	$h_{\ddot{O}} = 2.0$ $h_{\dot{O}} = 1.0$	$k_{C-O} = 0.8$ $k_{C=O} = 1.0$
PHOSPHORUS	$h_P = 0.0$	$k_{P-P} = 1.0^{\text{b.)}}$ $k_{P-O} = 0.9$ $k_{P-Oester} = 0.8$

a.) For an "aromatic" bond of about 1.40 \AA .

b.) For orbitals P_1, P_2, \dots, P_5 which are on the same atom.

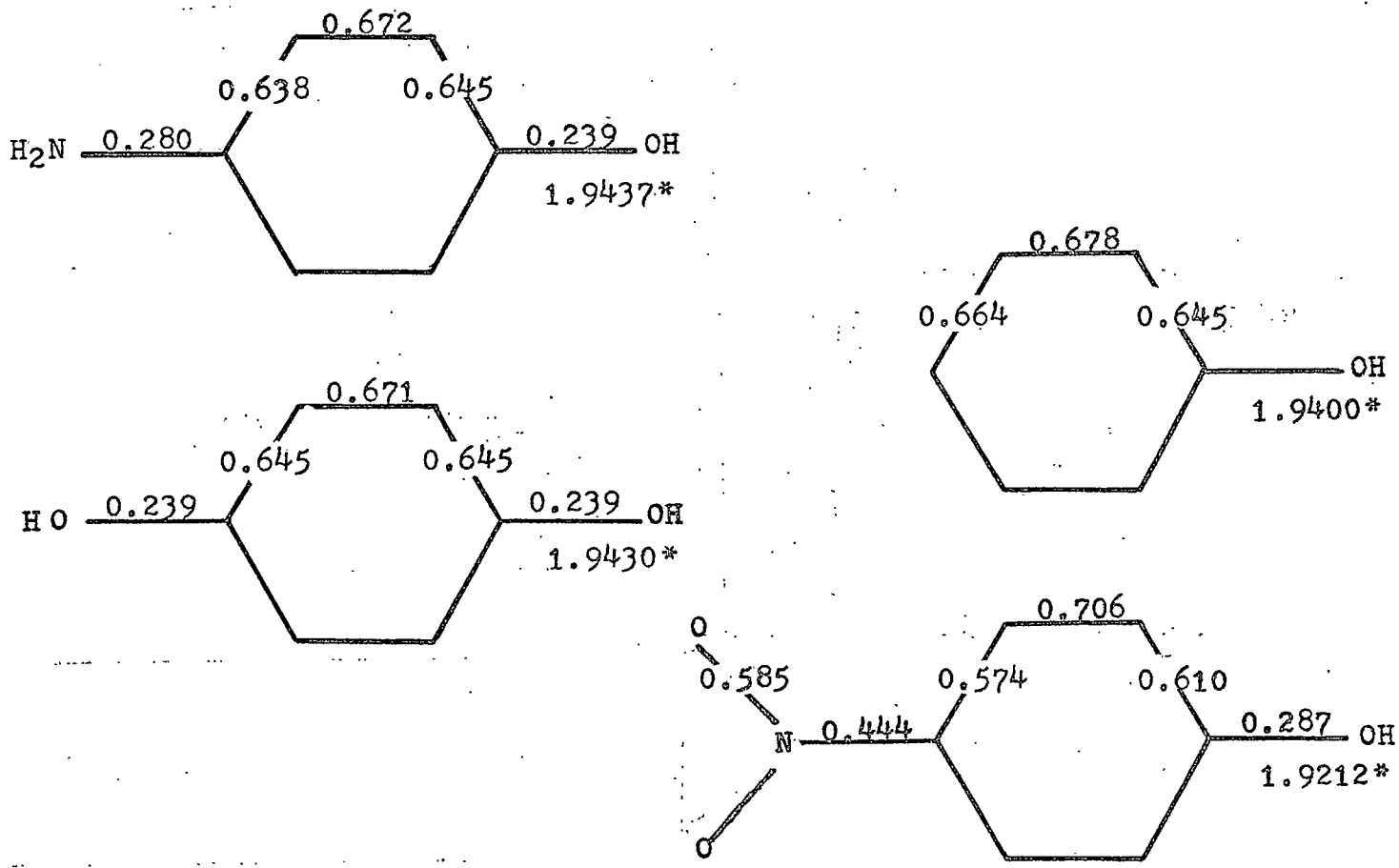
2. The phosphorus atom was assumed to have one empty 3d orbital available for overlap with the ester oxygen. The non-ester oxygens were ignored.
3. The same assumptions were made as in part 1. except each non-ester oxygen was assumed to have two 2p orbitals involved in the π -d system.

Similar calculations were carried out for both para-substituted phenols and benzoic acids.

III. RESULTS OF HMO CALCULATIONS

Substituted Phenols. Figure XIX indicates the π -bond order, p , for all bonds which have some π -character in the four phenols. The electron density on the phenolic oxygen is also shown. A plot of electron density on the phenolic oxygen versus σ is shown in Figure XX. The bond orders are in agreement with what should be predicted by studying resonance structures. The C-O bond in p-nitrophenol is expected to be shorter than the C-O bond in p-aminophenol.

Substituted Benzoic Acids. Figure XXI indicates the π -bond order, p , for all bonds which have some π -character in the four benzoic acids. The electron density on the acid oxygen is also shown. A plot of electron density on the acid oxygen versus σ is shown in Figure XXII. Although the



69

FIGURE XIX

HMO BOND ORDERS AND ELECTRON DENSITY ON THE PHENOLIC OXYGEN FOR p-SUBSTITUTED PHENOLS

*Calculated value of the electron density on the phenolic oxygen.

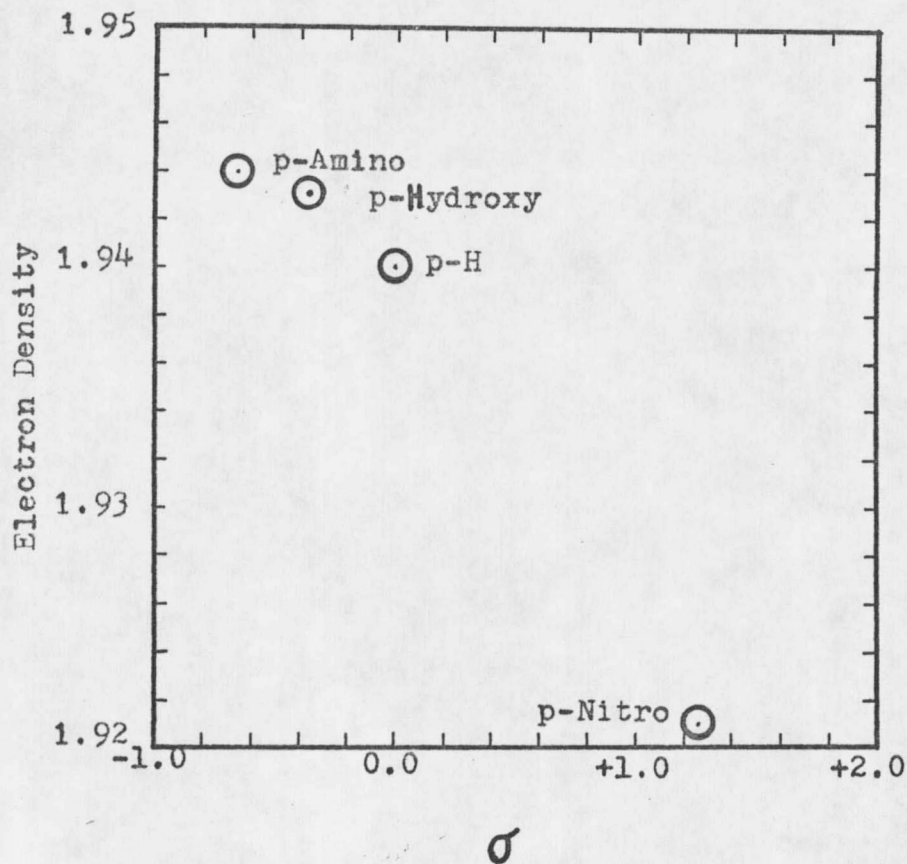
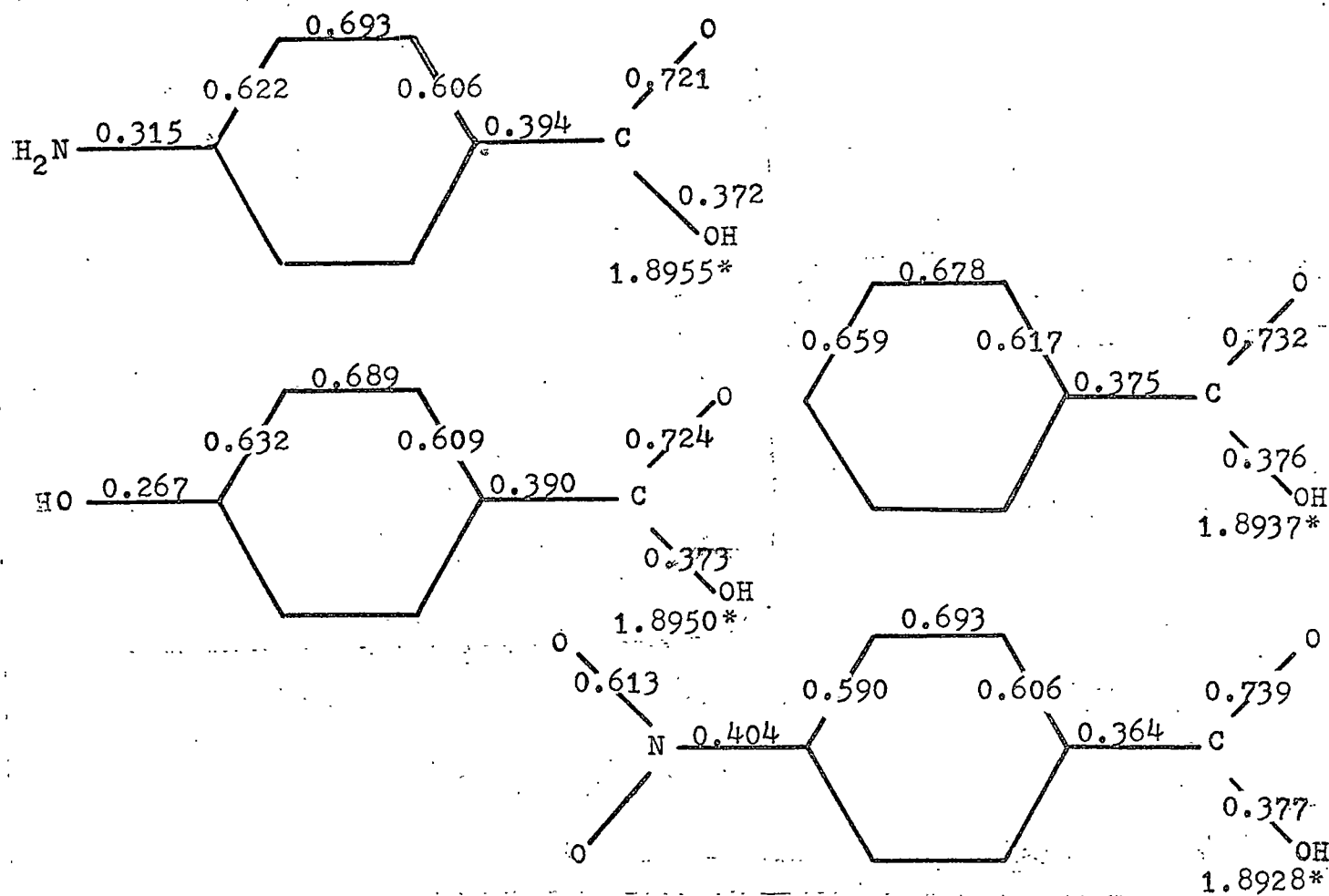


FIGURE XX

ELECTRON DENSITY ON THE
PHENOLIC HYDROXYL OXYGEN ATOM VERSUS σ

- a.) The σ -constant for the p-nitro group used here is the one for phenols and anilines (26).
- b.) The circles do not indicate standard deviations.



71

FIGURE XXI

HMO BOND ORDERS AND ELECTRON DENSITY ON ACID OXYGEN BENZOIC ACIDS

*Calculated value of the electron density on the acid oxygen.

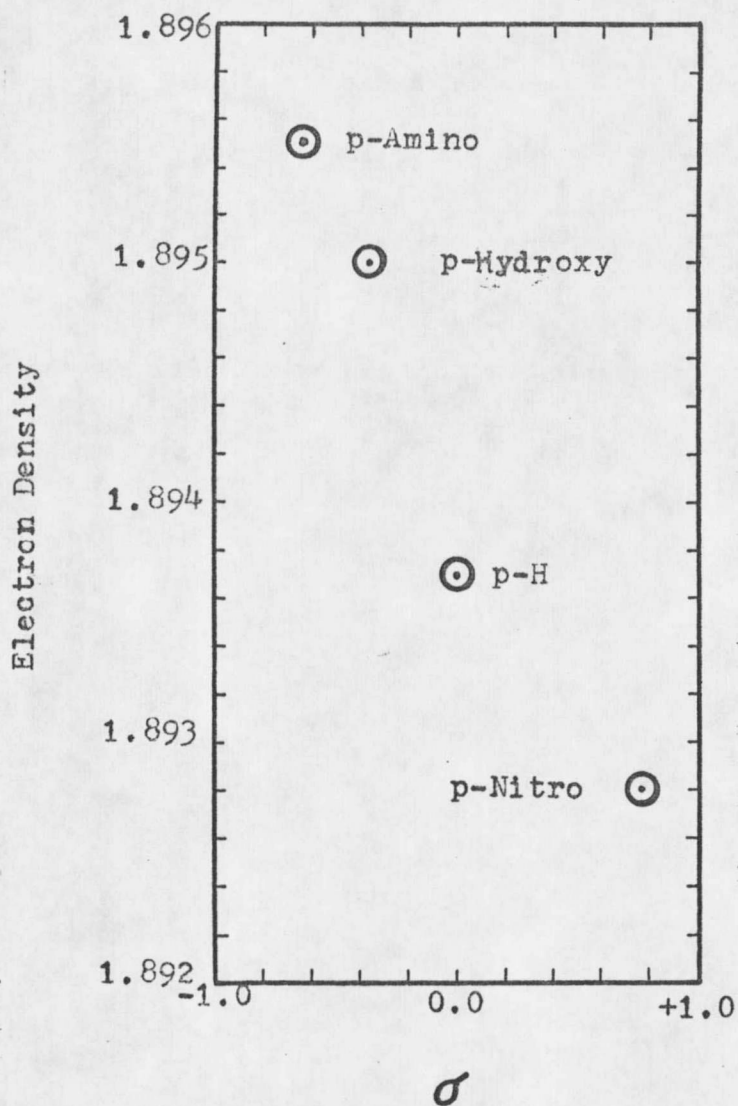


FIGURE XXII

ELECTRON DENSITY ON THE CARBOXYL OH OXYGEN ATOM OF
SUBSTITUTED BENZOIC ACIDS VERSUS σ

Circles do not indicate standard deviations.

variation in electron density is not as great as with the phenols, the plot is nearly linear.

Para-substituted Monophenyl Phosphates.

1.) Figure XXIII shows the π -bond order, p , for all bonds which have some π -character in the four phenyl phosphate dianions. The calculated electron density on the ester oxygen is also shown. A plot of electron density on the ester oxygen versus σ is shown in Figure XXIV. A plot of p for the P-O(ester) bond versus σ is shown in Figure XXV.

2.) Figure XXVI shows the π -bond order, p , for all bonds which have some π -character in the four phenyl phosphate dianions. The calculated electron density on the ester oxygen is also shown.

3.) Figure XXVII shows the π -bond order, p , for all bonds which have some π -character in the four phenyl phosphate dianions. The calculated electron density on the ester oxygen is also shown.

IV. CONCLUSIONS BASED ON HMO CALCULATIONS

The electron density on the phenolic oxygen is of some interest. Typically chemists have generalized that

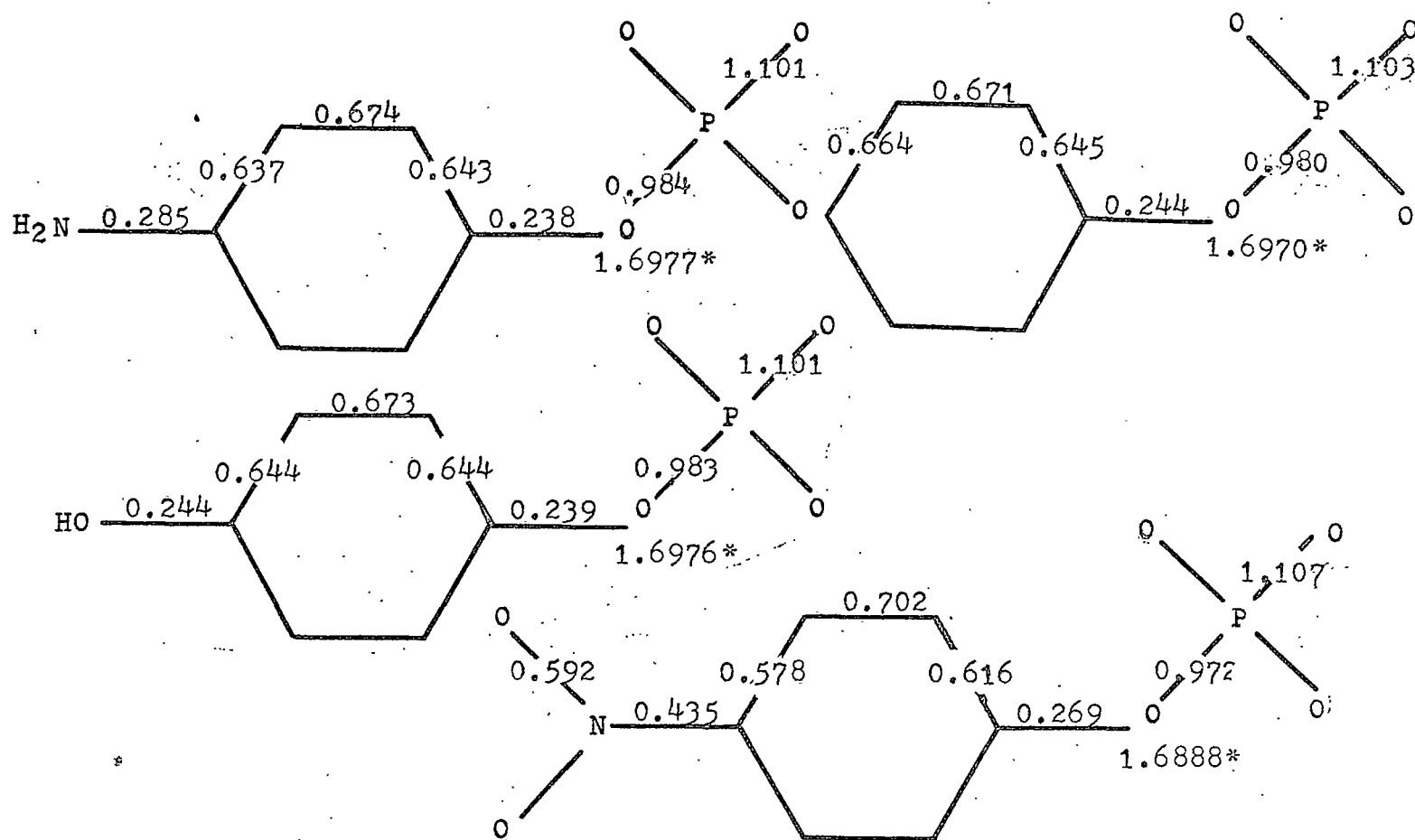


FIGURE XXIII

HMO BOND ORDERS AND ELECTRON DENSITY ON ESTER OXYGEN - FIRST HMO APPROXIMATION FOR PARA-SUBSTITUTED PHENYL PHOSPHATES

*Calculated value of the electron density on the ester oxygen.

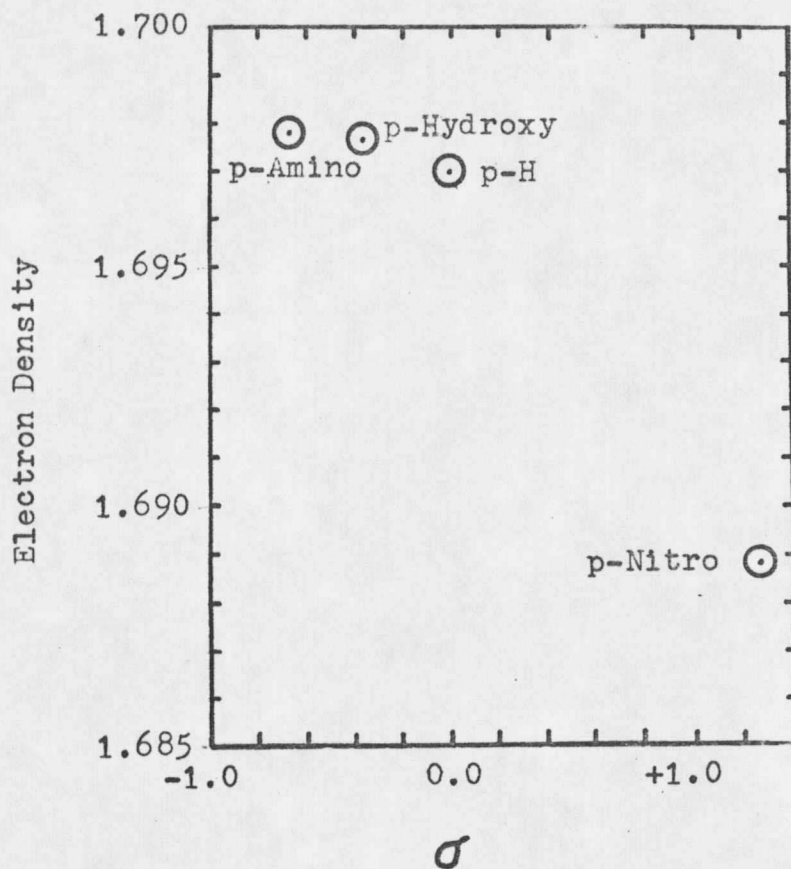


FIGURE XXIV

HMO FIRST SET OF ASSUMPTIONS.
ELECTRON DENSITY ON ESTER OXYGEN ATOM OF
SUBSTITUTED PHENYL PHOSPHATES VERSUS σ

(Circles are for clarity only.)

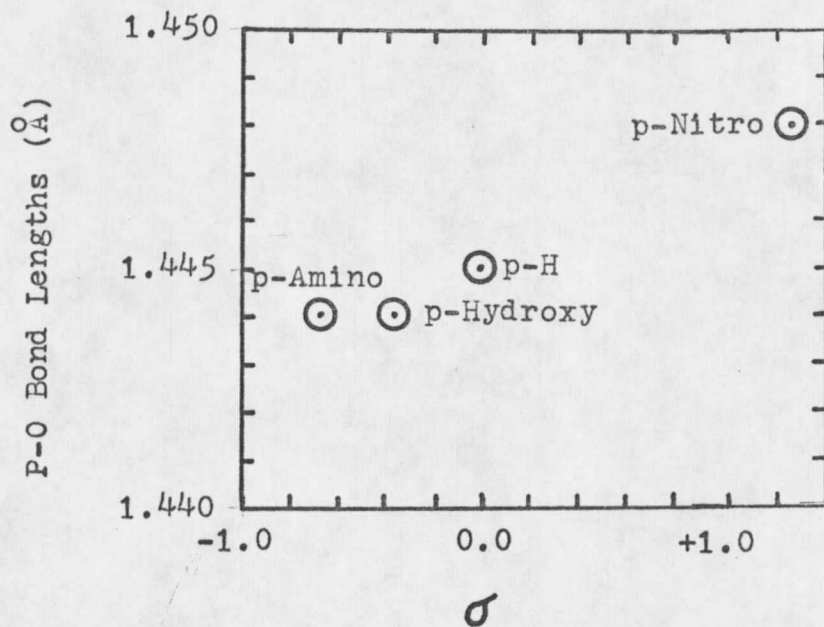
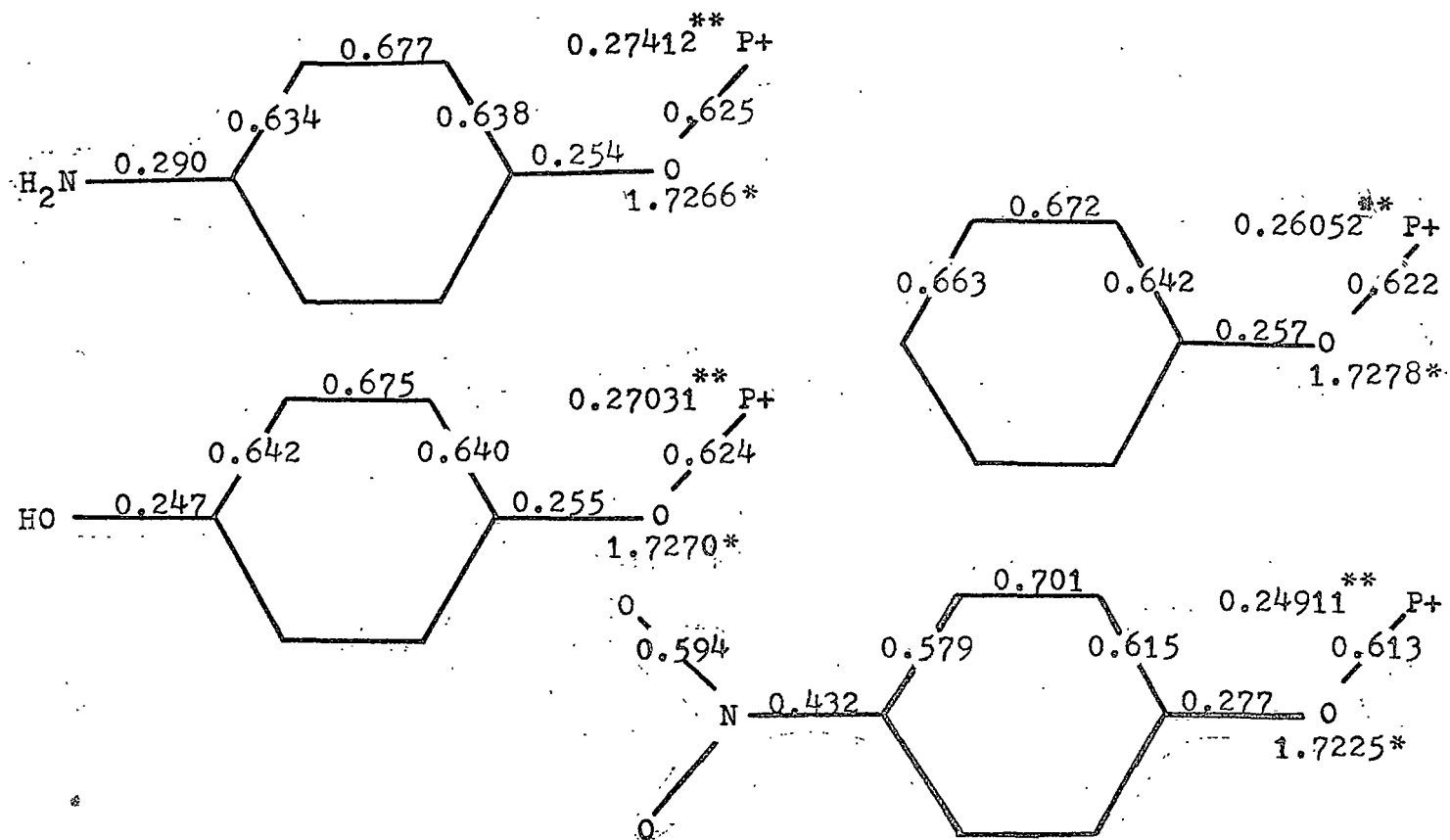


FIGURE XXV

BOND ORDER, ρ , FOR P-O(ESTER) BOND IN PHENYL PHOSPHATES
VERSUS σ

Circles do not indicate standard deviations.



77

FIGURE XXVI

HMO BOND ORDERS AND ELECTRON DENSITY ON ESTER OXYGEN - SECOND HMO APPROXIMATION
 FOR PARA-SUBSTITUTED PHENYL PHOSPHATES

*Calculated value of the electron density on the ester oxygen.

**Calculated value of the electron density on the P+ atom.

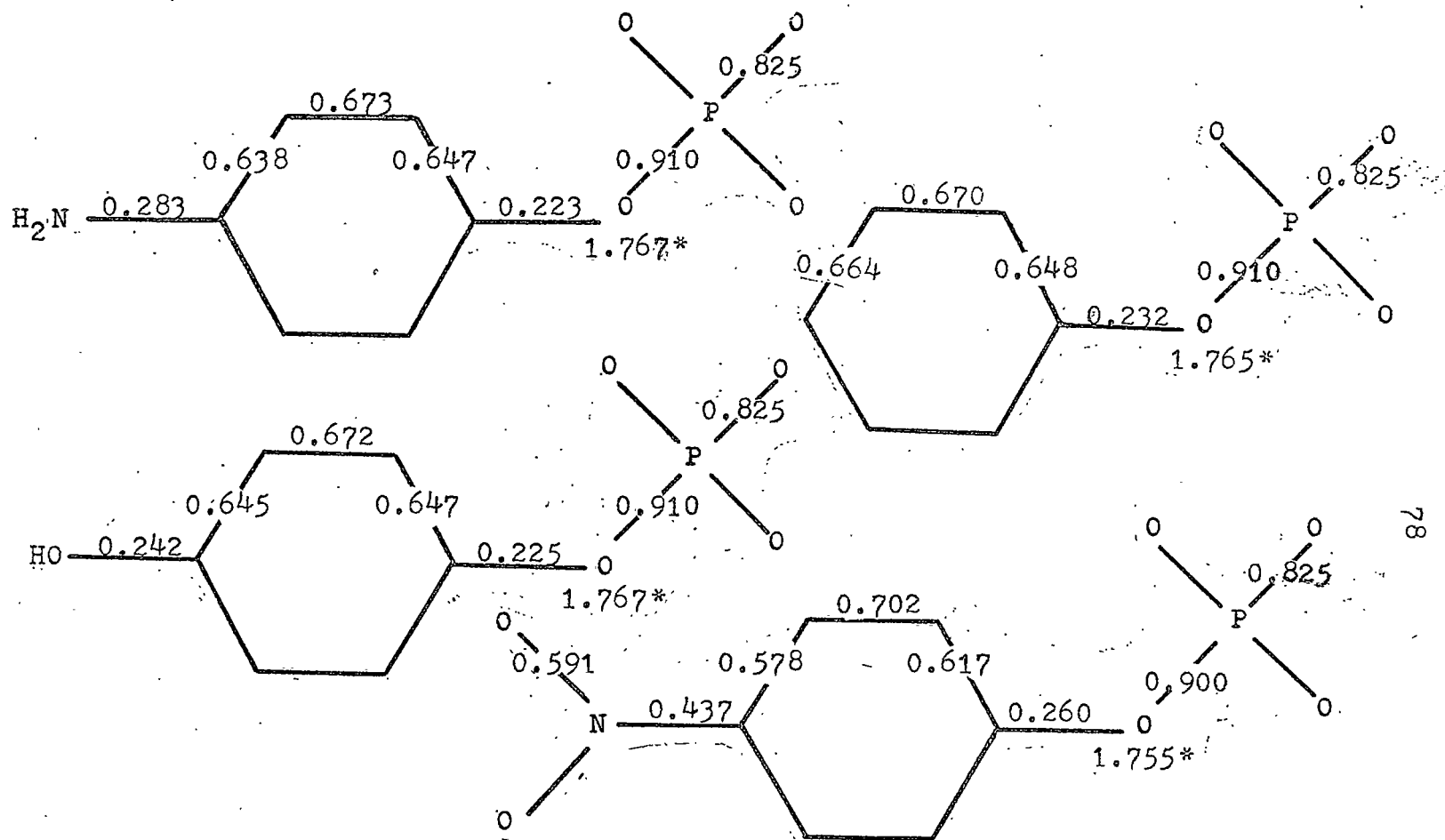


FIGURE XXVII

HMO BOND ORDERS AND ELECTRON DENSITY ON ESTER OXYGEN - THIRD HMO APPROXMIATION FOR PARA-SUBSTITUTED PHENYL PHOSPHATES

*Calculated value of the electron density on the ester oxygen.

the more electron density on a particular atom the stronger it acted as a base. Apparently little or nothing has been done to be more quantitative about this statement. If the variation in electron density is assumed to be linear when plotted against σ the implication is that electron density is proportional to $\log K_a$.

$$\text{e.d. (electron density)} = k \sigma_R$$

and

$$\log \left(\frac{K_R}{K_O} \right) = \rho \sigma_R$$

thus

$$\log \left(\frac{K_R}{K_O} \right) = \left(\frac{\rho}{k} \right) (\text{e.d.})$$

As can be seen from Figures XXIII, XXVI, and XXVII, the variation in π -bond order, p , in all three sets of assumptions is consistent with the hypothesis given in Chapter III. Likewise, the electron density on the ester oxygen varies in a manner that is reasonably consistent with the hypothesis. It has been proposed that the electron withdrawing ability of the p-nitrophenyl group reduces π -bonding in the phosphate group. This presumably makes the d-orbitals of the phosphorus more readily available for

bonding to a fifth oxygen in the activated complex (49). The kinetic data of Barnard, et al. (5), these calculations, the presumed mechanism of hydrolysis (49), and the hypothesis presented in Chapter III appear to be reasonably consistent.

One now needs to know if the calculated bond orders predict large enough differences in bond lengths to be observed. Coulson (14) has derived an equation which relates bond order to bond length:

$$x = s - \frac{s - d}{1 + k \left(\frac{1-p}{p} \right)}$$

where

s = the "natural" single-bond distance

d = the double bond distance

k = a parameter

p = the π -bond order

Let $s = 1.71\text{\AA}$ (16), $d = 1.44\text{\AA}$ (11), $k = 1.00$, and the values for p are those from Figure XXIII. Figure XXVIII shows a plot of calculated bond lengths versus σ for the first set of phenyl phosphate calculations (A). It is known that the Coulson equation underestimates bond lengths when calculated from bond orders (46). The variation indicated is expected to be a minimum. It appears that

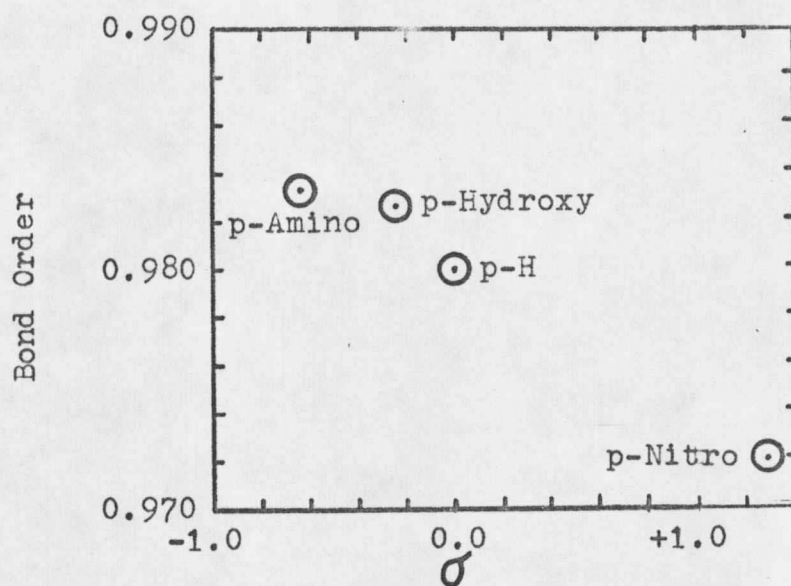


FIGURE XXVIII

CALCULATED (14) P-O(ESTER) BOND LENGTHS VERSUS σ
FOR PHENYL PHOSPHATES

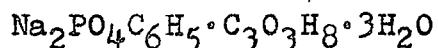
Approximation A

Circles do not indicate standard deviations.

three or four structures with very good data should be sufficient to test the hypothesis.

CHAPTER V

THE CRYSTAL AND MOLECULAR STRUCTURE OF DISODIUM PHENYL PHOSPHATE·2-METHOXYETHANOL·TRIHYDRATE



I. INTRODUCTION

The structure of the potassium salt of phenyl phosphate has previously been determined (11). Unfortunately, the estimated standard deviations of the bond lengths were too large to be of value as a test of the hypothesis proposed in Chapter III. The structure of the sodium salt of phenyl phosphate is presented here. This is the initial structure determination in the testing of the hypothesis.

II. PREPARATION

The crystal was one taken from a bottle of 99+% pure sodium phenyl phosphate purchased from MCB Chemical Company in October of 1962.

The crystal used for the crystal structure analysis was a nearly colorless, transparent, well-shaped parallelepiped of dimensions 0.07 x 0.25 x 0.45mm³.

III. CHOICE AND MOUNTING OF A CRYSTAL

Well-formed crystals from the reagent bottle observed

under a microscope show significant instability. In a time span of twenty minutes or less at room temperature and typical humidity conditions for Bozeman, the crystals decomposed to an opaque microcrystalline powder. The following procedure was used for mounting the crystal. The crystal chosen was placed in a Lindemann capillary tube, tapped gently into place with a fine glass rod and placed in a dessicator that contained an equilibrium mixture of solid compound in water. The crystal in the capillary was allowed to equilibrate for about four hours in the dessicator before the capillary tube was sealed. In the case of the present crystal the elapsed time between opening of the bottle and placing the capillary in the dessicator was less than five minutes. Initial work with the crystal indicated that it was very stable towards X-rays.

IV. DETERMINATION OF TENTATIVE CELL DIMENSIONS

Weissenberg and rotation photographs of the X-ray diffraction pattern of the crystal indicated the space group was monoclinic and that a glide plane was present perpendicular to the axis of rotation. The cell dimensions as determined from the photographs were $a \cong 14.7 \text{ \AA}$, $b \cong 8.0 \text{ \AA}$, $c \cong 13.5 \text{ \AA}$, and $\beta \cong 107^\circ$. The crystal was mounted with the b, b^* axis coinci-

dent with the spindle axis.

V. DETERMINATION OF SPACE GROUP AND ACCURATE CELL DIMENSIONS

The crystal was transferred to the General Electric XRD-5 Diffractometer and carefully aligned by centering on the 040 reflection at a $\lambda=90.00^\circ$ setting on the instrument. Systematic extinctions were

$$0k0: k = 2n + 1$$

$$h0l: l = 2n + 1$$

$$hkl: \text{none}$$

which unequivocally defined the space group as $P2_1/c$.

Precise measurements of $+2\theta$ and -2θ were made for 14 independent reflections. Cell dimensions were then refined by least squares analysis of the average 2θ value using a standard program from the Montana State University Crystallography Library. The crystal data are listed in Table XIV.

VI. DETERMINATION OF THE DENSITY

The experimental density of the compound was determined by flotation using a mixture of carbon tetrachloride and methanol which just suspended some of the compound taken directly from the reagent bottle. The observed density,

TABLE XIV
CRYSTAL DATA

Sodium phenyl phosphate·2-methoxyethanol·trihydrate

$C_9PO_9Na_2H_{19}$

F.W. 348.19

F(000) = 728

Monoclinic, space group $P2_1/c$

$$a = 14.69(2)\text{\AA}$$

$$b = 7.960(6)\text{\AA}$$

$$c = 13.68(1)\text{\AA}$$

$$\beta = 107.3(2)^\circ$$

Volume of the unit cell = 1526\AA^3

$D_{\text{calc}} = 1.52$ grams/cc.

Molecules/unit cell = 4

$D_{\text{exp}} = 1.52$ grams/cc.

Linear absorption coefficient, $\mu(\text{MoK}\alpha) = 2.86\text{cm}^{-1}$

Crystal dimensions: 0.07mm x 0.25mm x 0.45mm

D_{exp} was 1.52 grams/cc, and the calculated density, D_{calc} , assuming four molecules per unit cell, was 1.52 grams/cc.

VII. DATA COLLECTION

The intensities of 1424 unique reflections were measured out to $\Theta = 20^\circ$. The method of data collection was the same as in Chapter I. Three standard reflections, (500, $\bar{2}21$, 060 reflections) were collected approximately every three hours during the course of the data collection. A scale factor calculated from these was used to place each block of data on the same scale as the initial data block. The average value of the scale factor for all data blocks was 0.98 with a standard deviation of 0.03. This indicates little deterioration of the crystal or deviation of conditions over the course of the data collection.

VIII. TREATMENT OF DATA

The intensities were converted to structure factors (F_0) in the usual manner. The weights for each reflection were calculated assuming Poisson counting statistics and an instrument instability constant (k_2) of 0.05 as in Chapter I (45). Of the 1424 pieces of data collected 990 were considered observed at the three sigma level.

IX. STRUCTURE DETERMINATION

Preliminary examination of the Patterson map indicated it could be difficult (though not impossible) to interpret so the symbolic addition procedure for centrosymmetric structures was used (3). The structure factors were normalized and Σ_2 relations were calculated for those reflections with E's greater than 2.0. Of the 84 such reflections signs were determined for 50 of them when the reflections $\bar{7}34$, $\bar{1}25$, and $\bar{1}023$ were chosen to define the origin and given a positive sign. Using these 50 signed reflections as input the Σ_2 relationship was used to generate signs for as many additional reflections as possible down to an E value of 1.3. The 148 signed reflections were used for the calculation of an E-map (2) from which the positions of the phosphorus atom, the four oxygens bound to it and the first carbon of the phenyl group were determined. A structure factor calculation gave an R-index of 0.49. Several additional Fourier maps were required to reveal the positions of the remaining heavy atoms in the asymmetric unit.

X. REFINEMENT

Initially, all atoms other than those in the phenyl phosphate group were assumed to be oxygens. Two of these atoms gave large positive peaks on a difference map and the compound was thus shown to be the disodium salt. The presumed disodium phenyl phosphate octahydrate was refined with a unit weighting scheme to an R of 0.10. Positional and isotropic temperature factors were refined. Refinement then was carried out varying positional parameters and anisotropic thermal parameters. Use of the weighting scheme of Stout and Jensen (45) in this refinement produced an R of 0.09. Interatomic distances and thermal parameters of the water molecules were carefully inspected. It appeared that four of the oxygen atoms which were assumed to be water molecules were actually a molecule of ethylene glycol. One of the remaining oxygen atoms thought to be another water molecule appeared to act strangely due to incomplete occupation. Refinement of this model produced an R-index of 0.085. All of the hydrogen atoms attached to the various carbon atoms were located from a difference map and the model refined to an R-index of 0.068. The data were carefully inspected at this point and 21 (2.1% of the observed data) reflections

with $|\Delta F|/\sigma_F \geq 5.0$ were removed. Further refinement produced an R-index of 0.061.

When refined, the occupation factor of the incompletely occupied water site acted as though the atom was really a carbon rather than an oxygen. The NMR spectrum of the crystalline material was compared with that of a mixture of sodium phenyl phosphate (purchased from Sigma) and ethylene glycol and found to be similar with the exception of one large singlet peak.

Another difference map was calculated and particular attention was paid to the water molecule for which the occupation factor had been refined. At this point it was very apparent that there were three hydrogen atoms bound to this atom. Furthermore a symmetry related position was much too close to one of the oxygen atoms of the ethylene glycol to be a non-bonded oxygen atom. It appeared that, in fact, the ethylene glycol molecule was in reality a molecule of 2-methoxyethanol. All of the hydrogen atoms attached to the main oxygen atoms were located from this map.

Additional NMR spectra of a mixture of disodium phenyl phosphate and 2-methoxyethanol (methylcellusolve) were essentially identical in peak number, type, and placement to that observed for the crystalline material.

This model refined to an R of 0.056, an R'' of 0.065, $R_{\text{obs}} + \text{unobs}$ of 0.128, and an S of 1.89. The refinement was stopped when the shifts in the parameters of the heavy atoms were less than 10% of their standard deviations and the corresponding hydrogen atom parameter shift to standard deviation ratio were 0.4 or less. The observed and calculated structure factors are shown in Table XV. The positional parameters for the non-hydrogen atoms are shown in Table XVI and their respective anisotropic thermal parameters are shown in Table XVII. The hydrogen atom positional parameters and isotropic thermal factors are shown in Table XVIII. No absorption or extinction corrections were made. The linear absorption coefficient of this compound for $\text{MoK}\alpha$ radiation ($\lambda = 0.71069\text{\AA}$) was calculated to be 2.86cm^{-1} . The transmission factors for X-rays passing through the crystal between $\Theta = 0^\circ$ and $\Theta = 20^\circ$ were both calculated to be 0.96 (31). The crystal was assumed to be a cylinder of average radius 0.08mm and μR of 0.023. The data were not corrected for absorption. Scattering factor curves for the non-hydrogen atoms were taken from the International Table (31). Anomalous scattering corrections ($\Delta f'$ and $\Delta f''$) were used for both phosphorus and the sodium ions (31). The hydrogen atom scattering factor curve was that of Stewart,

TABLE XV

OBSERVED AND CALCULATED STRUCTURE FACTORS

1	2	3	4	5	6	7	8	9	10	11	12	13	14	15	16	17	18	19	20	21	22	23	24	25	26	27	28	29	30	31	32	33	34	35	36	37	38	39	40	41	42	43	44	45	46	47	48	49	50	51	52	53	54	55	56	57	58	59	60	61	62	63	64	65	66	67	68	69	70	71	72	73	74	75	76	77	78	79	80	81	82	83	84	85	86	87	88	89	90	91	92	93	94	95	96	97	98	99	100
---	---	---	---	---	---	---	---	---	----	----	----	----	----	----	----	----	----	----	----	----	----	----	----	----	----	----	----	----	----	----	----	----	----	----	----	----	----	----	----	----	----	----	----	----	----	----	----	----	----	----	----	----	----	----	----	----	----	----	----	----	----	----	----	----	----	----	----	----	----	----	----	----	----	----	----	----	----	----	----	----	----	----	----	----	----	----	----	----	----	----	----	----	----	----	----	----	----	----	-----

92

TABLE XVI

POSITIONAL PARAMETERS FOR THE NON-HYDROGEN ATOMS IN

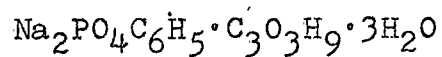
$$\text{Na}_2\text{PO}_4\text{C}_6\text{H}_5\cdot\text{C}_3\text{O}_3\text{H}_9\cdot 3\text{H}_2\text{O}$$

ATOM	<u>z/a</u>	<u>y/b</u>	<u>z/c</u>
P	.1504(1) ^a	.2352(2)	.0897(1)
O(1)	.2565(3)	.3060(5)	.1527(3)
O(2)	.1562(3)	.1762(5)	-.0125(3)
O(3)	.0880(3)	.3863(5)	.0856(3)
O(4)	.1304(3)	.0953(5)	.1549(3)
C(1)	.3397(5)	.2279(8)	.1505(5)
C(2)	.3737(5)	.2568(10)	.0661(6)
C(3)	.4571(7)	.1802(12)	.0672(7)
C(4)	.5104(6)	.0913(11)	.1499(9)
C(5)	.4777(6)	.0703(12)	.2317(7)
C(6)	.3921(6)	.1386(10)	.2310(6)
NA(1)	.0839(2)	.6208(3)	-.0298(2)
NA(2)	.0947(2)	.5676(3)	.2250(2)
O(5)	.2325(3)	.4384(6)	.3362(3)
O(6)	.0714(3)	.0956(6)	.3383(3)
O(7)	.0652(3)	.6108(6)	.3880(3)

^aThe number in parentheses is the standard deviation and refers to the least significant digits.

TABLE XVI (CONTINUED)

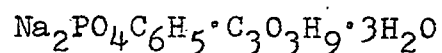
POSITIONAL PARAMETERS FOR THE NON-HYDROGEN ATOMS IN



<u>ATOM</u>	<u>z/a</u>	<u>y/b</u>	<u>z/c</u>
C(7)	.2859(5)	-.3519(10)	-.0948(5)
O(8)	.1619(3)	-.2330(5)	.1369(3)
O(9)	.2501(3)	-.3593(6)	-.0090(3)
C(8)	.2616(5)	-.2586(9)	.1571(5)
C(9)	.2942(5)	-.2350(9)	.0630(5)

TABLE XVII

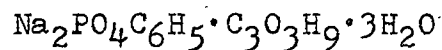
ANISOTROPIC THERMAL PARAMETERS FOR THE NON-HYDROGEN ATOMS IN



ATOM	β_{11}	β_{22}	β_{33}	β_{12}	β_{13}	β_{23}
P	•0024(1)	•0067(3)	•0022(1)	•0000(2)	•0003(1)	•0006(2)
O(1)	•0029(3)	•0079(9)	•0028(3)	•0010(4)	•0003(2)	•0019(4)
O(2)	•0033(3)	•0099(9)	•0022(3)	•0011(4)	•0006(2)	•0011(4)
O(3)	•0034(3)	•0059(9)	•0027(3)	•0006(4)	•0007(2)	•0002(4)
O(4)	•0034(3)	•0058(8)	•0031(3)	•0001(4)	•0011(2)	•0001(4)
C(1)	•0025(4)	•0051(13)	•0053(6)	•0008(7)	•0009(4)	•0003(8)
C(2)	•0037(5)	•0173(17)	•0059(6)	•0007(9)	•0024(4)	•0032(9)
C(3)	•0050(6)	•0199(20)	•0096(8)	•0033(10)	•0031(6)	•0057(11)
C(4)	•0027(5)	•0141(19)	•0145(11)	•0028(9)	•0000(7)	•0011(13)
C(5)	•0026(6)	•0195(20)	•0083(8)	•0015(9)	•0018(5)	•0019(11)
C(6)	•0032(5)	•0141(17)	•0050(6)	•0009(8)	•0002(4)	•0025(9)
NA(1)	•0037(2)	•0097(5)	•0030(2)	•0000(2)	•0006(1)	•0006(2)
NA(2)	•0033(2)	•0118(5)	•0028(2)	•0012(2)	•0007(1)	•0005(3)
O(5)	•0060(3)	•0182(12)	•0036(3)	•0018(5)	•0027(3)	•0013(5)

TABLE XVII (CONTINUED)

ANISOTROPIC THERMAL PARAMETERS FOR THE NON-HYDROGEN ATOMS IN



ATOM	β_{11}	β_{22}	β_{33}	β_{12}	β_{13}	β_{23}
O(6)	•0049(3)	•0171(10)	•0023(3)	=•0011(5)	•0011(3)	•0004(5)
O(7)	•0042(3)	•0111(10)	•0049(4)	•0024(4)	•0009(3)	•0004(5)
C(7)	•0044(5)	•0187(18)	•0045(6)	=•0002(8)	•0017(4)	=•0004(8)
O(8)	•0047(3)	•0074(9)	•0039(3)	=•0001(4)	•0016(2)	=•0012(4)
O(9)	•0036(3)	•0175(11)	•0031(3)	=•0020(5)	•0016(2)	=•0023(5)
C(8)	•0041(5)	•0104(15)	•0041(5)	•0005(7)	•0004(4)	=•0011(7)
C(9)	•0048(5)	•0117(15)	•0037(5)	•0004(7)	•0024(4)	•0012(7)

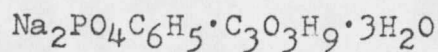
(e.s.d.'s in parentheses)

The expression for the anisotropic thermal parameters is of the form:

$$\exp(-\beta_{11}h^2 - \beta_{22}k^2 - \beta_{33}l^2 - 2\beta_{12}hk - 2\beta_{13}hl - 2\beta_{23}kl)$$

TABLE XVIII

HYDROGEN ATOM POSITIONS AND THERMAL PARAMETERS FOR



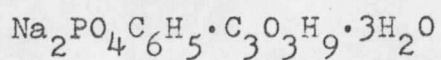
ATOM	<u>z/a</u>	<u>y/b</u>	<u>z/c</u>	<u>B_{iso}</u>	
H(1)	.34010	.32654	.01079	2.0	*
H(2)	.489(5) ^a	.225(8)	.016(5)	5.(2)	
H(3)	.566(4)	.041(8)	.162(4)	5.(2)	
H(4)	.502(5)	-.001(9)	.303(5)	6.(2)	
H(5)	.367(3)	.133(6)	.285(4)	1.(1)	
H(6)	.275(3)	-.378(6)	.181(3)	1.(1)	
H(7)	.293(3)	-.182(6)	.210(4)	2.(1)	
H(8)	.369(5)	-.264(10)	.083(5)	8.(2)	
H(9)	.288(5)	-.126(9)	.038(5)	6.(2)	
H(10)	.151(4)	-.135(8)	.143(4)	5.(2)	
H(11)	.281(5)	-.228(9)	-.136(5)	7.(2)	
H(12)	.355(4)	-.400(7)	-.066(4)	3.(1)	
H(13)	.239(4)	-.420(7)	-.140(4)	3.(1)	
H(14)	.262(4)	.403(7)	.311(4)	3.(1)	
H(15)	.216(3)	.396(7)	.375(4)	2.(1)	

^a The number in parentheses is the standard deviation and refers to the least significant digits.

*Calculated values for positions and assigned value for the isotropic temperature factor.

TABLE XVIII (CONTINUED)

HYDROGEN ATOM POSITIONS AND THERMAL PARAMETERS FOR



<u>ATOM</u>	<u>z/a</u>	<u>y/b</u>	<u>z/c</u>	<u>B_{iso}</u>	
H(16)	.08300	.20700	.37000	2.0	*
H(17)	.10400	.10000	.29300	2.0	*
H(18)	.089(2)	.548(4)	.399(2)	2.0	**
H(19)	.003(7)	.580(12)	.383(7)	2.0	**

**Assigned value for the isotropic temperature factor.

et al. (43).

XI. DISCUSSION OF THE MOLECULAR STRUCTURE

A drawing showing the thermal ellipsoids (32) for the asymmetric unit is shown in Figure XXIX. The bond lengths and bond angles are shown in Figures XXX and XXXI.

The Phenyl Phosphate Dianion. The bond distances and angles are not significantly different from those found in a previous determination of the phenyl phosphate dianion (11). Analysis of all the intramolecular distances in the dianion by use of a half-normal probability plot was carried out (1, 42). The statistic δ_{p_1} where

$$\delta_{p_1} = \left| |p(1)_1| - |p(2)_1| \right| / \left\{ \sigma^2_{p(1)_1} + \sigma^2_{p(2)_1} \right\}^{\frac{1}{2}}$$

is plotted against the expected value of δ_{p_1} which is calculated assuming a normal distribution of errors. A linear half-normal probability plot with a slope of unity and a zero intercept may generally be interpreted as being due to good agreement between the two structures and correctly estimated standard deviations. The half-normal probability plot is shown in Figure XXXII. The plot is described by two different lines. The differences in

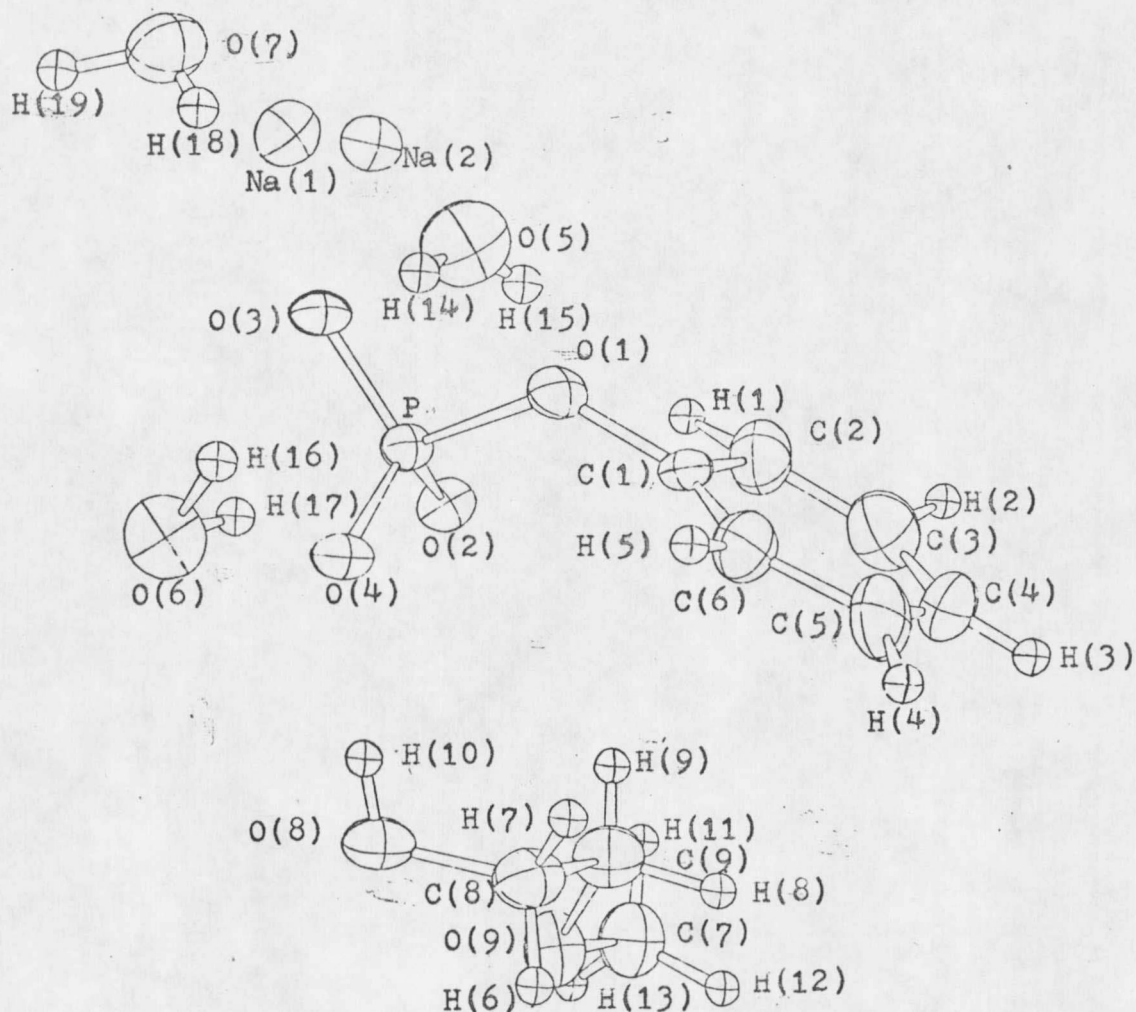


FIGURE XXIX

a-b PROJECTION OF THE MOLECULAR STRUCTURE OF
 $\text{Na}_2\text{PO}_4\text{C}_6\text{H}_5 \cdot \text{C}_3\text{O}_3\text{H}_9 \cdot 3\text{H}_2\text{O}$ ILLUSTRATING THE THERMAL ELLIPSOIDS
 AT THE 50% PROBABILITY LEVEL
 The hydrogen atoms were arbitrarily assigned isotropic tem-
 perature factors of 1.0 in this illustration.

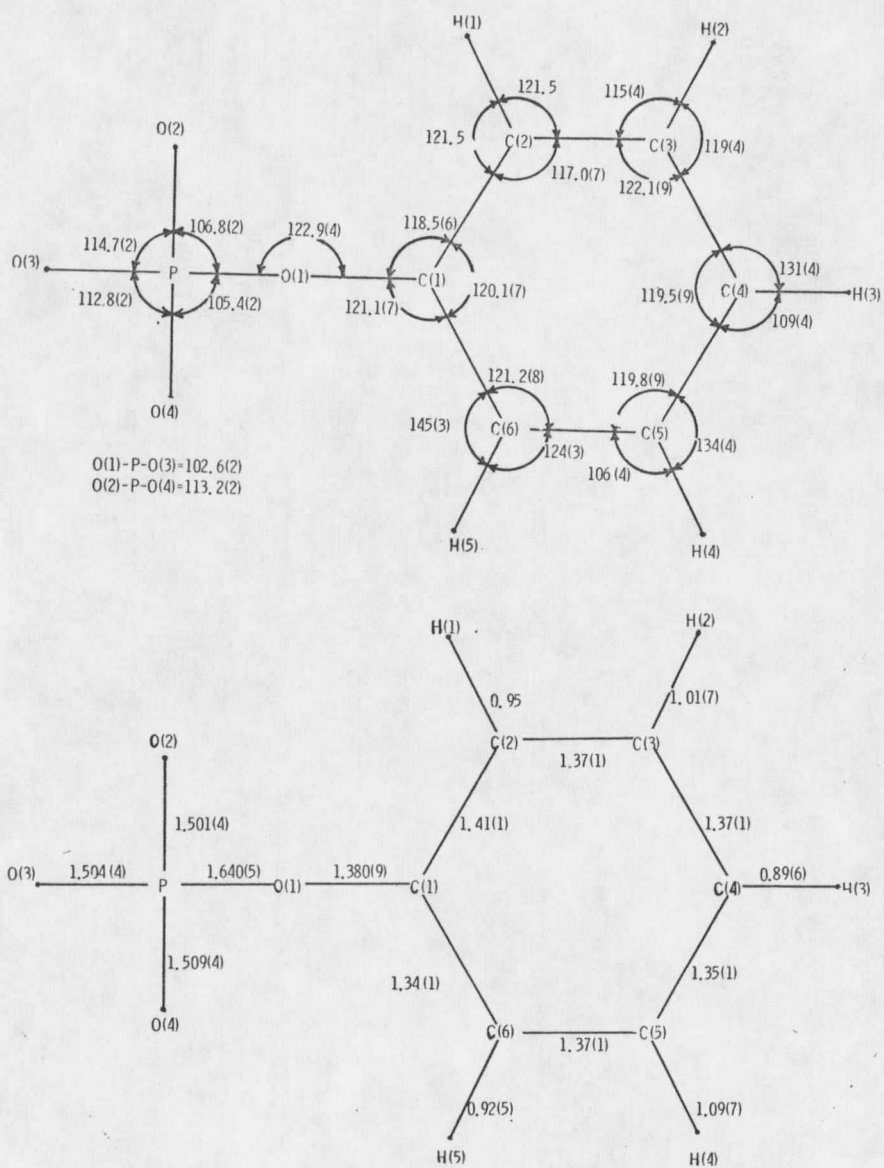


FIGURE XXX

BOND DISTANCES AND ANGLES FOR THE PHENYL PHOSPHATE DIANION

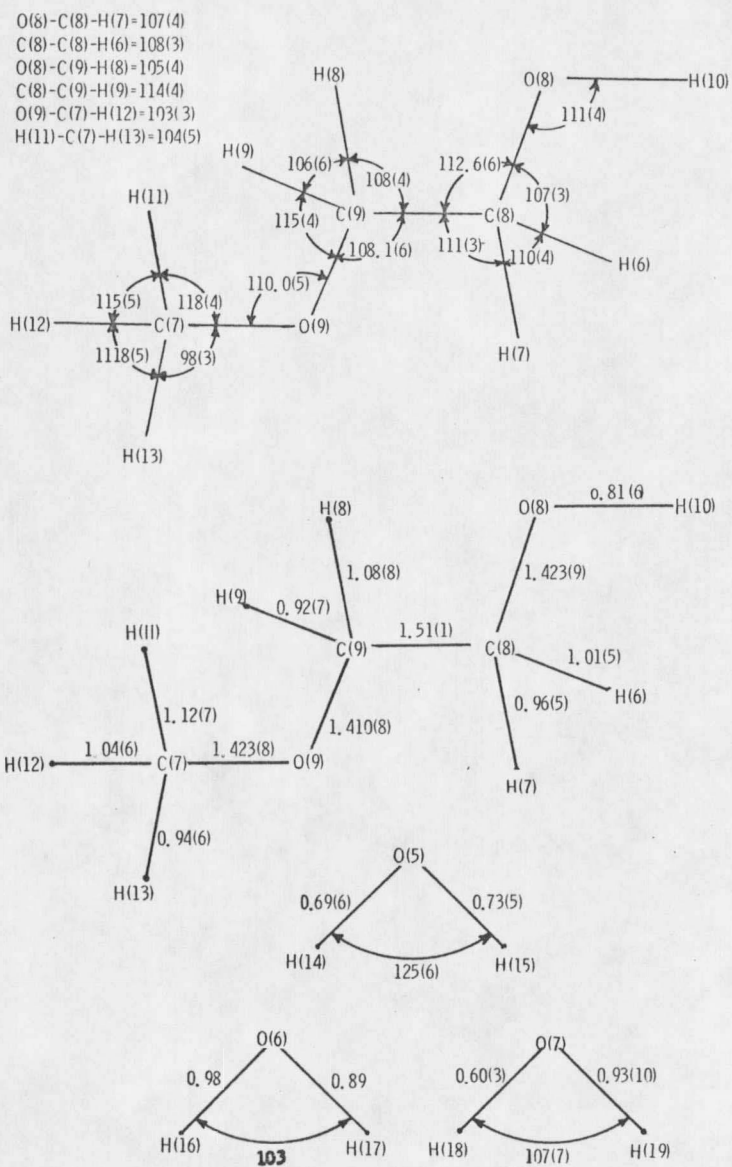


FIGURE XXXI

BOND DISTANCES AND ANGLES FOR THE SOLVATION MOLECULE AND THE WATER OF HYDRATION

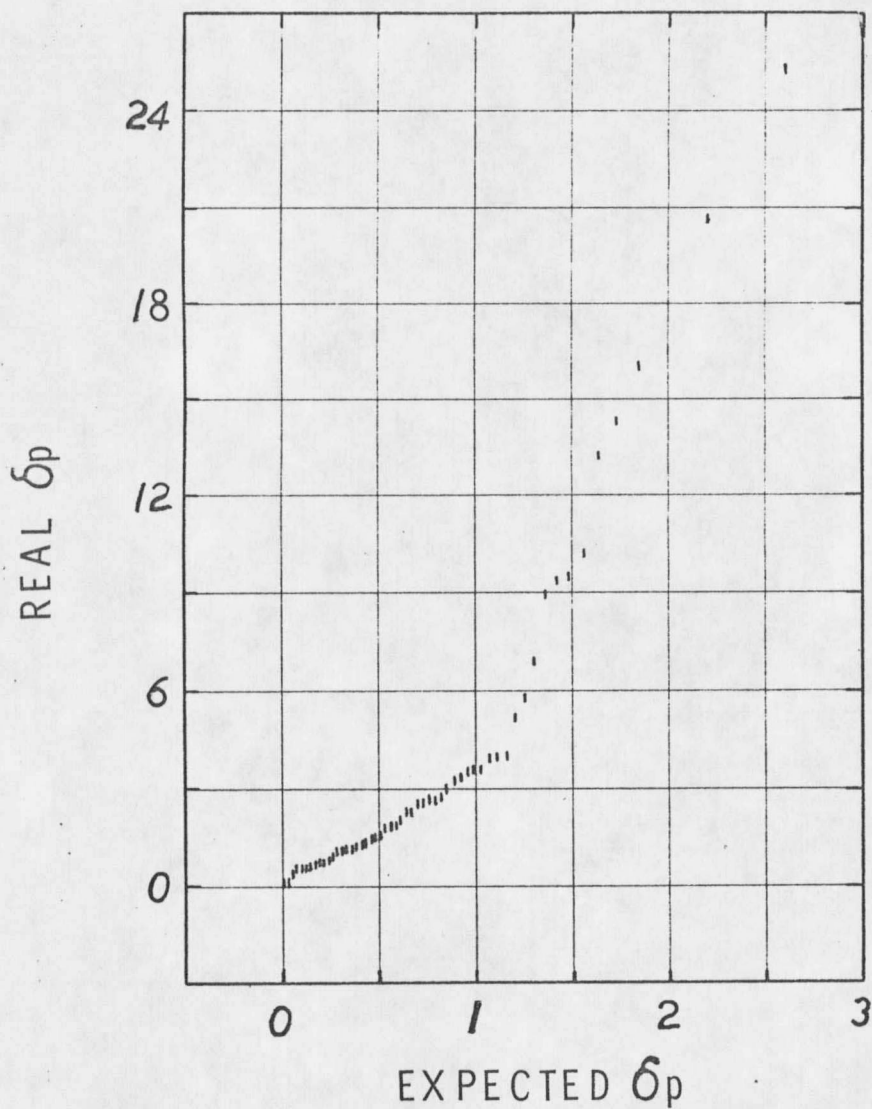


FIGURE XXXII

HALF-NORMAL PROBABILITY PLOT FOR ALL INTRAMOLECULAR DISTANCES IN THE PHENYL PHOSPHATE DIANION FROM TWO STRUCTURE DETERMINATIONS

distances nearly follows a normal distribution except for some portion of the dianion which is significantly different in the two structures. The variation is due to the ortho- and meta-carbon atoms of the phenyl group. Calculation of the angles between the plane of the phenyl group and the P-O(1)-C(1) plane seems to explain this difference. In the earlier determination this angle was found to be 52° while in this work the angle is 77° . The equations for all planes of interest (including those of the earlier structure)(11) are shown in Table XIX.

Half-normal plots prepared for the two apparently different distributions are shown in Figures XXXIII and XXXIV.

The least squares line through the data in Figure XXXIII has a slope of 1.8 and an intercept of 0.34. This indicates that the differences between the parameters do not follow a normal distribution and the standard deviations of both studies have been underestimated by an average factor of 1.8. The non-zero intercept indicates that there is a small systematic error in this group of parameters.

The least squares line through the data in Figure XXXIV has a slope of 10.9 and an intercept of 2.0 which suggests that there are systematic errors in the parameters. Since the phenyl ring in one structure is

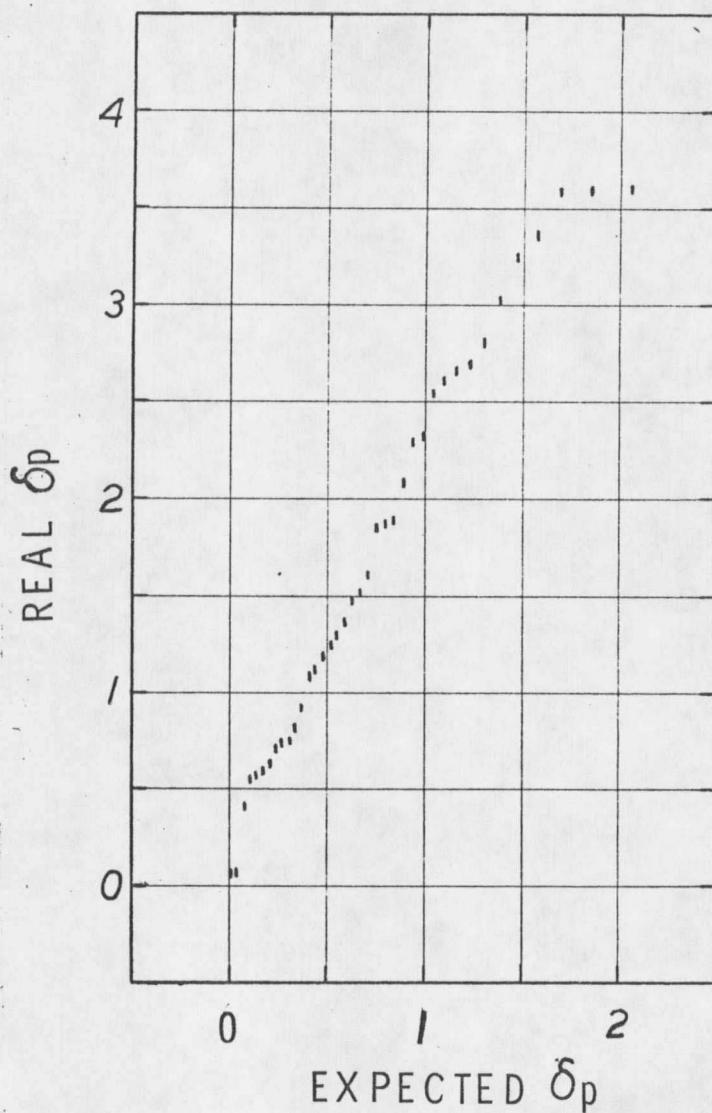


FIGURE XXXIII

HALF-NORMAL PROBABILITY PLOT FOR THE INTRAMOLECULAR
DISTANCES EXPECTED TO BE IDENTICAL IN THE TWO
PHENYL PHOSPHATE DIANION STRUCTURES

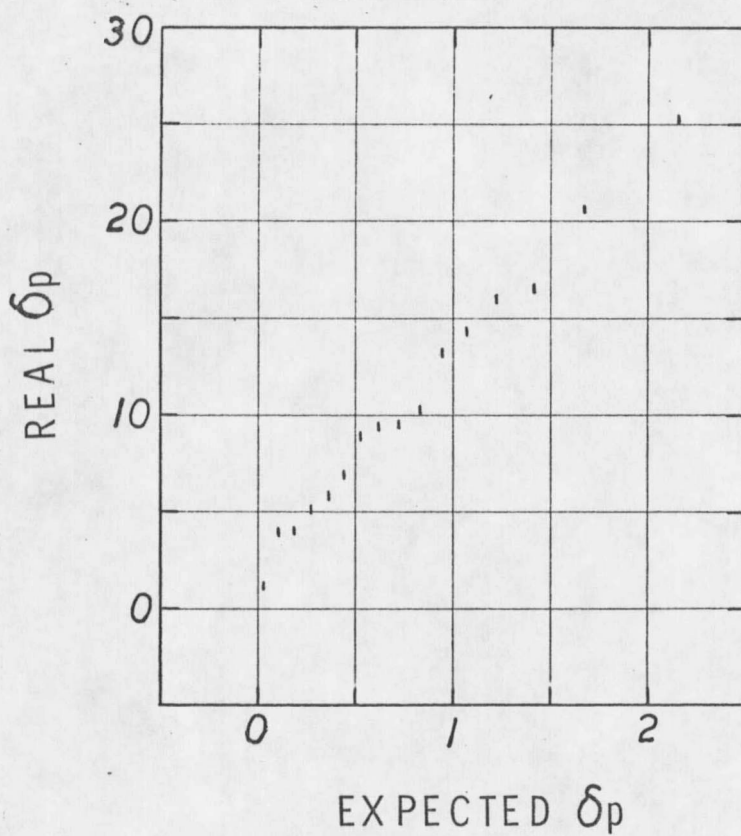


FIGURE XXXIV

HALF-NORMAL PROBABILITY PLOT FOR THE INTRAMOLECULAR
DISTANCES EXPECTED TO BE DIFFERENT IN THE TWO PHENYL
PHOSPHATE DIANION STRUCTURES

TABLE XIX

LEAST SQUARES PLANES^{a.)} REFERRED TO ORTHOGONAL AXES IN
 SODIUM PHENYL PHOSPHATE·2-METHOXYETHANOL·TRIHYDRATE^{b.)}

<u>ATOMS IN PLANE</u>	<u>l</u>	<u>m</u>	<u>n</u>	<u>p</u>	<u>S(Δ^2)^{c.)}</u>
C(1), C(2), C(3), C(4), C(5), C(6)	0.368	0.831	0.417	3.95	0.00165
P, O(1), C(1)	0.261	0.553	-0.791	0.589	0.00
O(8), C(8), C(9)	-0.101	-0.970	-0.219	1.224	0.00
O(9), C(8), C(9)	0.804	0.120	0.582	3.527	0.00

PLANES OF INTEREST FROM PREVIOUS STRUCTURE (11)

C(1), C(2), C(3), C(4), C(5), C(6)	0.472	-0.439	0.764	1.320	0.00290
P, O(1), C(1)	0.058	0.953	-0.297	1.064	0.00

- a.) Least squares plan: $lX + mY + nZ - p = 0.0$.
- b.) Coordinate system for plane is: X along a, Y in a-b plane, Z along c*.
- c.) $S(\Delta^2)$ is the sum of the squares of deviations of atoms from plane.

rotated by 25° with respect to the rest of the molecule when compared to the other structure, this is as expected.

A δ_R plot was constructed for the current structure. To do this, the statistic $\delta_{R_1} = \frac{\Delta_F}{\sigma_{F_0}}$ is plotted against the expected error X_1 , where X_1 is evaluated from the normal probability function

$$P(x) = \frac{1}{\sqrt{2\pi}} \int_{-x}^x e^{-\alpha^2/2} d\alpha$$

A linear plot with a slope of unity and an intercept of zero indicates that the errors follow a normal distribution and the σ_{F_0} have been correctly estimated. The δ_R plot is shown in Figure XXXV. The slope of the least squares line is 1.56 with an intercept of 0.04 indicating that the σ_{F_0} are underestimated by a factor of about 1.56 and that the distribution of errors follows a normal probability function.

The phenyl phosphate dianions in the two studies exist in quite different environments and are of significantly different conformation (with respect to the rotation of the phenyl group). The P-O(1) distances are identical in the two studies [1.640(5)Å versus 1.64(2)Å (11)]. Perhaps the P-O(1)-C(1) π -overlap (d-p-p) is of the same magnitude in the two conformations. Showing that this is

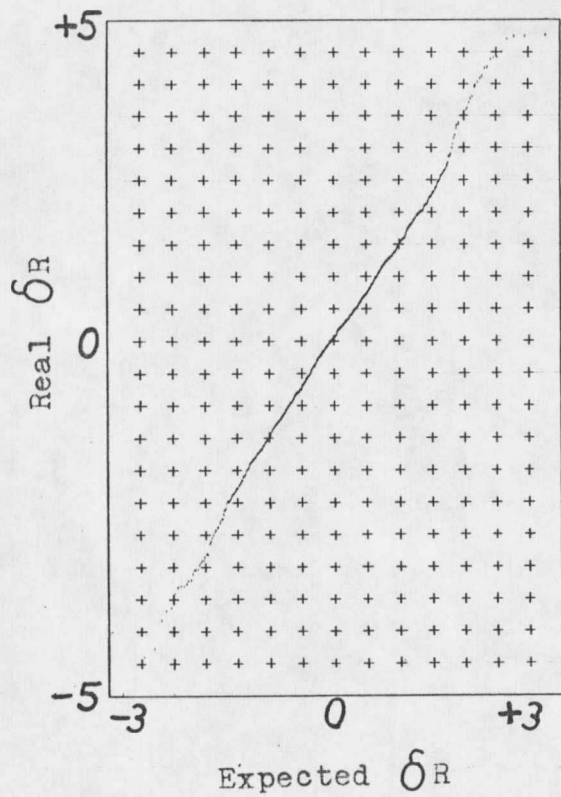


FIGURE XXXV

NORMAL PROBABILITY PLOT OF 969 δ_{R_1} BASED ON
OBSERVED STRUCTURE FACTORS F_o

so is extremely difficult if not impossible.

The hydrogen atoms on the phenyl ring were not considered in the comparison as they were not located in the first structure (11). The hydrogen atoms on the phenyl ring in the current structure were located from a difference map and refined. Refinement of the positional and isotropic temperature parameters of H(1) resulted in an unreasonable bond distance and very high standard deviations for these parameters. The position of H(1) was calculated using a C-H distance of $0.95\overset{\circ}{\text{A}}$ and an isotropic temperature factor of 2.0 was assigned to it. These values are in reasonable agreement with the other phenyl hydrogen parameters. The C(1)-C(2) and C(1)-C(6) distances in the phenyl ring are significantly different. These distances are expected to be the same and no obvious explanation exists for the difference observed. A final difference map showed a semi-circular ridge of electron density of about $+0.2e\overset{\circ}{\text{A}}^{-3}$ height at about $1.5\overset{\circ}{\text{A}}$ from C(2). Whether this ridge is due to errors in the data or is real is unknown.

The 2-Methoxyethanol Molecule. The bond distances and angles in the molecule are not significantly different from expected values. It is interesting that, although the molecule is not in the lowest energy staggered ("anti")

conformation, it is very close to the skew ("gauche") conformation which is also an energy minimum close to that of the staggered conformation. The predicted value for the skew conformation dihedral angle is 60° while in this case the dihedral angle formed by the O(8)-C(8)-C(9) and C(8)-C(9)-O(9) planes is 71° . This conformation allows O(8) to coordinate with both Na(1) and Na(2). Also, O(9) is involved in the Na(1) coordination sphere while H(10) forms a hydrogen bond with O(4) of the phosphate group. It is not surprising that this conformation is preferred over the slightly more favorable staggered conformation. Figure XXXI shows the bond angles and distances with the estimated standard deviations for the 2-methoxyethanol molecule.

Sodium Ion Coordination. The sodium ion coordination scheme is part of the hydrophilic planes that exist in the crystal coincident with the b-c plane. The coordination about Na(1) forms a distorted octahedron while that about Na(2) is a distorted trigonal bipyramid. Figure XXXVI shows the coordination scheme with coordination angles and distances included. Figure XXXVII is a packing diagram showing a portion of four adjacent unit cells emphasizing the sodium ion coordination. O(1) and O(2) of the phosphate

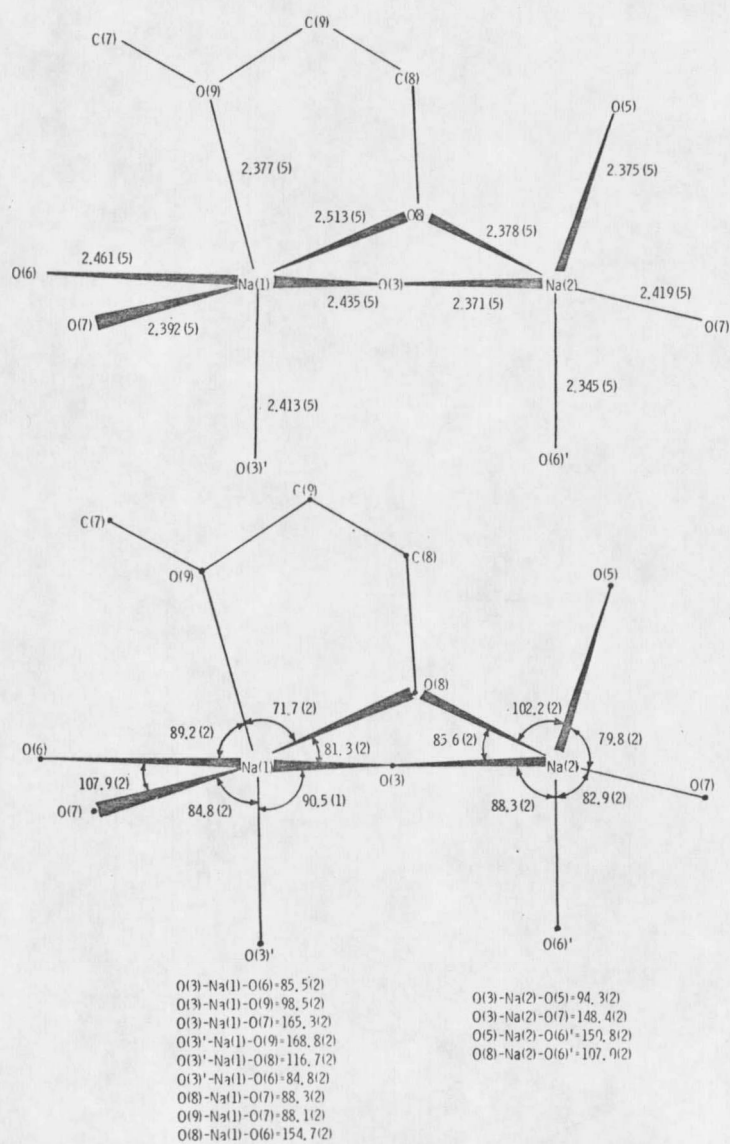


FIGURE XXXVI

SODIUM ION COORDINATION ANGLES AND DISTANCES

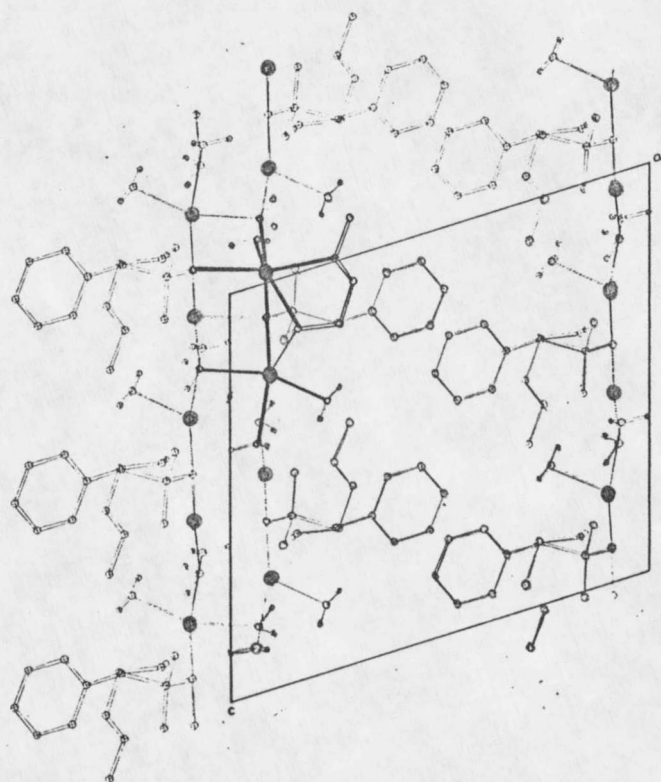


FIGURE XXXVII
PACKING DIAGRAM EMPHASIZING SODIUM ION COORDINATION

group participate only in hydrogen bonding and are not involved in the sodium ion coordination.

Hydrogen Bonding Scheme. Figure XXXVIII is a partial packing diagram illustrating the hydrogen bonding that occurs in the crystal. There is extensive hydrogen bonding between molecules which are in the a-c plane along the c-axis. Helices involving alternating water and phosphate groups held together by hydrogen bonds are very evident about the 2_1 axes that lie in the b-c plane. In addition, H(10) clearly forms a hydrogen bond with O(4) of the phosphate group.

Water of Hydration. Figure XXXI shows the bond angles and bond lengths for the three water molecules. The hydrogen atoms were located from a difference map. Some difficulty was experienced in attempting to refine the hydrogen atoms attached to O(6) and O(7). It appears that these hydrogen atoms are at least partially disordered. The refined isotropic temperature factors for H(16) and H(17) were unrealistically large. The positional parameters refined to produce an H(16)-O(6)-H(17) angle of $73(8)^\circ$. For these reasons the H(16) and H(17) atoms were not refined but were assigned positional parameters as determined from the difference map. The H(16)-O(6)-H(17)

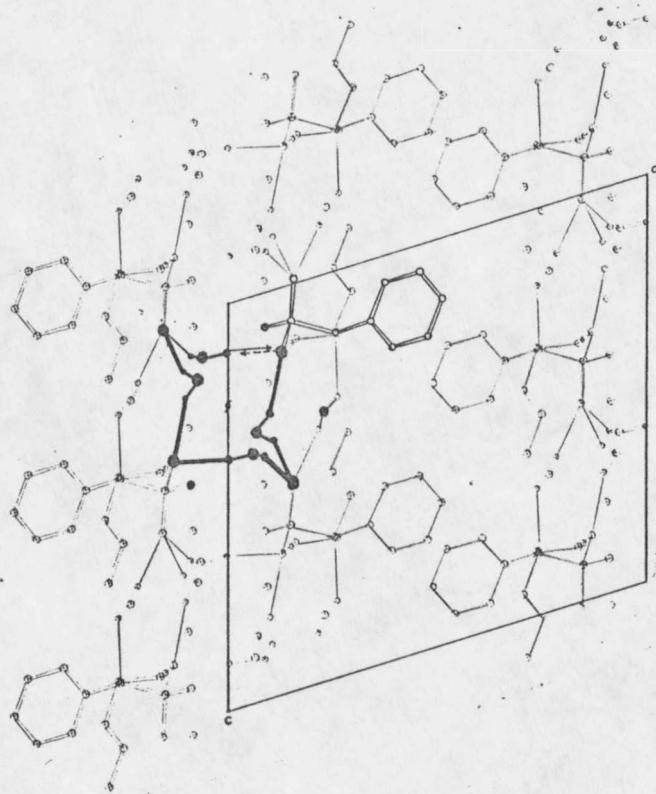
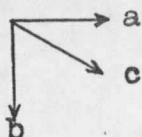
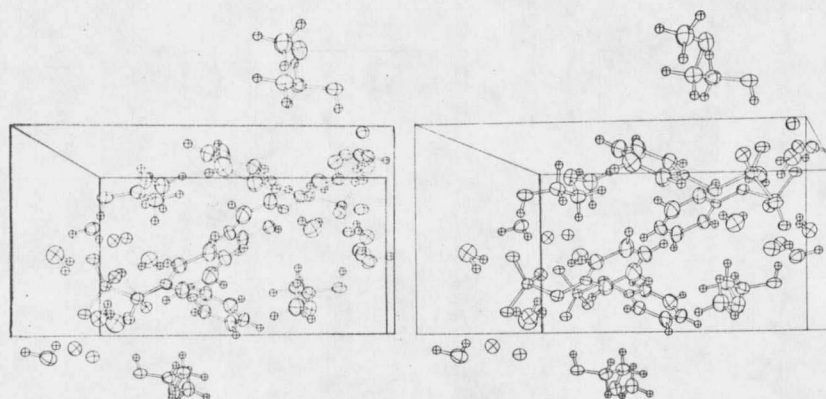


FIGURE XXXVIII
PACKING DIAGRAM EMPHASIZING HYDROGEN BONDING

angle without refinement was 103° . Isotropic temperature factors of 2.0 were assigned in agreement with those observed for H(14) and H(15). The positions of H(18) and H(19) were refined but the isotropic temperature factors were assumed to be 2.0 and not refined. Attempted refinement of these quantities produced isotropic temperature factors of -3.0 and +12.0 for H(18) and H(19) respectively. None of the three H-O-H angles appear to be significantly different from the expected value of 109° .

XII. DISCUSSION OF THE CRYSTAL STRUCTURE

Figure XXXIX shows a stereoscopic view of the contents of one unit cell. In the a-direction of the crystal both hydrogen-bonding and coordination with the sodium ions occur in the hydrophilic sections of the crystal with van der Waal interactions occurring in the hydrophobic portions of the crystal. In the b-direction the largest interactions seem to be due to coordination about the sodium atoms. The 2-methoxyethanol molecule which is coordinated to both Na(1) and Na(2) is actually in the unit cell above the one containing the sodium ions. Likewise, the water oxygen, O(5), coordinated to Na(2) is in the unit cell above the one containing the sodium ion. In the c-direction both hydrogen-bonding and chains of



ORIENTATION OF UNIT CELL

FIGURE XXXIX
STEREOGRAPHIC PACKING DIAGRAM FOR
 $\text{Na}_2\text{PO}_4\text{C}_6\text{H}_5 \cdot \text{C}_3\text{O}_3\text{H}_9 \cdot 3\text{H}_2\text{O}$

of sodium-oxygen linkages occur.

CHAPTER VI

SUMMARY AND CONCLUSIONS

The three-dimensional structure of 2,2,3,3,4-pentamethyl-1-phenylphosphetane 1-oxide has been determined. This represents the first structure determination of an unsymmetrical phosphetane oxide. The single α -methyl group is trans to the phenyl group. The P-C bond to the least substituted α -carbon is significantly shorter than the other P-C bond. This result is in opposition to the predicted relative bond lengths based on ring-opening reactions (37). A reaction mechanism for basic hydrolysis of this type of compound has been proposed. The reaction mechanism is consistent with both the increased reactivity of the less highly substituted compounds and the observed products. The proposed transition state involves a pseudo-rotation from an initial activated complex, A, to a more stable activated complex, B. The axial-equatorial arrangement of the two oxygen atoms in the trigonal bipyramid of A is less stable than the equatorial-equatorial arrangement of the atoms in B. This is felt to be the main reason for the observed cleavage of the P-C bond to the least substituted α -carbon.

The stereochemistry of some ten related compounds has

been determined as a result of the crystal and molecular structure determination of 1-iodomethyl-3-methyl-1-phenylphosphonium iodide. The phenyl group is trans to the 3-methyl group. The 3-methyl phosphonium ring system exists in the half-chair form as opposed to the envelope form predicted for methylcyclopentane (39). Either the predicted conformation for methylcyclopentane is incorrect, or, more likely the methylphosphonium ring system is not a good analogue due to perturbations in bond angles and distances caused by the phosphorus atom. The iodide-iodine intermolecular distance of $3.672(1)\overset{\circ}{\text{A}}$ is apparently one of the shortest iodine-iodine distances observed to this date.

A hypothesis has been proposed relating the free-energy of hydrolysis of aryl phosphates to the length of the P-O bond being hydrolyzed.

Hückel molecular orbital calculations were carried out as an initial test of the hypothesis. The results are consistent with the hypothesis. In addition, HMO calculations on para-substituted benzoic acids and phenols indicate that $\log K_a$ is proportional to the electron density on the oxygen atom donating the proton.

The crystal and molecular structure of disodium phenyl phosphate·2-methoxyethanol·trihydrate has been determined. This structure represents the first of several

structure determinations to be carried out in testing the hypothesis. The 2-methoxyethanol molecule is apparently stabilized in the "skew" form by sodium ion coordination and hydrogen bonding. The structure of the phenyl phosphate dianion is compared to that present in dipotassium phenyl phosphate-sesquihydrate. The P-O(ester) bond is the same length (1.640^oÅ) in the two structure determinations although the phenyl phosphate dianions exist in different conformations in the two structures.

BIBLIOGRAPHY

123
BIBLIOGRAPHY

1. Abrahams, S. C., and Keve, E. T., (1971). Acta Cryst., A27, 157.
2. Ahmed, F. R., (1966). "Fouriers for Distorted and Undistorted Nets," National Research Council, Ottawa, Ontario, Canada.
3. Ahmed, F. R., (1968). "Symbolic Addition Procedure (Centrosymmetric)," National Research Council, Ottawa, Ontario, Canada.
4. Alver, E., and Holtedahl, B. H., (1967). Acta Chem. Scand., 21, 359.
5. Barnard, P. W. C., Bunton, C. A., Kellerman, D., Mhala, M. M., Silver, B., Vernon, C. A., and Welch, V. A., (1966). J. Chem. Soc., 227.
6. Bryan, R. F., (1967). J. Chem. Soc., (B), 1311.
7. Burkhardt, G. N., Ford, W. G. K., and Singleton, E., (1936). J. Chem. Soc., 17.
8. Busing, W. R., and Levy, H. A., (1959). "A Crystallographic Least Squares Program for the IBM 704," ORNL 59-4-37. Oak Ridge National Laboratory, Tenn. As modified for use in the Montana State University Crystallographic Library of Programs.
9. Callis, P. R., Craig, A. C., and Howald, R. A., (1973). Program and Abstracts, Amer. Chem. Soc. Northwest Regional Meeting, Pullman, Washington, Paper CI.5.
10. Calleri, M., and Speakman, J. C., (1964). Acta Cryst., 17, 1097.
11. Caughlan, C. N., and Haque, M. U., (1967). Inorg. Chem., 6, 1998.
12. Caughlan, C. N., Wang, C. K., and Fitzgerald, A., (1972). Program and Abstracts, Inter. Union of Cryst. Meeting, Tokyo, Japan, Paper III, Section on High Energy Phosphates.

13. Corfield, J. R., Harger, M. J. P., Shutt, J. R., and Trippett, S., (1970). J. Chem. Soc., (C), 1855.
14. Coulson, C.A., (1939). Proc. Roy. Soc., A169, 413.
15. Cromer, D. T., and Mann, J. B., (1968). Acta Cryst., A24, 321.
16. Cruickshank, D. W. J., (1961). J. Chem. Soc., 5486.
17. Davies, W. C., and Lewis, L. P. G., (1934). J. Chem. Soc., 1599.
18. Davies, W. O., and Stanley, E., (1962). Acta Cryst., 15, 1092.
19. Demény, L., (1931). Rec. trav. chim., 50, 60.
20. Eliel, E. L., (1962). "Stereochemistry of Carbon Compounds," p.250, New York, McGraw-Hill, Inc.
21. Ezzel, B. R., (1970). J. Org. Chem., 35, 2426.
22. Fitzgerald, A., Caughlan, C. N., and Smith, G. D., (1971). Program and Abstracts, Amer. Cryst. Assoc. Meeting, Ames, Iowa, Paper 07.
23. Fitzgerald, A., Caughlan, C. N., and Smith, G. D. (1972). Program and Abstracts, Amer. Cryst. Assoc. Meeting, Albuquerque, New Mexico, Paper E1.
24. Grey, G., and Cremer, S. E., (1972). J. Org. Chem., 37, 3458.
25. Hammett, L. P., (1935). Chem. Rev., 17, 125.
26. Hammett, L. P., (1937). J. Am. Chem. Soc., 59, 96.
27. Haque, M. U., and Caughlan, C. N., (1970). Acta Cryst., B26, 1528.
28. Haque, M. U., (1970). J. Chem. Soc., (B), 938.
29. Haque, M. U., (1971). J. Chem. Soc., (B), 117.

30. Hine, J., (1962). "Physical Organic Chemistry," Second Edition, McGraw-Hill, New York; Kosower, E.M., (1968). "An Introduction to Physical Organic Chemistry," John Wiley and Sons, Inc., New York; Leffler, J.E., and Grunwald, E., (1963). "Rates and Equilibria of Organic Reactions," John Wiley and Sons, Inc., New York.
31. International Tables for X-Ray Crystallography, (1962). Vol. III, Tables 3.3.1A, 3.3.2C, 5.3.5B. Kynoch, Birmingham, England.
32. Johnson, C. K., (1965). "ORTEP: A Fortran Thermal Ellipsoid Plot Program for Crystal Structure Illustration," ORNL-3794, Oak Ridge National Laboratory, Tennessee.
33. Ketelaar, J. A. A., Gersman, H. R., and Koopmans, K., (1952). Rec. trav. chim., 71, 1253.
34. Lai, T. F., and Marsh, R. E., (1967). Acta Cryst., 22, 885.
35. Meulenaer, J. de, and Tompa, H., (1965). Acta Cryst., 19, 1014
36. Mislow, K., (1970). Accts. of Chem. Res., 3, 321.
37. Moret, C., and Trefonas, L. M., (1969). J. Am. Chem. Soc., 91, 2255.
38. Pauling, L., (1960). "The Nature of the Chemical Bond," Third Edition, Cornell Univ. Press, Ithaca, N.Y.
39. Pitzer, K. S., and Donath, W. E., (1959). J. Am. Chem. Soc., 81, 3213.
40. Sakore, T. D., and Pant, L. M., (1966). Acta Cryst., 21, 715.
41. Sim, G. A., Robertson, J. M., and Goodwin, T. H., (1955), Acta Cryst., 8, 157.
42. Smith, G. D., (1973). Programs for Evaluation of Both Normal and Half-Normal Probability Functions and for Plotting the Data. Hydrogen atom positions were calcu-

lated with a program written by K. Raymond as modified by G. D. Smith. Montana State University Crystallographic Library of Programs.

43. Steer, R. J., Watkins, S. F., and Woodward, P., (1970). J. Chem. Soc., (C), 403.
44. Stewart, R. F., Davidson, E. R., and Simpson, W. T., (1965). J. Chem. Phys., 42, 3175.
45. Stout, G. H., and Jensen, L. H., (1968). "X-Ray Structure Determination," Macmillan, New York.
46. Streitwieser, A., (1963). "Molecular Orbital Theory for Organic Chemists," John Wiley and Sons, New York.
47. Svetich, G. W., and Caughlan, C. N., (1965). Acta Cryst., 19, 645.
48. Toussaint, J., (1951). Acta Cryst., 4, 71.
49. Van Wazer, J. R., (1958). "Phosphorus and Its Compounds," Vol. I. Interscience Publ., Inc., New York.
50. Wang, C. G., Caughlan, C. N., and Haque, M. U., Unpublished Data.
51. Wang, C. K., Caughlan, C. N., and Haque, M. U. Unpublished Data.

